CALCULATIONS OF ELECTRONIC POTENTIAL ENERGY SURFACES

A thesis presented for the degree

of

Ph.D. in the University of Glasgow

by

Alan C. Roach

June 1967

Calculations of Electronic Potential
Energy Surfaces

It is ordinarily possible to simplify the treatment of the
dynamics of a general polyatomic system by first considering only
the electronic motions, for all possible configurations of
artificially fixed nuclei. Any particular electronic eigenvalue,
as a function of nuclear geometry, then constitutes an effective
potential energy surface, which governs the nuclear motion.

The calculation of potential energy surfaces for practical
systems represents a major quantum mechanical undertaking which
in general becomes tractable only within a framework of approximation
and semi empiricism.

The major part of this thesis describes calculations developed
to estimate the lower lying potential surfaces for the reactive
system $K + NaCl = KCl + Na$. A model treatment is developed and
discussed in detail. Essentially the problem is reduced to the
consideration of the motion of a single electron in the fields of
the closed shell ions Na^+, K^+ and Cl^-. There is good evidence
that these ions can be treated as classical polarisable charged
spheres in their longer range electrostatic interactions and also
that their structures are not seriously modified by the presence of
the single valence electron. The electronic eigenfunction is
expanded in terms of a basis set of alkali atom valence s and p-orbitals
The most difficult problem is the evaluation of certain close range

interactions between the electron and the ions and this matter is discussed in detail. The electronic problem is first solved in neglect of the polarisation of the ion cores and this latter effect is afterwards introduced, resulting in a first order perturbation correction to the energy surfaces. Empirical evidence used consists of values for ionic polarisabilities and radii, together with experimental ionisation potentials.

A suitably reduced version of this model is applied to the calculation of potential curves for the diatomic ions Na_2^+, K_2^+ and NaK^+ and yields encouragingly close agreement with experimentally observed properties.

The results for the complete system are presented and discussed. The reaction exothermicity is slightly overestimated. There is no calculated activation barrier, the reaction appearing to conform to the "early downhill" classification. A potential well indicates that, if the excess energy were removed, a triangular complex molecule could be formed, some 13 Kcal more stable than the product. Finally there appears to be some qualitative evidence that highly energetic collisions of the reactants may lead to electronically excited product atoms, a phenomenon observed experimentally for the reaction $Na + KBr = NaBr + K$.

The shorter second part of the thesis presents an estimate of the Jahn-Teller effect in rhenium hexafluoride. This effect arises from the coupling between electronic and nuclear motions

when two or more potential surfaces have the same energy in a non linear symmetrical configuration. In such cases the degeneracy is relieved by certain vibrational displacements, leading to a distortion in the equilibrium geometry and a complication of the vibrational spectrum. In rhenium hexafluoride it is assumed that this effect arises from a purely electrostatic interaction between the fluorine atoms and the non-bonding $5d$ rhenium electron in a degenerate Γ_8 state arising from strong spin orbit coupling of the t_{2g} configuration. The electrostatic potential of a fluorine atom is taken as that of a fluoride ion less some variable fraction of an electron, depending on bond ionicity, taken from a hybrid orbital directed towards the central rhenium atom. The rhenium $5d$ orbital is taken of Slater form with variable exponent. The results, which depend essentially on the potential surface gradients in the octahedral configuration are relatively insensitive to physically reasonable choices of these parameters. A large splitting in the V_2 band of the Raman spectrum is predicted, in good order of magnitude agreement with experiment. There is a corresponding very small distortion of the molecular geometry calculated, probably in a tetragonal sense.

Preface

The major section of this thesis, Part I, gives an account of a calculation of electronic potential energy surfaces for the reaction $K + NaCl = KCl + Na$. A model is developed at length which considers basically the motion of a single valence electron in the fields of the three ions Na^+, K^+, Cl^-, and which, when applied to the calculation of potential curves for the diatomic ions Na_2^+, K_2^+, and NaK^+, gives very satisfactory agreement with experiment. The most interesting predictions arising from the calculated results for the system $K + NaCl$ are that there is no activation barrier to reaction, that, on the contrary, the reaction complex NaKCl is over 10 Kcal/mole more stable than the products, and that under normal conditions an essentially adiabatic mechanism should apply.

Part II is devoted to a calculation of the magnitude of the Jahn-Teller effect in ReF_6, assuming that it arises from a purely electrostatic interaction between the single Re non-bonding t_{2g} electron and the fluorine atoms. The results, in addition to suggesting a small ($\sim 0.005 \overset{\circ}{A}$) tetragonal distortion in the equilibrium geometry of the molecule, give order of magnitude agreement with the experimentally observed splitting

($\sim$170 cm^{-1}) in the ω_2 band of the vibrational spectrum.

This account describes original work carried through in pursuit of the degree of Ph. D. in the University of Glasgow. Although a small pilot calculation on the subject of Part II was performed in partial fulfillment of the requirements of the degree of B. Sc., the work recorded here constitutes a very considerable expansion and amplification of the earlier probe.

June 1967.   Alan C. Roach.

Acknowledgements

The author wishes to indicate his deep indebtedness to Dr M. S. Child, who supervised this work, making many valuable suggestions and devoting much time and energy to helpful discussions.

The author also wishes to express his thanks to the Carnegie Trust for the Universities of Scotland, who provided him with a grant, and to his wife, Anne, who typed this manuscript.

Contents

Introduction

In the study of the properties of a general chemical system, composed of several nuclei and electrons, it is usually possible for the problem to be divided conveniently into two parts by taking advantage of the relative lightness and mobility of the electrons. In a quantum mechanical treatment the many particle hamiltonian, in neglect of small spin and magnetic effects, may be written in the form

$$\hat{H} = \sum_N \frac{\hat{p}_N^2}{2M_N} + \sum_E \frac{\hat{p}_E^2}{2m} + V, \tag{1}$$

where the successive terms represent the nuclear and electronic kinetic energy operators, and the total potential energy arising from the coulomb interaction between every pair of particles. $\hat{p}_N$ and $\hat{p}_E$ are nuclear and electronic momentum operators and M_N and m are the respective particle masses. Grouping the latter two terms together, and collectively representing nuclear coordinates by R and electronic coordinates by r, (1) may be rewritten:

$$\hat{H}(r, R) = \sum_N \frac{\hat{p}_N^2}{2M_N} + \hat{H}_e(r; R) \tag{2}$$

where $\hat{H}_e(r; R)$ is the "electronic" hamiltonian. The electronic wavefunctions at fixed R, $\psi_n(r; R)$, are chosen to satisfy the Schrodinger equation

$$\hat{H}_e(r; R)\, \psi_n(r; R) = U_n(R)\, \psi_n(r; R), \tag{3}$$

and $U_n(R)$ is the corresponding electronic energy. The eigenvalues U_n and the normalised eigenfunctions ψ_n depend parametrically on and vary continuously with R. Since the ψ_n always constitute a complete orthonormal set of functions over the electronic coordinates, it is possible to write the wavefunction for the total system in the form:

$$\Psi(r,R) = \sum_n \chi_n(R)\, \psi_n(r;R), \qquad (4)$$

where the χ_n depend only on the nuclear coordinates. Substituting into the full Schrodinger equation, multiplying by ψ_m^* and integrating over the electronic coordinates, using (3), coupled equations of the following type result for the χ_n :

$$\left[\sum_N \frac{\hat{p}_N^2}{2M_N} + \int \psi_m^*\left(\sum_N \frac{\hat{p}_N^2}{2M_N}\right)\psi_m\, dr + U_m(R) - E\right]\chi_m$$
$$+ \sum_{n\neq m}\left[\sum_N \frac{1}{2M_N}\left\{\int \psi_m^*\hat{p}_N^2\psi_n\, dr + 2\left(\int \psi_m^*\hat{p}_N\psi_n\, dr\right)\hat{p}_N\right\}\right]\chi_n = 0, \quad (5)$$

where, as is always possible, the ψ_m have been chosen to be real, so that $\int \psi_m^*\hat{p}_N\psi_m\, dr = 0$.

It can be shown that the electronic integrals involving the nuclear momentum operators are ordinarily of the relative order of the square root of the ratio of the electronic to the nuclear mass.[1,2] Neglect of these terms leads to the adiabatic approximation:

$$\left[\sum_N \frac{\hat{p}_N^2}{2M_N} + U_n(R)\right]\chi_n(R) = E\,\chi_n(R). \qquad (6)$$

For a system in the state $\Psi_n(r; R)$, the nth electronic eigenvalue, a function of nuclear configuration, constitutes the potential energy surface governing the motions of the nuclei. Within the framework of this approximation, the whole motion of the system may be described in terms of a single, continually adjusting, electronic solution of (3). No transitions between electronic states occur as a result of the motion.

There are, however, situations in which the adiabatic approximation is inadequate. The circumstances in which this may occur can be demonstrated by considering the simplest and most usual situation in which breakdown is caused at some configuration through appreciable coupling between two electronic states, a and b, by motion along a single nuclear coordinate Q_ν, with corresponding momentum operator

$$\hat{p}_\nu = -i\hbar\frac{\partial}{\partial Q_\nu} \tag{7}$$

Neglecting the second derivative of the electronic functions Ψ_i with respect to Q_ν, equation (5) for the coupled nuclear motions takes the form:

$$\left[\sum_{\nu}\frac{\hat{p}_\nu^2}{M_\nu} + U_a - E\right]\chi_a + \left[\left(\int\Psi_a^*\hat{p}_\nu\Psi_b\,dr\right)\frac{\hat{p}_\nu}{M_\nu}\right]\chi_b = 0. \tag{8}$$

If the coupling is treated as a perturbation and if the zero order (adiabatic) state corresponds to motion over the potential surface U_a, with total wavefunction

$$\Psi^{(0)} = \psi_a \chi_a, \tag{9}$$

then the corrected wavefunction and energy are

$$\Psi^{(1)} = \psi_a \chi_a + \sum_{\chi_b} \left\{ \frac{\left(\int \psi_a^* \hat{p}_\nu \psi_b \, d\tau\right)\left(\int \chi_a \frac{\hat{p}_\nu}{M_\nu} \chi_b \, dR\right)}{E_a^{(0)} - E_b^{(0)}} \right\} \psi_b \chi_b, \tag{10}$$

and $\quad E^{(2)} = E_a^{(0)} + \sum_{\chi_b} \left\{ \frac{\left|\left(\int \psi_a^* \hat{p}_\nu \psi_b \, d\tau\right)\left(\int \chi_a^* \frac{\hat{p}_\nu}{M_\nu} \chi_b \, dR\right)\right|^2}{E_a^{(0)} - E_b^{(0)}} \right\}$

where the complete set of nuclear functions χ_b is included in the summation (or integration if a continuum is involved). In the free particle case the only non zero nuclear integrals $\int \chi_a^* \frac{\hat{p}_\nu}{M_\nu} \chi_b \, dR$ will couple states χ_a and χ_b corresponding to identical de Broglie wavelengths, and hence identical nuclear momenta. It may be supposed that these interactions are predominant even in the general case and hence only this χ_b need be considered. In this event

$$\int \chi_a^* \frac{\hat{p}_\nu}{M_\nu} \chi_b \, dR \sim O(\nu),$$

$$\text{and} \quad E_a^{(0)} - E_b^{(0)} \sim U_a - U_b, \tag{11}$$

where ν is the classical nuclear velocity conjugate to Q_ν.

Further, from the electronic Schrodinger equation(3), it can be shown[3] that

$$\int \psi_a^* \hat{p}_\nu \psi_b \, d\tau = \frac{1}{u_a - u_b} \int \psi_a^* \left(-i\ell \frac{\partial V}{\partial Q_\nu} \right) \psi_b \, d\tau.$$ (12)

It is apparent from equations (10-12) that the adiabatic approximation is unreliable in two cases. Firstly for exceptionally high nuclear velocities [4] the nuclear integral (11) becomes large, but the more important case at ordinary temperatures occurs at configurations where there is a near or actual degeneracy of electronic levels when the denominator of the electronic integral (12) becomes small, the integral diverging at an actual degeneracy unless the numerator on the right hand side of (12) also vanishes because of some symmetry property.

In regions where the adiabatic approximation fails coupled equations of form (5) must be employed to determine the nuclear motions. After passage through such a region there is a finite probability that a transition will have occurred to a different electronic state. For the case discussed above where two electronic surfaces "cross" as a result of motion along a single nuclear coordinate, Q_ν, an approximate estimate of the transition probability, P, is given by the Landau-Zener formula: [5-7]

$$P = \exp\left\{ -\frac{\pi}{2\hbar v} \frac{\Delta^2}{\left| \frac{\partial}{\partial Q_\nu}(u_a - u_b) \right|} \right\},$$ (13)

where v is the classical nuclear velocity along Q and Δ
is the separation between the two potential surfaces at
their point of closest approach, at which position also the
gradient difference $\frac{\partial}{\partial Q}(U_a - U_b)$ is evaluated.

In Part I of this thesis a calculation is described
of a set of electronic potential energy surfaces
relevant to the gaseous chemical reaction K+NaCl = KCl+Na.
In general the documentation of potential surfaces over a
wide range of nuclear configurations constitutes a complex
and lengthy quantum mechanical enterprise, even for
rather simple systems, and relatively few reliable
calculations have been performed, these employing for the
most part serious approximation or varying degrees of
empiricism.[8]   In the present work it is argued that the
electronic problem can be reduced essentially to the
consideration of the motion of a single valence electron
in the fields of the ions Na^+, K^+ and Cl^-.   It is shown,
however, that considerable care must be exercised in
the estimation of the closer range interactions between
the electron and the ions.   A detailed model is developed
for the calculation and this is shown to stand up well
when put to the test in the production of potential
curves for the diatomic ions Na_2^+, K_2^+ and NaK^+, in

that excellent agreement is found between calculated and
experimental properties.   Finally the full results for the
reactive system are laid out and discussed.   It is predicted
that there will be no activation barrier to reaction, and
that, if excess energy were removed, a triangular molecule
KNaCl could be formed with a dissociation energy of
approximately 13 Kcal/mole.   For the most part the reaction
may be expected to conform to an adiabatic model though it
is estimated that certain near collinear collisions
could lead with significant probability to electronic
transitions, though these could only manifest themselves
in excited product states in the case of highly energetic
collisions between the reactant species.

This work constitutes the necessary first step towards
a calculation of the detailed dynamics of the reaction
$K+NaCl \rightleftharpoons KCl+Na$, and the results provide material to
which various approaches for tackling the problem of the
nuclear motions could be applied.   The reason for the
choice of this particular system as a suitable one for which
to produce information for such a project is worthy of
mention.   The full detail available from the results
of such calculations involves unaveraged information for
collisions at particular relative velocities, internal

energies and impact parameters. The only experimental
method capable of providing a comparable range of
detail is the observation of reactions using crossed
molecular beams. This technique, as applied to neutral
reactive species, is still in its infancy, though it is
at present enjoying a very rapid expansion.[9] One of
the principal problems involved is detection of the very
small flux of molecules scattered in a given direction.
Alkali metal atoms, and some of their compounds, have
been capable of observation at fluxes corresponding to the
deposition of a monolayer a month[10] by means of the
surface ionisation detector[11] which produces on impact
alkali ions which can subsequently be counted by measuring
the current they carry. For this reason most of the
reactions studied to date experimentally have involved
alkali metal atoms, and such reactions thus provide the
most useful testing ground for theoretical treatments of
the reactive scattering process, though it might be argued
that as a class they are not quite typical of the
chemically more interesting simple reactions. Within this
range the present choice allows the formulation of a relatively
simple model which seems to contain the seeds of a fairly
reliable treatment. This model is equally applicable

to any similar reaction involving other alkali metals or
halogens. The example chosen might be expected to be a
fairly typical member of this series.

Part II sets out a rather less extensive calculation
on the molecule ReF_6. In an octahedral configuration, the
ground electronic state of this molecule is expected to
be degenerate. According to the theorem of Jahn and
Teller [12,13], therefore, the octahedral geometry must
be unstable with respect to certain asymmetric modes of
displacement in which the degeneracy is relieved. If
the distortion of the equilibrium arrangement from the
octahedral geometry is small, then in the ordinary vibrations
of the molecule, the octahedral crossing point is frequently
traversed and the various electronic states are strongly
coupled. [14] It is assumed in ReF_6 that the instability
of the octahedral configuration arises from a purely
electrostatic interaction between the single non-bonding
rhenium 5d-electron and the fluorine atoms. On this
basis a fairly uninvolved calculation of the shapes of the
potential surfaces around the degenerate configuration
leads to the conclusion that the molecule will be subject to
a very small tetragonal distortion, corresponding to a
change in an equatorial bondlength of approximately 0.005 Å.

In addition, the observed splitting in the ω_2 band of
the Raman spectrum is successfully accounted for. The
results are on the whole insensitive to the precise details
of the model employed, and provide a satisfactory
demonstration of the applicability of Jahn-Teller theory
to this molecule.

Part I

A CALCULATION OF POTENTIAL SURFACES

FOR THE REACTION   K + NaCl = KCl + Na.

Chapter 1.   Introduction

The documentation of a set of potential surfaces
for the reaction $K + NaCl = KCl + Na$ effectively involves
the solution of a static triatomic, 47 electron problem
at some thousands of configurations, there being three
internal nuclear coordinates.   It is clear that any
hopeful calculation must make use of some simplified,
and at least partially empirical model, both on the
grounds of tractability and of accuracy.   The object of
this work is to produce the best possible estimate of
the shape of the potential surfaces for this system and
as such is not intended as a demonstration of the power
and purity of the basic quantum mechanical postulates.
The use of empirical data and the treatment of various
factors as separate fragmentary model problems are
judged, therefore, purely on grounds of the likelihood
that they might lead to greater reliability in the
eventual results.

In chapter 2 it is argued that the electronic problem
can be reduced to a consideration of the motion of a single
valence electron in the fields of the ions Na^+, K^+ and Cl^-,
where these latter entities retain their essential identity
at all configurations of interest, and behave in their

longer range electrostatic interactions as charged
polarisable spheres. The wavefunction of the single
electron is expanded in terms of valence s- and p-atomic
orbitals on the alkali centres. The solution of a set
of secular equations is thus required to determine the
eigenstates of this valence electron.

Chapter 3 presents a discussion of the solution of
these secular equations, in neglect of the contribution
to the electronic energy arising from the ion core
polarisabilities. A variety of integrals have to be
evaluated. Experimental ionisation potentials are used
to avoid all one centre and kinetic energy integrations,
but, for the remaining two and three centre integrals,
expressions are required for the various atomic orbitals
and for the interaction potentials between the electron
and the ions. The orbital forms used are chosen to
fit fairly closely the outer lobes of the relevant self
consistant field valence s-wavefunctions. An important
disadvantage incurred by the use of atomic functions,
however, is that an orbital centred on a given atom is
not fully orthogonal to the occupied orbitals of the
other ion cores, leading to a partial breach of the
Pauli exclusion principle in the final calculated
eigenfunction. This problem is discussed at length

and an adequate correction for it proves vital to the
success of the whole project.   The correction applied
is basically in the spirit of the theory of pseudopotentials,
in that the energetic effects of proper orthogonalisation
are reproduced by suitably altering the close range
interaction potential between the valence electron and the
ion cores.[15]   Simple forms are proposed for the
pseudopotential of each ion.   Finally, the methods of
integration and of solution of the secular equations are
given.

The interactions between the ion cores are discussed
in chapter 4, and at this point also the electronic
interactions involving the core polarisabilities are
introduced as a first order perturbation to the energies
of the eigenstates.   In chapter 5 calculations and results
are described for the potential curves of the diatomic
ions Na_2^+ , K_2^+ and NaK^+.   The model as developed is
extremely successful in the reproduction of experimentally
known properties and the great importance of the earlier
pseudopotential arguments is demonstrated.   The inclusion
of p-atomic orbitals is shown to be essential for the
estimation of accurate binding energies and also for the
proper description of the interactions at large separations.

The results for the calculation on the reactive

system are presented in chapter 6, and there also
their principal features are discussed, namely the absence
of any activation barrier to reaction, the appearance of
a well corresponding to the potential existence of a bound
triangular complex molecule, and the possibility of small
non adiabatic effects in near collinear collisions.
Finally two appendices deal respectively with the
calculation of electrostatic potentials for the ions
Na^+, K^+ and Cl^- from Hartree Fock electronic distributions,
and with a discussion of the situations in which the
Cizek approximation for the evaluation of multicentre
integrals[16] cannot be applied.

Chapter 2   The model

In 1951 E.S. Rittner[17] demonstrated that the
binding energies, dipole moments and vibrational
frequencies of the gaseous diatomic alkali halides
could be calculated with remarkable accuracy on the
assumption that these molecules are constituted of pure
and discrete ions.   This postulate is well supported
by calculation [18] and experimentally on crystalline
NaCl by accurate X-ray diffraction studies,[19] and by
nuclear quadrupole coupling investigations[20], where the
latter method has been used to quantify the ionic
character with a figure of 99%.   Rittner further assumed
that these ions could be treated as uniform classical
charged spheres, each polarised in the electrostatic field
of the other.   The straightforward electrostatic
interactions involving the ionic charges and the point
dipoles induced at their centres then provide the major
contribution to the stability of the molecules, being
supplemented by a weak van der Waals attraction and
opposed by a strong close range Pauli overlap repulsion
term.

Taking the alkali to halogen direction as positive
the induced dipoles D_+ and D_- are given in terms of the ion

polarisabilities P_+, P_- and the internuclear separation
R by solution of the simultaneous equations

$$D_+ = P_+ \left(\frac{1}{R^2} + \frac{2D_-}{R^3} \right) , \tag{2.1}$$

$$\text{and} \quad D_- = P_- \left(\frac{1}{R^2} + \frac{2D_+}{R^3} \right) ,$$

where atomic units are employed. The brackets express
the fields at each ion centre due to the unit charge and
the induced dipole of the other ion. Pauling [21] lists
values for the ion polarisabilities, P_+ and P_- . The
electrostatic contribution to the molecular potential
energy curve is thus

$$Q = - \frac{1}{R} - \frac{D_+ + D_-}{R^2} - \frac{2D_+ D_-}{R^3} + \frac{D_+^2}{2P_+} + \frac{D_-^2}{2P_-} , \tag{2.2}$$

where the negative terms represent the charge-charge,
charge-dipole and dipole-dipole interactions. The two
final positive contributions give the quasi-elastic
energies of formation of the induced dipoles.

Additional terms are included for the attractive van
der Waals dispersion force and also an exponential form
is chosen to take account of the close range Pauli overlap
repulsion. Thus the resulting potential curve is given by

$$V = Q + A \exp(-R/\rho) - c/R^6 , \tag{2.3}$$

where A, ρ and c are parameters.

c may be evaluated by the London formula [22]

$$c = \frac{3}{2} \frac{I_+ I_- P_+ P_-}{(I_+ + I_-)} , \tag{2.4}$$

where I_+, I_- are the ionisation potentials of the ions.
Values for A and ρ can be chosen to reproduce the
experimental bondlengths, R_o, and force constants, p, so
that

$$\left(\frac{dV}{dR}\right)_{R=R_o} = 0, \quad \text{and} \quad \left(\frac{d^2V}{dR^2}\right)_{R=R_o} = p. \qquad (2.5)$$

If this is done ρ is found to be substantially constant
throughout the alkali halides, with a value, typically
0.31 Å , some 10% less than that applicable in the
crystal phase.   Rittner thus used this averaged value
so that the second condition (2.5) had not in general to be
invoked and in fact the calculations could be used to
predict vibrational frequencies with considerable accuracy.

For the crystalline alkali halides A and ρ can be
determined experimentally within the context of the theory
of Born and Mayer.[23]   Use of these values for the gaseous
molecules, however, leads to unsuccessful predictions of
binding energies and bondlengths.   One possible reason
for this inconsistency is the inadequacy of a single
exponential expression over a wide range of internuclear
separations as has been shown by Amdur's experimental
investigations of inert gas collisions.[24]   Bonding
properties are sensitive to the repulsion term over a
relatively narrow region close to the equilibrium bondlength
and the bonds of the diatomic molecules are some 10% shorter
than corresponding crystalline values.   However, a much

more probable explanation here is the effect on these
"hard" interactions of even small dipolar distortions of
the ions, which are absent in the crystal.

With this approach, Rittner was able to calculate
binding energies within 3% of the experimental values.
A more conclusive test of the essential veracity of the
electrostatic model is its ability to reproduce dipole
moments with about 5% accuracy, these values being of
order 30% lower than would apply if the ions were unpolarised.
The polarisation interactions contribute typically 15% of the
total binding energies.

It is possible to set up a table of gaseous ionic
radii for the alkali and halide ions exactly analogous
to Pauling's crystalline set [25], though the values are
around 10% smaller.[17]   These figures can be used to
provide further support for the model.   If the ions were
treated not as uniform polarisable spheres but, more
drastically, as classical conducting spheres of definite
radius, then their polarisabilities would be equal to the
cubes of their radii.   In fact the gaseous ionic radii
of the halide ions are only 2 to 3% larger than the cube
roots of their respective Pauling polarisabilities.
Agreement for the less polarisable, and electronically

more tightly bound alkali ions is less spectacular,
but still around 20%.   If these radii were used, therefore,
together with the assumption that the ions behaved as
conducting spheres, reasonable agreement with experiment
would still be found.   The fact that this cruder method
would not fail, strongly supports the idea that the ions
can be treated electrostatically as having definite sizes,
and the fact that their actual polarisabilities are
close to the limiting value for conducting spheres also
supports the assumption that they are uniform in their
electrostatic behaviour.

In the light of the success of these calculations the
system $K + NaCl$ will be treated as an assembly of the three
ions Na^+, K^+ and Cl^- and a single valence electron.   The
interactions between the ions will be evaluated by an
extension of Rittner's method; the main difficulties arise
from the interactions between the electron and the ions.

It must be noted, however, that this treatment applies
only for configurations where the chlorine unit is close to
an alkali atom, so that it can be permanently described as
a negative ion.   Interest, in the reaction under study, is
in fact confined to such situations.

The immediate question as to the validity of this

model concerns the assumption that the close presence

of the valence electron does not seriously disturb the nature

of the ion cores.

A direct measure of the effect of an electron on a

core is given by the core relaxation energy, the energy

released by the remaining core electronic system when it

adjusts to its new ground state on ionisation of a valence

electron.   This quantity may be estimated from Hartree-Fock

self consistent field calculations [26-28] by comparing

the total calculated energy of the isolated ion with the

total energy of the atom less the one electron energy of

the valence electron.   Relevant results, in atomic units,

are collected in table 2.1.

Table 2.1

	Na	K
Total energy of atom	161.85857	599.16447
Valence electron energy	0.18199	0.14742
Core energy in atom	161.67658	599.01705
Core energy in ion	161.67676	599.01711
Relaxation energy of ion	0.00018	0.00006
Experimental ionisation potential[29]	0.18883	0.15946

The values derived for the relaxation energies are less than

0.1% of the experimental ionisation potentials, though it is
possible that the potassium value quoted may be an
underestimate as in that case the ion and atom calculations
referred to involved rather less comparable basis sets
of analytical functions than were employed in the two
sodium calculations.   It does not seem likely that there
will be any significant additional contribution from
electronic correlation to the true relaxation energies.
On the strength of these figures therefore, relaxation
effects may be neglected.

It is as well to emphasise that the only assumptions
inevitably implied up to this point are that the ions can
be treated as definite entities whose structures are never
seriously altered and which approximate to charged
polarisable spheres in their long range electrostatic
behaviour (as, for example, with one another).   The neglect
of such factors as Pauli exclusion, exchange or correlation
in the short range interactions with the valence electron is
not an automatic result of this subdivision.

The quantum mechanical problem is therefore reduced
to that of finding the eigenstates of a single electron in
the fields of the Na^+, K^+ and Cl^- cores.   In the reactants
region of the nuclear configuration space this electron

occupies a K 4s-orbital, whereas in the products region it
fills a Na 3s-orbital.   It is thus natural to expand the
electronic eigenstate at any configuration in terms of
Na and K valence states.   In an obvious notation

$$|e\rangle = c_1 |Na, s\rangle + c_2 |Na, p_1\rangle + c_3 |Na, p_2\rangle$$
$$+ c_4 |K, s\rangle + c_5 |K, p_1\rangle + c_6 |K, p_2\rangle. \quad (2.6)$$

This summation is taken over the s- and p-states of the
lowest unoccupied shells of Na^+ and K^+, where, on each
atom, only the two valence p-orbitals, p_1 and p_2, which lie in
the plane of the three nuclei, are included; p-orbitals
perpendicular to the plane cannot interact with the lower
energy s-functions.   The inclusion of p-terms contributes
significantly to binding forces and is essential to account
for the long range interactions in which a K atom is
polarised by the dipole of an NaCl molecule, and vice versa.
(The K atom is approximately 70 times as polarisable as
a K^+ ion.[30])   The orbitals used do not of course
constitute a complete set but the inclusion of higher
Na and K valence orbitals, whilst considerably increasing
the size of the problem, would probably effect little
improvement in the final results.   Equally there should
be no necessity to improve the set by the inclusion of
orbitals centred on Cl^-, since it is doubtful if stable

unfilled orbitals even exist; Slater's rules,[31] for
instance, estimate a 4s-radial maximum at around 30 Å, and
in such circumstances the rules most certainly underestimate
the degree of screening.

The theory is developed in the following way. The
electronic hamiltonian is written in two parts:

$$\hat{\mathcal{H}}_e = \hat{\mathcal{H}}_0 + V(core),$$

$$\text{where} \quad \hat{\mathcal{H}}_0 = -\tfrac{1}{2}\nabla^2 + V(Na^+) + V(K^+) + V(Cl^-). \tag{2.7}$$

The potentials $V(Na^+)$, $V(K^+)$ and $V(Cl^-)$ represent the
spherically symmetric interactions between the electron and
the ions, including possible exchange and correlation terms.
All the interactions between the ions, and the polarisation
of the ions by the electron are retained in the term
$V(core)$, which is in itself large by virtue of containing
the charge-charge and overlap repulsion interactions
between the ions. These larger influences are independent
of the electronic coordinates and may be evaluated
separately from the computation of the electronic eigenstates,
giving a uniform additional contribution to the total
energies. The terms in $V(core)$ resulting from the effect
of the electron in inducing and interacting with ion core
dipoles are of course dependent on the electronic position
but are of a small order of magnitude.

The electronic eigenstates are found from the zero

order equation:

$$\hat{\mathcal{H}}_c \, |e^c, n\rangle = E_n^0 \, |e^c, n\rangle, \tag{2.8}$$

and the effect of V(core) is introduced as a first order

perturbation, with the corrected energy levels given by

$$E_n^{(1)} = E_n^{(0)} + \langle e^c, n | V(core) | e^c, n\rangle. \tag{2.9}$$

The advantages of this procedure will in due course be

elucidated.

Chapter 3   The zero-order eigenstates

This chapter concerns the approximate solution of
equation (2.8) when the electronic eigenfunction takes
the form of equation (2.6).   In matrix form these equations
can be rewritten:

$$H \underset{\sim}{c}_n = S \underset{\sim}{c}_n E_n^0 ,$$

(3.1)

where H and S are the 6 x 6 real symmetric hamiltonian
and overlap matrices respectively. $\underset{\sim}{c}_n$ is the vector
of coefficients in (2.6) corresponding to the nth
eigen vector with eigenvalue E_n^0.

The first step is to determine the elements of the
matrices H and S.   Ionisation potentials are known
experimentally for all of the atomic orbitals employed,[29]
and these values can be used to avoid performing one centre
and all kinetic energy integrals.   Thus, for example,

$$\langle Na, s | -\tfrac{1}{2}\nabla^2 + V(Na^+) | Na, s \rangle = I(Na, s) ,$$

(3.2a)

and $$\langle Na, s | \tfrac{1}{2}\{-\nabla^2 + V(Na^+) + V(k^+)\} | K, p_\sigma \rangle = \tfrac{1}{2}\{I(Na, s) + I(K, p)\} \langle Na, s | K, p_\sigma \rangle ,$$

(3.2b)

where I's represent the appropriate ionisation potentials.
Within the framework of a one electron problem these
relationships are exact, and the consistency between variants

of type (3.2b) can be used as a test of the expressions

chosen to represent the atomic orbitals.   Furthermore

the use of ionisation potentials automatically includes

exchange, correlation and relaxation contributions to

these integrals.   In particular the relations of type

(3.2a) ensure the inclusion of the largest of these

effects, namely those arising in one centre interactions.

   To complete the H and S matrices overlap and nuclear

attraction integrals must be evaluated.   These involve 31

two centre and 9 three centre quadratures for which forms of

the orbitals and potentials are required.   In such multicentre

integrals only the outer lobes of the atomic orbitals

contribute significantly.   Analytical expressions for six

term Na 3s- and eleven term K 4s-orbitals are available

from Hartree-Fock calculations.[28]   The outer lobes of

these were fitted by single term Slater type expressions

with exponents optimised by least squares.   This process

gives (in atomic units)

$$|Na,s\rangle \propto r^2 \exp(-0.85r),$$

$$\text{and} \quad |K,s\rangle \propto r^3 \exp(-0.736r).$$

(3.3)

Tests indicate that with these expressions the required

integrals can be reproduced to within about 2% of the

values obtained using the full Hartree-Fock functions.

Expressions for the p-functions are less readily available.   The lower potential surfaces, however, will not be comparatively as sensitive to these as to the s-expressions so that it is assumed adequate to use the same radial variation as for the respective s-orbitals, with the appropriate angular modifications.

One point worthy of mention, and whose consequences will be apparent later, is the large size of these orbitals.   The mean radii are 2.0 Å for $|Na\rangle$ and 3.5 Å for $|K\rangle$ Even when the atoms are as much as 8 Å apart, the s-orbital overlap is still in excess of 0.1.

3.1   The spherical ionic potentials

The potential expressions $V(Na^+)$, $V(K^+)$ and $V(Cl^-)$ have to be chosen to embody the two and three centre interactions of the valence electron with the unpolarised ion cores.   Table 3.1 gives a breakdown of the interactions of the Na 3s- and K 4s-electrons with their own ion cores.

Table 3.1

	$|Na,s\rangle$	$|K,s\rangle$
Electrostatic energy	~ -246 Kcal/mole	~ -210 Kcal/mole
Exchange energy	~ -7 "	~ -7 "
Correlation energy	-4 "	-6 "
Relaxation energy	$+0.1$ "	$> +0.03$ "

The electrostatic and exchange values are estimated
from the results of calculations described below; the
correlation energies have been calculated by Clementi,[32,33]
and the relaxation terms have already been discussed.   The
sum of the exchange and correlation energies amounts to less
than 5% of the corresponding electrostatic energy.   The
strong one-centre interactions quoted are all accounted for
in the present calculations by the use of ionisation
potentials, and it is only the weaker multicentre contributions
for which potential expressions are required.   Since exchange
and correlation interactions are relatively short range
in character it is expected that they will form an even
smaller percentage of multicentre terms, and they are
neglected.

Calculations on a purely electrostatic model with
the potentials calculated from Hartree-Fock charge
distributions give unrealistic results, however, for a
very fundamental reason.   The valence electron cannot be
treated independently unless its molecular orbital is
orthogonal to all occupied core orbitals.   In the present
formulation the electron is assigned to a linear combination
of atomic orbitals of the form $|Na,x\rangle + |K,y\rangle$ of which
$|Na,x\rangle$ is orthogonal to $\langle Na,cores|$ but not to $|K,cores\rangle$

and vice versa for $|K,y\rangle$.   This constitutes a partial

breach of the Pauli exclusion principle; the molecular

orbitals may be of altogether an incorrect appearance

in the immediate neighbourhood of the core nuclei, where

electrostatic interactions are at their strongest.

If one considers that, for example, the one electron energy

of a K 1s-electron is 133 A.U.,[28] whereas the valence

electron energy will be of the order of 0.2 A.U., it is

apparent that even a small spurious overlap of the

valence orbital with the K 1s- core orbital is capable

of introducing a large negative discrepancy in the

computed energy.

Ideally the basis set atomic orbitals should be

orthogonalised to all the occupied orbitals belonging to

"foreign" cores.   Such a task would be prohibitive in

itself, involving the evaluation of up to ten overlap

integrals per atomic orbital at every configuration.

The orbital expressions would by this process be

considerably complicated, vastly increasing the effort

required in computing the integrals involved in the

completion of the H and S matrices.

When one considers that the orbitals are appreciably

modified only in restricted regions of space, it seems

reasonable to attempt to bypass this effort.   Even if

computational labour were no obstacle one would have to

recognise in a complete treatment that small but troubling

effects are introduced such as the removal of orthogonality

between different atomic orbitals based on the same centre,

and also in the last resort it is incorrect to associate

atomic ionisation potentials with appreciably modified

orbitals.

One method which was considered, in an attempt

to find a tractable solution to this problem, was to

represent each ion core by a single function of 1s-,

but suitably expanded, form and to **orthogonalise foreign**

valence orbitals to these.   This, however, gives no

guarantee of improving orthogonalisation to individual core

orbitals and in practice was found to worsen the situation.

The effect of proper orthogonalisation is to introduce

radial nodes into a function within a foreign core.

Locally the function is forced to behave in the manner of

a valence shell orbital of that core.   Thus, in addition

to the potential energy stabilisation obtainable by an

electron penetrating close to a nucleus, there is also an

increased kinetic energy contribution within the same

region, arising from the augmented curvature of the

wavefunction.

The object of the following discussion is to determine suitable potential functions so that the energetic effects of orthogonalisation may be approximated using the unmodified atomic orbitals.   Consider the interaction between an electron in a valence orbital of atom A and the core of another atom B.   Let ψ_A represent the unmodified atomic orbital of A and ψ_A' the wavefunction which results when orthogonalisation to the occupied orbitals on core B is carried out.   Further let χ_B be the lowest lying unoccupied valence orbital of B.

Far from B the A orbital is unaffected by orthogonalisation so that

$$\psi_A' = \psi_A \qquad\qquad (3.4)$$

Deep inside the B core, on the other hand, the orthogonalised A orbital will vary as the B valence function, and thus

$$\psi_A' = \lambda \chi_B \qquad\qquad (3.5)$$

where λ is a small numerical constant, which allows for the fact that relatively little of the electronic charge in orbital ψ_A' is distributed around the foreign core B.   In between these two extremes of behaviour there will be, in

reality, a region of transition.   For the purposes of
this current investigation, however, it will be assumed
that the transition between (3.4) and (3.5) is a sharp one.
B is assigned a "core radius", σ , outside of which the A
orbital is assumed to be unaltered, but within which the
core influence is sufficient to cause total modification
to the form (3.5).   This assumption is essentially that
the core is hard edged.   For the ions Na^+, K^+ and Cl^-
the natural choice for σ is the gaseous ionic radius, although
it is found that results are not crucially sensitive to the
value chosen.

Within this radius a modified potential V_B' is defined
so that

$$\left(\psi_A \,\middle|\, V_B' \,\middle|\, \psi_A \right) = \left(\psi_A' \,\middle|\, -\tfrac{1}{2} \nabla^2 + V_B \,\middle|\, \psi_A' \right), \tag{3.6}$$

where rounded brackets are used in this context to signify
that integration is restricted to the volume of the core B,
pointed brackets being reserved for integrals over all space.
The right hand side of (3.6) gives the sum of the local
potential and kinetic energy contributions to the interaction
when the A orbital has been properly orthogonalised, V_B
representing, to a close approximation, the electrostatic
potential of core B.   On the left hand side V_B' has to be
chosen in such a manner that its interaction with the

unmodified function Ψ_A preserves the equality. (3.5) and (3.6) taken together give

$$\left(\Psi_A \mid V_B' \mid \Psi_A \right) = \lambda^2 \left(\chi_B \mid V_B^{eff} \mid \chi_B \right) , \tag{3.7}$$

where V_B^{eff} is an effective point charge potential defined so that

$$\left(\chi_B \mid V_B^{eff} \mid \chi_B \right) = \left(\chi_B \mid -\tfrac{1}{2} \nabla^2 + V_B \mid \chi_B \right). \tag{3.8}$$

The determination of a suitable expression for V_B' therefore involves an evaluation of the integral $\left(\chi_B \mid V_B^{eff} \mid \chi_B \right)$ and of the constant λ. Before completing such calculations expressions must be set out for the electrostatic potential V_B and for the valence orbital χ_B.

For the ions Na^+, K^+ and Cl^- electrostatic potentials may be obtained by applying Poisson's equation to numerical Hartree-Fock electronic charge distributions[34-36] and then fitting the results to a suitable analytical expression by a least squares process.[37-38] These calculations, which are described in appendix A, result in the following expressions (in atomic units):

$$V_{Na^+} = \{-1-13.902 \exp(-3.4244r) + 3.902 \exp(-18.836r)\} \ /r$$
$$+62.646 \exp(-10.733r),$$

$$V_{K^+} = \{-1-31.637 \exp(-2.5689r) + 13.637 \exp(-29.040r)\} \ /r$$
$$+128.54 \exp(-5.6428r) + 261.27 \exp(-19.210r),$$

$$V_{Cl^-} = \{1-20.589 \exp(-1.6308r) + 2.589 \exp(-40.683r)\} \ /r$$
$$+47.688 \exp(-4.0146r) + 89.361 \exp(-21.097r). \tag{3.9}$$

<center>Table 3.2^(a)</center>

Table 3.2$^{(a)}$

		Na^+	K^+	Cl^-
1.	$\sigma^{(b)}$	1.70	2.23	3.00
2.	$\langle \chi_B | V_B | \chi_B \rangle$	-0.3909	-0.3320	(0.2171)
3.	$\langle \chi_B | V_{SCF} | \chi_B \rangle^{(c)}$	-0.4019	-0.3427	-
4.	$\langle \chi_B | -\tfrac{1}{2}\nabla^2 | \chi_B \rangle$	0.2266	0.2032	(0.2709)
5.	$(\chi_B | V_B | \chi_B)$	-0.1316	-0.1249	-0.1454
6.	$(\chi_B | -\tfrac{1}{2}\nabla^2 | \chi_B)$	0.1377	0.1299	0.1734
7.	$(\chi_B | 1/r | \chi_B)$	0.0311	0.0205	0.0368
8.	$\langle \chi_B | V_B | \chi_B \rangle - (\chi_B | V_B | \chi_B)$	-0.2593	-0.2072	(0.3625)
9.	$\{ \langle \psi_B | q/r | \psi_B \rangle - (\psi_B | q/r | \psi_B) \}^{(d)}$	-0.2637	-0.2127	(0.3775)

(a) Atomic units are used throughout. Curved brackets,( ), refer to integrals restricted to the core volume and pointed brackets, $\langle\rangle$, to integrals over all space.

(b) σ = core radius.

(c) $\langle \chi_B | V_{SCF} | \chi_B \rangle$ = self consistent field one electron energy less kinetic energy.

(d) $\{ \langle \psi_B | q/r | \psi_B \rangle - (\psi_B | q/r | \psi_B) \}$ = potential energy contribution from outside the core, calculated on a point charge model and including only the outer lobe of χ_B .

In the first instance it is convenient to treat together
the two alkali ions Na^+ and K^+.   The valence s-functions
used are those derived from minimal basis set Hartree-
Fock calculations.[28]

$$\chi_{Na} = 0.697461 \exp(-10.6259r) - 0.928038r \exp(-3.28570r)$$
$$+ 0.06400048r^2 \exp(-0.83576r) \qquad\qquad (3.10)$$

$$\chi_K = -0.7903487 \exp(-18.48950r) + 2.3164226r \exp(-6.50312r)$$
$$- 0.8851556r^2 \exp(-2.89329r) + 0.01749141r^3 \exp(-0.87375r).$$

Table 3.2 presents an analysis of the contributions to
various atomic integrals; the results involving Na and K
are contained in columns 2 and 3.   Comparison of the
second and third rows shows that the total potential energy
calculated for the valence electron using the electrostatic
potentials (3.9) comes within 3% of the difference between
the published self consistent field one electron energy
and the kinetic energy.   This close agreement illustrates
the relative smallness of the exchange contribution to the
self consistent field energy. (The estimates of exchange
energies given in table 2.1 were obtained from these
figures.)

From rows 5 and 6 it may be seen that within the
core radii are concentrated approximately two thirds of
the total kinetic energy and one third of the total
potential energy and that these contributions cancel to

within about 4%.   This cancellation would be even more
complete and possibly slightly reversed in sign if a
suitable proportion of the exchange energies were
included.   Row 7 gives the contribution from within
the core which would result if V_8^{eff} $(\sim -\frac{1}{2}\nabla^2 + V_8)$ were taken
as $1/r$.   The conclusion drawn is that for both Na^+ and K^+
within the ion core,

$$V_{M+}^{eff} = 0 \pm \frac{0.2}{r}. \qquad (3.11)$$

The maximum uncertainty incurred by use of $V_{M+}^{eff} = 0$ within
the cores in the atomic integrals of table 3.2 is of the
order of 4 Kcal/mole.   For the multicentre integrals
with which this discussion is ultimately concerned, however,
λ^2 of (3.5) is small (of order 0.1 to 0.01) so that the
possible error incurred within the core is reduced to
an acceptable level.

Comparison of rows 8 and 9 shows that the remaining
contribution to the potential energy from outside the core
can be accounted for to within 2% by computing only the
interaction between the net ionic point charge and the
outermost lobe of the valence orbital.

The final conclusion, therefore, is that for an
alkali ion a suitable expression, V_{M+}', for the modified
potential to be used to interact with a foreign atomic

orbital is

$$V'_{M+}(r) = \begin{cases} 0 & r < \sigma \\ -1/r & r > \sigma \end{cases} \tag{3.12}$$

there being no requirement in this case to find λ. This
form is very considerably different from the electrostatic
potential, which near a K nucleus approaches $-19/r$.
Calculations with other choices of core radius suggest that
the ionic radius is a reasonable choice for this parameter,
though the conclusions reached are not crucially altered
by a deviation of up to 20% in σ. Whereas this implies
that the potential form (3.12) derived by the above
arguments is not critically sensitive to σ, it does not
provide evidence for the wisest choice of radius to
represent the discontinuity from unperturbed to totally
modified behaviour of a foreign atomic orbital.

The choice of a modified potential V'_{cc} for the Cl^-
ion is more difficult. As suggested above it is extremely
unlikely that a stable valence orbital even exists.
Certainly no expression has been published. The ion is,
however, isoelectronic with K^+, and, acknowledging that
an orthogonalised foreign orbital will be approximately
of 4s- disposition within the core the form χ_{cc} is taken
as a suitably expanded version of the K 4s-function (3.10);

the scaling factor, which allows for the difference in
size between the two ions, is taken as the ratio of the
gaseous ionic radii.   Thus, within the Cl⁻ core, a foreign
orbital Ψ_A after orthogonalisation takes the form

$$\Psi_A' = \lambda \chi_{ce}, \text{ where } \chi_{ce}(r) = \chi_\kappa(0\cdot75r). \tag{3.13}$$

The final column of table 3.2 lists the Cl⁻ one
centre integrals calculated using this unnormalised form
for χ_α, together with the Cl⁻ electrostatic potential (3.9).
In this case within the core the kinetic energy contribution
overwhelms the attractive potential energy to an extent
equivalent to a net repulsive potential,

$$V_{ce^-}^{eff} \sim + \frac{0\cdot75}{r}, \tag{3.14}$$

where this form is not very sensitive to the choice of
core radius.   Since $V_{ce^-}^{eff}$ does not vanish, a value for λ
must be estimated in this case.

If the final, modified potential, V_{ce^-}' is sought in the
form

$$V_{ce^-}' = \beta/r, \tag{3.15}$$

then equation (3.7) shows that

$$\beta = \frac{\lambda^2 (\chi_{ce}|V_{ce^-}^{eff}|\chi_{ce})}{(\Psi_A|1/r_{ce}|\Psi_A)}. \tag{3.16}$$

The two centre restricted integral on the denominator of

(3.16) is evaluated by using an approximate expression
for the unperturbed atomic orbital ψ_A within the Cl⁻ core.
If ψ_A is a Slater-type orbital it may be written

$$\psi_A = N\, r_A^p \exp(-\alpha r_A) \; , \tag{3.17}$$

where any angular part (centred on A) is assumed to be
invariant over the volume of the Cl⁻ core, and is included,
together with the normalisation factor, in N.   To further
facilitate the integration, which is over a small region
where ψ_A changes slowly, only the linear variation of ψ_A
parallel to the bond axis is included, and to this approx-
imation,

$$\psi_A = \gamma\left(1 - \delta r \cos\theta\right) \tag{3.18}$$

where $\gamma = N R^p \exp(-\alpha R)$ and $\delta = \left(\frac{p}{R} - \alpha\right)$.

In (3.18) ψ_A has been expressed in polar coordinates centred
on the Cl⁻ nucleus, with the A-Cl bond as principal axis. γ
is the magnitude of ψ_A and δ is its gradient, both
evaluated at the Cl nucleus.   These approximations are
adequate for all but the shortest bondlengths, R.   Thus

$$\left(\psi_A \,\middle|\, 1/r_{ce} \,\middle|\, \psi_A\right) = 2\pi\,\sigma^2\gamma^2\left(1 + \frac{\delta^2\sigma^2}{6}\right). \tag{3.19}$$

If the further postulate is made that λ is equal to the
mean ratio of ψ_A to χ_{ce} on the core boundary (so that ψ_A' is as

closely as possible continuous) then, taking σ = 3.0 A.U.,

$$\lambda \sim \frac{\gamma}{0.020} ,$$ (3.20)

so that, substituting in (3.16)

$$\beta \sim \frac{5}{4 + 6\delta^2} .$$ (3.21)

For Na and K atomic orbitals, giving R physically reasonable
values for appreciable core effects (2-5 Å), δ lies in the
range 0.0 to -0.5, and hence a suitable modified potential
within the core is

$$V'_{c\ell^-} = + 1/r .$$ (3.22)

Whilst this expression is not completely reliable it
should certainly be of the correct order.   Outside the
ionic radius only the point charge repulsion is significant
so that (3.22) provides an extremely convenient and simple
representation for the Cl^- potential throughout space, and
again diverges markedly from the electrostatic potential
which in the immediate vicinity of the nucleus behaves as
$-17/r$.

The above derivation of the expression (3.22) for $V'_{c\ell^-}$
can be supported in order of magnitude by another consideration
based on the acceptance of the zero net potential within
alkali ion cores.   Close to a K^+ nucleus an orthogonalised

valence wavefunction gives rise on average to no net
energy contribution from any particular small region of
space.   If two protons are removed from the nucleus to
yield a Cl⁻ isotope the valence energy must rise.   An upper
bound to the new net repulsive potential is provided by + 2/r
arising from the removal of the nucleons. On relaxation,
however, the energy is reduced in two ways;   the potential
energy falls because the nucleus is less screened by the
expanded core electron distribution, and there is a decrease
in kinetic energy as a result of a smoothing of the
oscillations of the valence orbital.   These arguments are
consistent with (3.22).

The discussion presented above is essentially in the
spirit of the theory of pseudopotentials in which also
the energetic effects of orthogonalisation to core functions
are reproduced by the inclusion of an extra repulsive
potential in the close range hamiltonian.   It can be shown[15]
that, if this potential is suitably chosen, the modified
hamiltonian has rigorously the same eigenvalues as the
original genuine hamiltonian, but its eigenfunctions, whilst
closely approximating those of the true hamiltonian outwith
the core, are smoothed in the interior, and the constraint
of orthogonalisation is removed.   A complete treatment in

this problem would be prohibitive since the precise

pseudopotential naturally depends on the forms of all

of the core orbitals and also on the particular foreign

orbital and bondlength to which it is applied.   In

practice the advantage of this approach seems to lie not

in eliminating the labour required to satisfy the Pauli

principle but in simplifying the forms of the valence

eigenfunctions so that they may be more closely

approximated by means of a relatively small basis set.

The fixed potentials derived above are thus approximations

to pseudopotentials.

In this approach the pseudohamiltonian, which should

have the same valence eigenvalues as the real hamiltonian (2.7)

and essentially similar eigenfunctions outside of the cores,

becomes

$$\hat{\mathcal{H}}_o = V'_{Na^+} + V'_{K^+} + V'_{Cl^-} + \begin{cases} -\tfrac{1}{2}\nabla^2 & \text{outside alkali cores} \\ 0 & \text{inside alkali cores.} \end{cases} \qquad (3.23)$$

The corresponding pseudohamiltonian for an alkali ion is

$$\hat{\mathcal{H}}_{M^+} = \begin{cases} -\tfrac{1}{2}\nabla^2 - 1/r & r > \sigma \\ 0 & r < \sigma \end{cases} \qquad (3.24)$$

The valence atomic orbitals of $\hat{\mathcal{H}}_{M^+}$ are not oscillatory

functions and should be fairly closely represented by the

single term smooth fits to the outer lobes of the true
alkali orbitals.   In table 3.3 it is demonstrated that
the simple atomic expressions (3.3) taken with the
hamiltonian (3.24) do in fact lead to encouragingly
accurate estimates of the valence orbital ionisation
potentials.

Table 3.3

	$\lvert$Na,s$\rangle$	$\lvert$Na,p$\rangle$	$\lvert$K,s$\rangle$	$\lvert$K,p$\rangle$
I.P. calc. (A.U.)	-0.1849	-0.1046	-0.1388	-0.1021
I.P. expt.[29] (A.U.)	-0.1888	-0.1115	-0.1595	-0.1002

A very high level of accuracy is desirable in these
large one centre terms, however, and the experimental
values are retained in the evaluation of the integrals (3.2).
Thus the matrix H is constructed from the matrix elements
of V'_{Na^+} , V'_{K^+} and $V'_{C\ell^-}$ and from overlap integrals.

3.2   Calculation of integrals

Equipped with expressions for the potentials and
orbitals it is possible to proceed with the necessary
integrations.   All of the two centre integrals can be

treated analytically in terms of confocal ellipsoidal
coordinates as series of products of the well known
A and B functions:[39]

$$A_n(a) = \int_1^\infty \mu^n e^{-a\mu} d\mu,$$ (3.25)

$$\text{and } B_m(b) = \int_{-1}^1 \nu^m e^{-b\nu} d\nu.$$

Some care is required in the calculation of the A_n and B_m.
In most configurations the recursion formulae

$$A_n(a) = \frac{1}{a} \left\{ e^{-a} + n A_{n-1}(a) \right\}$$ (3.26)

$$\text{and } B_m(b) = \frac{1}{b} \left\{ (-1)^m e^b - e^{-b} + m B_{m-1}(b) \right\}$$

give accurate values, but for b<1 cancellations in (3.26)
leads to a rapid loss of significant figures and the B_m
are best calculated from the series:[40]

$$B_m(b) = \sum_{n=0}^\infty \frac{\{(-1)^m + (-1)^n\}}{(m+n+1)n!} b^n$$ (3.27)

Another complication, which is less well known, arises
for nuclear attraction integrals, I, at large values of
the internuclear separation, R.

$$I = \int \psi_A^*(r_A) \frac{1}{r_B} \psi_A(r_A) d\tau.$$ (3.28)

If $\psi_A = N r_A^p e^{-\alpha r_A}$ this integral in elliptical coordinates
reduces to an expression of the general form

$$I \propto R^{2+2p} \left\{ \sum_{r,s} c_{rs} A_r(\alpha R) B_s(\alpha R) \right\},$$ (3.29)

where the c_{rs} are the appropriate expansion coefficients.
Now for large R, according to (3.26),

$$A_r(\alpha R) \sim \frac{1}{\alpha R} e^{-\alpha R},$$
$$B_s(\alpha R) \sim \frac{(-1)^s}{\alpha R} e^{\alpha R}. \tag{3.30}$$

so that each term in the bracket of (3.29) is of order R^{-2}.
The integral, however, must tend to R^{-1} and so the bracketed
sum is of order R^{2p+1} times smaller than its individual
terms.   Direct summation in equation (3.29) for large p
or R may therefore lead to drastic rounding errors.   In
these situations the integral (3.28) is best calculated
by making the substitution:

$$\frac{1}{r_B} = \begin{cases} \frac{1}{R} \sum_{n=0}^{\infty} \left(\frac{r_A}{R}\right)^n P_n(\cos\theta_A) & r < R, \\ \frac{1}{r_A} \sum_{n=0}^{\infty} \left(\frac{R}{r_A}\right)^n P_n(\cos\theta_A) & r > R. \end{cases} \tag{3.31}$$

In the present work, performed on a computer carrying 11
significant figures, this effect becomes important only
at such large R ($\sim$15$\overset{o}{A}$) that sufficient accuracy is
obtained retaining only the first term in the expansion (3.31)

The calculation of integrals involving the
discontinuous alkali ion potentials (3.12) is performed by
first assuming that the expression

$$V'(r) = -1/r \tag{3.32}$$

applies throughout space.   The contribution which accrues

to this integral from within the alkali core is then
subtracted.   This latter bounded integral is
evaluated by approximating the foreign orbital expression in
the core as linear and axially symmetric, in the manner
proposed in equation (3.18).   Errors incurred by this
technique are insignificantly small, except possibly at
uninterestingly close internuclear separations, and are
expected to be at least an order of magnitude smaller
than the error arising from the uncertainty in the close
range part of $V'(r)$.

The computation of the nine three centre integrals
of form $\langle Na | V'_{ce^-} | K \rangle$ is more difficult.   Comparison with
numerical quadrature shows that Mulliken's approximation,[41]

$$\langle Na | V'_{ce^-} | K \rangle = \frac{1}{2} \left\{ \langle Na | V'_{ce^-} | Na \rangle + \langle K | V'_{ce^-} | K \rangle \right\} \langle Na | K \rangle, \quad (3.33)$$

can provide typically 10% accuracy for s-functions but
otherwise may not even give the correct sign, and as such
is totally inadequate.   An elaborate method for
approximating multicentre integrals in terms of two centre
forms was proposed by Cizek and shown to work excellently
in some simple examples.[16]   The model through which
this method is applied, however, cannot in practice always
be set up, and in this problem it was found that breakdowns

were frequent. This point is discussed in appendix B.

The three centre integrals are therefore evaluated numerically using confocal ellipsoidal coordinates based on the alkali ion centres. Gaussian quadrature is employed[42] and use of two separate 8x8x8 grids over the ranges $1 \leq \mu \leq 2.5$ and $2.5 \leq \mu \leq 12$ is sufficient to guarantee 1% accuracy $(\mu = \{r_{Na} + r_{K}\} / R_{NaK})$. This constitutes the most time consuming part of the whole calculation.

Once all integrals are evaluated, the H and S matrices can be set up and the eigenvalue equation (3.1) obtained.

3.3.   Solution of the eigenstate problem

Equations (3.1) can be combined to give an equation for all six eigenvectors simultaneously,

$$HC = SCE \tag{3.34}$$

where C is the matrix whose columns are the eigenvectors $c_1, c_2, \ldots, c_6$ and E is the diagonal matrix of eigenvalues. This equation is solved under the constraint that the set of eigenvector solutions are orthonormal, so that

$$C^{\dagger} S C = 1 \tag{3.35}$$

where 1 is the unit matrix.   The first step in the

solution is to find the real orthogonal matrix U which
diagonalises S, which is positive definite. Taking

$$\widetilde{u} S u = \lambda \tag{3.36}$$

then $S^{-\frac{1}{2}}$ can be uniquely chosen as

$$S^{-\frac{1}{2}} = u \, \lambda^{-\frac{1}{2}} \widetilde{u}, \tag{3.37}$$

where the elements of the diagonal matrix $\lambda^{-\frac{1}{2}}$ are the
inverse positive square roots of the elements of λ.
Multiplying by $S^{-\frac{1}{2}}$, equation (3.34) may be rewritten

$$S^{-\frac{1}{2}} H S^{-\frac{1}{2}} (S^{\frac{1}{2}} c) = (S^{\frac{1}{2}} c) E, \tag{3.38}$$

where $S^{\frac{1}{2}}$ is uniquely defined as the inverse of $S^{-\frac{1}{2}}$.
Putting $X = S^{\frac{1}{2}} c$ and $H' = S^{-\frac{1}{2}} H S^{-\frac{1}{2}}$, (3.38) becomes

$$X^{-1} H X = E. \tag{3.39}$$

$S^{-\frac{1}{2}}$ is real symmetric and therefore so is H'.   The
matrix X is then orthogonal, as it must be according to
(3.35), and can be determined, along with E, by a second
diagonalisation.   The matrix of eigenvectors is finally
obtained as

$$C = S^{-\frac{1}{2}} X. \tag{3.40}$$

This method requires the diagonalisation of two real
symmetric matrices.   This can conveniently be achieved

by the Jacobi method,[43] involving successive elementary orthogonal transformations chosen to nullify each off-diagonal element in turn, and iterating over the matrix until all remaining off-diagonal elements are smaller than a specified allowable threshold (taken as 10^{-7} A.U. in the present work).

Chapter 4   The core polarisation interactions.

The final stage in the calculation is to
determine the energy of interaction between the ion
cores and to compute to first order the electronic
interactions involving core polarisation.   The
largest contributions to the energy are the charge-
charge terms and the short range exponential repulsions
between the ions;   the influence of the induced
dipoles and of the van der Waals dispersion forces are
relatively weak.   The full, non-perturbation, treatment
would be to solve analytically the polarisation problem
for arbitrary electronic position.   The total
hamiltonian thus derivable would be exceedingly complex
and the evaluation of its matrix elements would involve
a large number of arduous integrations.   The extra
labour thus introduced into the problem would be totally
disproportionate to the smallness of the contribution of
the electron to the polarisation terms.   A perturbation
treatment is more appropriate.

The dipoles induced on the cores must by symmetry
lie in the plane of the three nuclei so that a total
of six dipole components must be specified.   Each of
these is the product of the appropriate ion polarisability

and the parallel component of the electrostatic field
at its centre, arising from the charges of the other
ions and of the valence electron and from the induced
dipoles at the other nuclei. Applying the full
analogue of the diatomic alkali halide treatment would
lead to six linear equations for the induced dipole
components, and these could be systematically solved.
The pairwise charge-dipole and dipole-dipole interactions
between the centres could then be accounted for, together
with the quasi-elastic energies of the dipoles.

The precise determination of the field components
at the nuclei due to the valence electron, and of the
interaction between the electronic charge and the core
dipoles would involve the determination of some 70 two
and three centre integrals of the types:

$$\langle Na | \tfrac{1}{r_\kappa^2} | Na \rangle \, , \quad \langle Na | \tfrac{\cos\theta_\kappa}{r_\kappa^2} | \kappa \rangle , \tag{4.1}$$

$$\text{and} \quad \langle Na | \tfrac{1}{r_{c\acute{c}}^2} | \kappa \rangle .$$

Of these not even the two centre terms can be tackled in
closed form, unless as a convergent Maclaurin series in
integrals involving the A and B auxiliary functions.[44]
Exact evaluation would be much more laborious than the whole
remainder of the project.   Instead the following method

has been adopted.

For the purposes of illustration consider the effect
of an electron in a hybrid Na orbital:

$$|e\rangle = |Na, sp_{\underline{y}}^{\lambda}\rangle = \frac{1}{\sqrt{1+\lambda^2}}\left\{|Na, s\rangle + \lambda |Na, p_x\rangle\right\}, \qquad (4.2)$$

where λ is a hybridisation coefficient and the unit
vector $\underline{y}$ specifies the axis (in the plane) of the
p-orbital.   The electron, together with the Na^+ ion
constitutes a polarised Na atom, which, in addition to
any core dipoles, exhibits a resultant "electronic dipole",
given by

$$\underline{D}_{Na} = \frac{-2\langle r\rangle \lambda}{\sqrt{3}\,(1+\lambda^2)}\,\underline{y}, \qquad (4.3)$$

where $\langle r\rangle$ represents the mean radius of the Na valence
orbitals.   If any eigenstate solution of the zero order
equation (2.8) is rewritten in the form:

$$|e^0, n\rangle = c_{Na}|Na, sp_{\underline{y}}^{\lambda}\rangle + c_K |K, sp_{\underline{w}}^{\mu}\rangle, \qquad (4.4)$$

where c_{Na} and c_K are constants, a fraction of an electron,

$$\rho_{Na} = \frac{c_{Na}^2}{c_{Na}^2 + c_K^2}, \qquad (4.5)$$

can be formally assigned to the Na hybrid and the
remaining fraction $(1 - \rho_{Na})$ to the K hybrid.   In this
approach there is situated on Na, for example, a residual
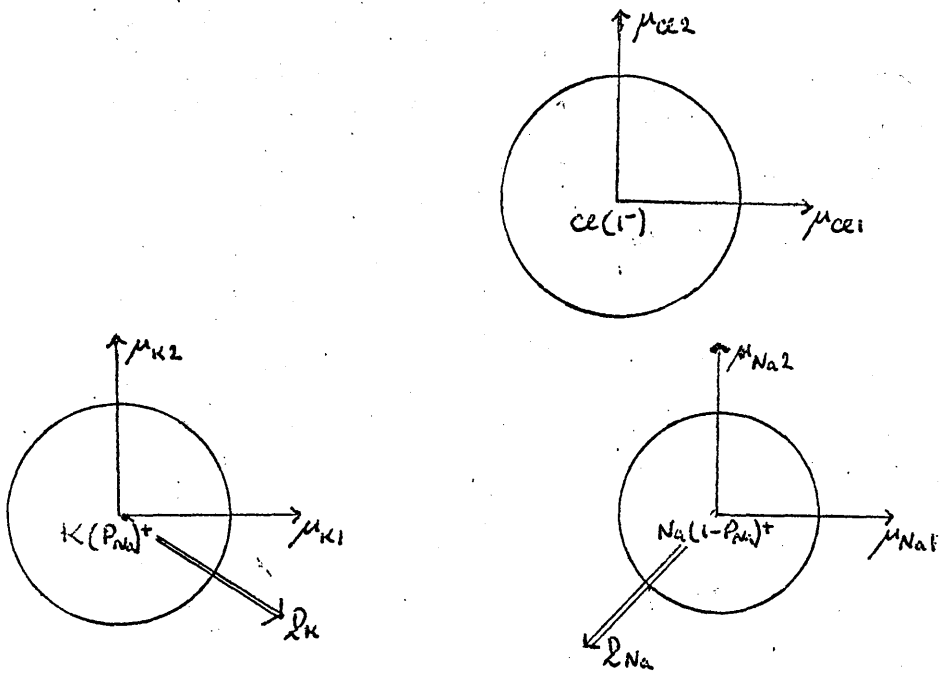
Figure 4.1: The electrostatic point charges, electronic dipoles, $\underset{\sim}{D}$, and induced core dipoles, $\underset{\sim}{\mu}$.

positive charge of $(1 - P_{Na})$ together with a partial

electronic dipole given by

$$\mathcal{D}_{Na} = \frac{-2 \langle r \rangle P_{Na} \lambda}{\sqrt{3}(1+\lambda^2)} \underset{\sim}{\nu}.$$ (4.6)

For each eigenstate, therefore, the core electrostatic

interactions can be approximated in terms of point

charges, electronic dipoles, $\underset{\sim}{\mathcal{D}}$, and core dipoles, $\underset{\sim}{\mu}$,

as illustrated in figure 4.1.

The problem is thus reduced to one of simple

electrostatics.   Since typically the electronic dipoles

are very much larger than the core dipoles, the

interactions between one core dipole and another are

neglected.   These will be of the order of the errors

in the above treatment of the electron.   In fact these

effects, of order R^{-7} and smaller, were noted to be

insignificant contribuents to the binding energies of

the alkali halides.[17]   Dipole induction is therefore

supposed to be due only to the point charges and the

electronic dipoles, giving non-coupled equations for the

core dipoles.   The polarisation contribution to the

energy of each eigenstate now simply decomposes into

charge-core dipole, electronic dipole-core dipole and

core dipole quasi-elastic terms.

It is to be noted that in this approximate treatment
it has been implicitly assumed that each foreign core
experiences the average field of the valence electron,
whereas, since the core electronic kinetic energies are
typically much higher than that of the valence electron,
the cores might be expected to respond to the instantaneous
position of the electronic charge.   The errors
introduced by this assumption should not be great, however;
the larger "own core" instantaneous polarisations are
built-in parts of the ionisation potentials.

The van der Waals terms are computed using
coefficients straightforwardly obtained with the aid of
the London formulae (2.4) and the $Na^+- Cl^-$ and $K^+- Cl^-$
exponential repulsion expressions are available from the
alkali halide calculations.[17]

No equivalent expression is available for the short
range $Na^+ - K^+$ repulsion and there is no direct method
by which it can be obtained.   Whilst the coulomb repulsion
will ensure that close $Na^+ - K^+$ separations will be
energetically unfavourable, an additional repulsion term
is necessary to overpower the inner trends of dipolar and
van der Waals forces.   The necessary parameters may be
estimated in the following way.

Some calculations have been reported, [45] on the assumption that the exponential repulsion between two ions is proportional to the square of the total overlap between their respective core orbitals:

$$A e^{-r/\rho} \propto S_{ab}^2 \tag{4.7}$$

This work leads to ρ- values for the alkali ion - halide ion repulsions in rough agreement with values derived elsewhere.   The computed results given for alkali ion - alkali ion parameters are listed in table 4.1.

Table 4.1

Ion pair	$Cs^+ - Cs^+$	$Rb^+ - Rb^+$	$K^+ - K^+$	$Li^+ - Li^+$
ρ (Å)	0.278	0.241	0.217	0.109

A typical alkali halide repulsion parameter is $\rho = 0.31$Å. These smaller values indicate steeper repulsion curves, consistent with the relative "hardness" of the more tightly bound positive ions.   For the $Na^+ - K^+$ repulsion a value of $\rho = 0.20$ Å appears to be of the correct order of magnitude.

The parameter A may be estimated by analysing the significance of the assignment to each ion of a fixed

ionic radius.   For ions of opposite sign equilibrium
between the electrostatic attraction and the closed shell
repulsion forces occurs at a bondlength equal to the sum
of their radii.   The closed shell repulsion is not directly
electrostatic in nature.   Hence, if the sign of the
electrostatic interactions between Na^+ and K^+ is reversed,
the resulting potential curve should show a minimum at a
separation equal to the sum of the sodium and potassium
gaseous ionic radii. A is chosen by insisting that this
criterion should be satisfied.

<u>Tables 4.2</u>

	Na^+	K^+	Cl^-
s-orbital ionisation potential[29]	0.18883	0.15946	
p-orbital ionisation potential[29]	0.1115	0.1002	
orbital mean radius [28]	4.75	7.05	
ion polarisability [21]	1.22	5.67	24.90
ion ionisation potential [29][46]	1.730	1.164	0.1367
gaseous ionic radius [17]	1.70	2.23	3.00

Exponential repulsion parameters[17][45]

	A	e
Na^+ - Cl^-	124.2	0.586
K^+ - Cl^-	248.4	0.586
Na^+ - K^+	966.0	0.378
Na^+ - Na^+	535.6	0.350
K^+ - K^+	1247	0.416

It is now possible to complete the entire calculation
and to arrive at the first order energy levels $E_n^{(1)}$
corresponding to the zero-order eigenfunctions $|e^\circ, n\rangle$.
Tables 4.2 contain (in atomic units) all of the empirical
data employed.

Chapter 5   The potential curves of Na_2^+, K_2^+ and NaK^+

In the course of the previous chapters a rather
elaborate edifice has been constructed within the
framework of which the proposed potential surface
calculation can be performed.   This chapter describes
the application of the basic essentials of the model in
some situations where experimental evidence is available
for the purposes of comparison.   It would otherwise be
extremely difficult to assess the reliability of the
results obtained for the system $K + NaCl$, in the absence
of any detailed experimental knowledge.

The diatomic ions Na_2^+, K_2^+ and NaK^+ are ideal for
this purpose.   They each, according to the above theory,
may be decomposed into systems involving the interactions
of a single electron and a pair of Rittner ions, and the
treatment outlined above may be very easily simplified to
deal with them.   In particular these calculations provide
a direct test of the pseudopotential expressions for
Na^+ and K^+ although they cannot measure the reliability
of the Cl^- pseudopotential.   Nonetheless a test of the
former functions does in itself provide a check on the
validity of the general reasoning involved in the evolution

of all of these potentials.

The treatment used in these calculations is precisely equivalent to the application of the model developed above in full detail to the system $M + NCl$, for configurations in which the halide ion is infinitely removed. Only the four sigma states derivable from the alkali valence orbitals are calculated. The diatomic systems lend themselves to experimentation with alternative techniques and parameters since the size of the problem is considerably eased as a result of the loss of the third centre, the smaller basis set of only four atomic orbitals, and particularly by the reduction to a single internal coordinate.

The experimental data to be compared with these calculations is all provided by studies of the neutral molecules and is listed in table 5.1.

Table 5.1

	Na_2	Na_2^+ (expt.)	Na_2^+ (calc)	K_2	K_2^+ (expt.)	K_2^+ (calc)	NaK	NaK^+ (calc.)
D_e^o (Kcal/mole)	16.8	22.9	22.8	11.8	17.5	16.5	14.3	12.5
R (Å)	3.08	~3.6	3.44	3.91	~4.7	4.86		3.91
ω (cm^{-1})		~105	132		~60	62		74
x (cm^{-1})		~-0.50	-0.55		~-0.13	-0.17		-0.32

The neutral molecule dissociation energies,[47] D_o^o, and bondlengths,[48] R, are derived direct from experimental work. The dissociation energies of Na_2^+ and K_2^+ are obtained by completing the cycle:

$$e^- + M_2 \longrightarrow M^+ + M + e^-$$
$$\downarrow I(M_2) \qquad \qquad \uparrow I(M)$$
$$M_2 \xrightarrow{\quad D(M_2) \quad} M + M \qquad \qquad (5.1)$$
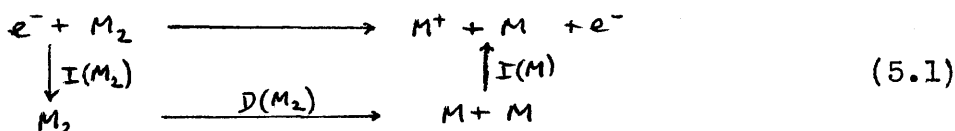
The ionisation potentials of the homonuclear neutral molecules and also the "experimental" bondlengths, vibrational frequencies, ω, and anharmonicities, x, for Na_2^+ and K_2^+ are obtained by extrapolation of the corresponding properties of series of Rydberg excited states of the neutral molecules.[49,50] (The bondlengths of Na_2^+ and K_2^+ are estimated from extrapolated rotational constants). It may be noted in passing that, although there is an increase in bondlength from Na_2 to Na_2^+ and from K_2 to K_2^+, there is also an increase in dissociation energy. This observation, which has been the subject of some discussion,[51-53] is supported by other calculations,[51,54] and the quoted dissociation energy of K_2^+ has recently been supported by photoionisation studies.[52]

The potential curves for the four lowest sigma states obtained by the present calculation are plotted in figures 5.1 - 5.3 and recorded numerically in tables 5.2 - 5.4.

Figure 5.1:

Potential curves for Na_2^+
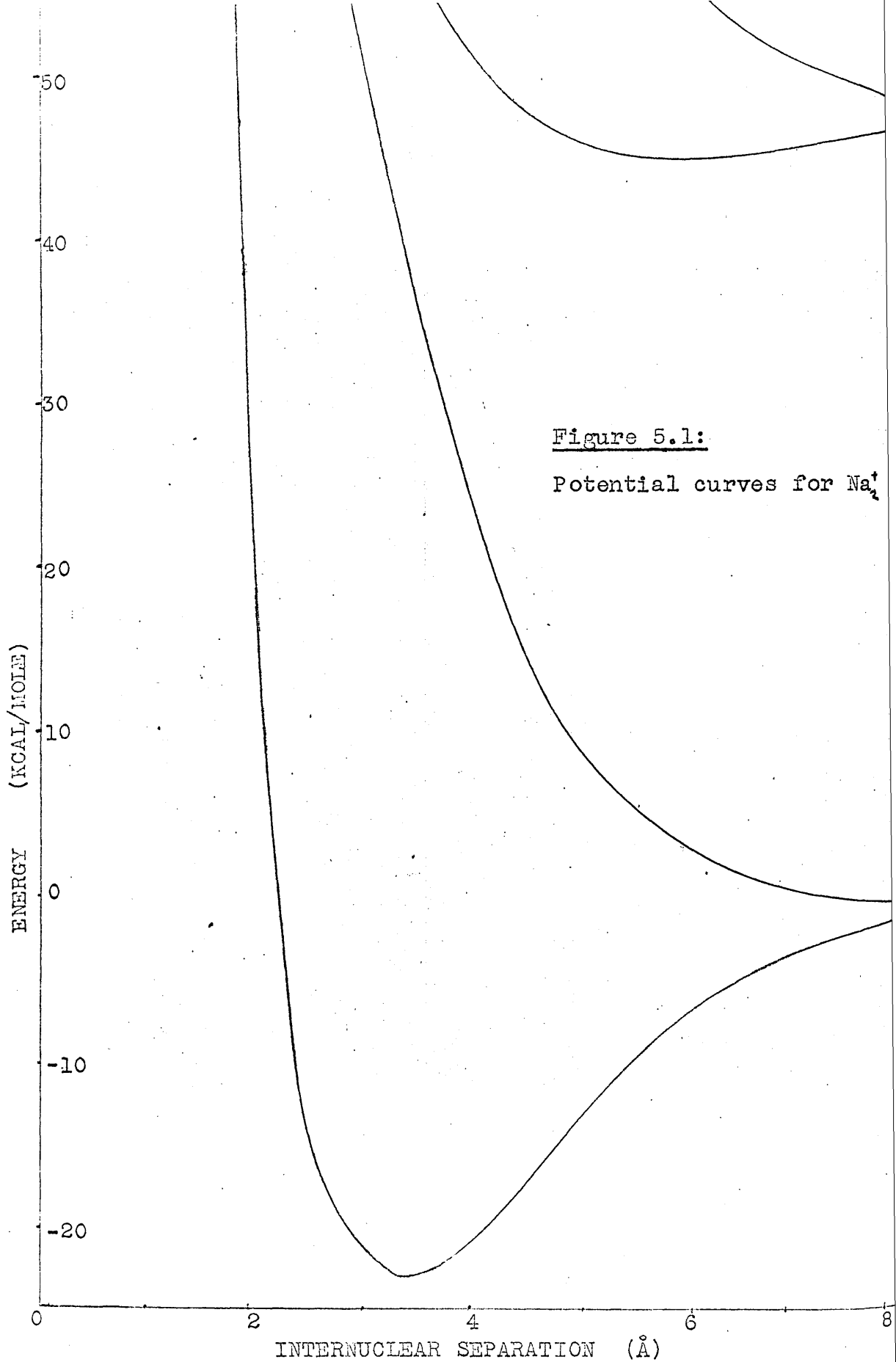
Table 5.2   Potential curves of Na_2^+

r(Å)	VI (-Kcal/mole)	V2	V3	V4
I.5	-55.I40	-I07.I33	-I60.602	-450.529
2.0	93.442	I7.263	I.I98	-232.37I
2.5	I27.675	46.599	37.9I9	- 97.775
3.0	I39.0I4	67.3I4	53.697	- 24.422
3.2	I40.600	74.400	57.756	- 7.5I2
3.4	I4I.I70	80.664	6I.032	6.268
3.5	I4I.I65	83.5I4	62.435	I2.I57
3.6	I4I.006	86.I9I	63.705	I7.439
3.8	I40.32I	9I.064	65.897	26.643
4.0	I39.274	95.346	67.697	34.I42
4.5	I35.793	I03.776	70.865	47.505
5.0	I3I.967	I09.5I7	72.602	55.76I
5.5	I28.452	II3.26I	73.3I0	60.98I
6.0	I25.558	II5.6I7	73.3I8	64.34I
7.0	I2I.790	II7.886	72.365	67.939
8.0	II9.994	II8.59I	7I.344	69.420
I0.0	II8.854	II8.703	70.4I4	70.I47
I2.0	II8.597	II8.583	70.I79	70.I5I
I5.0	II8.487	II8.487	70.065	70.064
20.0	II8.438	II8.438	69.989	69.989
∞	II8.4I5	II8.4I5	69.922	69.922

Energies refer to stability relative to the dissociation limit
$Na^+ + Na^+ + e^-$

Figure 5.2:

Potential curves for
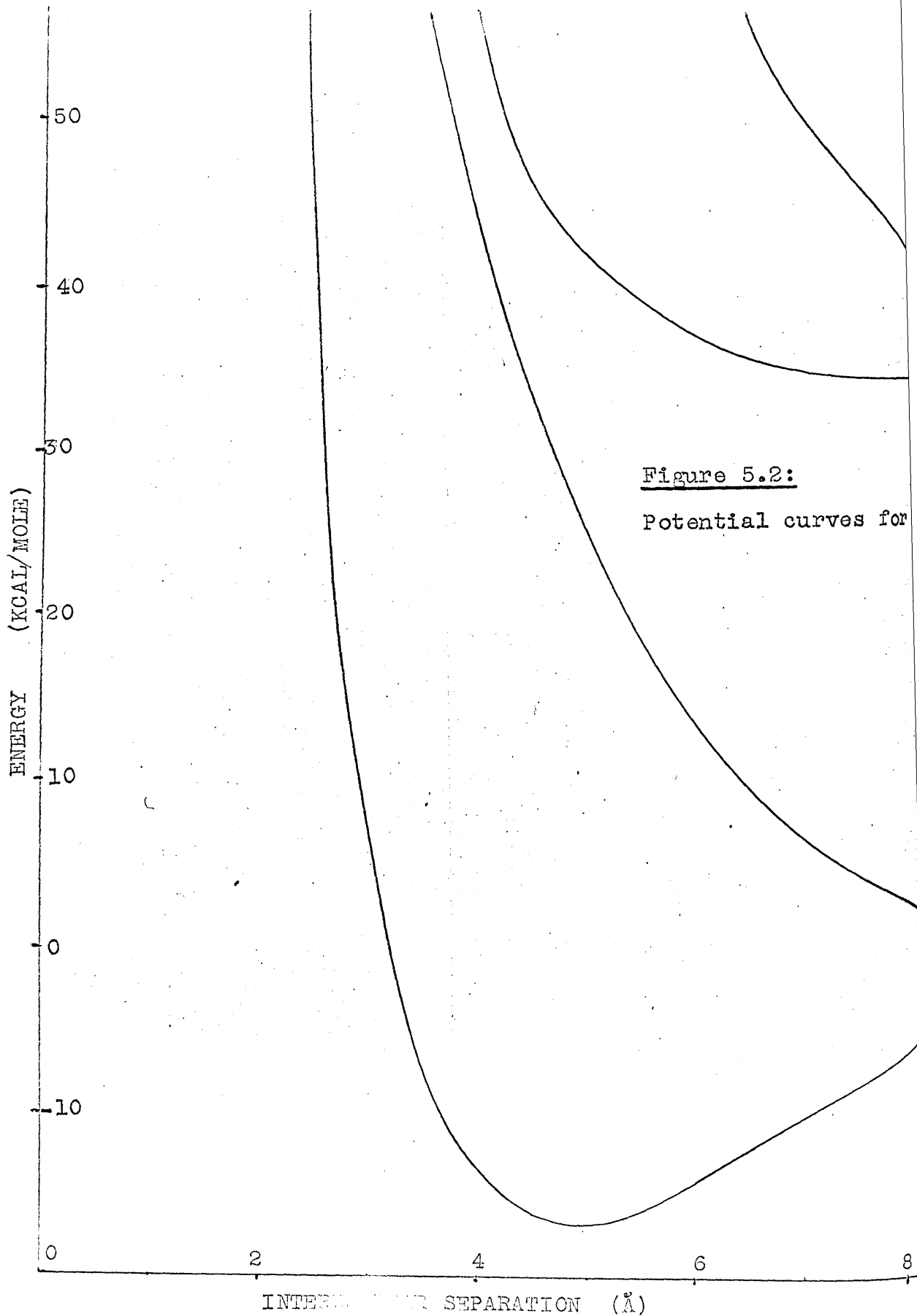
Table 5.3   Potential curves of K_2^+

r(Å)	VI(-Kcal/mole)	V2	V3	V4
2.0	-38.439	-87.129	-105.612	-136.445
2.5	65.872	9.335	- 2.491	- 31.320
3.0	93.241	33.348	25.666	9.646
3.5	106.387	45.992	39.837	29.632
4.0	113.155	58.106	48.589	16.994
4.4	115.641	66.064	53.383	8.475
4.6	116.207	69.432	55.278	9.127
4.7	116.360	71.002	56.125	10.432
4.8	116.436	72.505	56.912	12.200
4.9	116.446	73.947	57.644	14.296
5.0	116.396	75.332	58.326	16.605
5.5	115.463	81.498	61.097	28.705
6.0	113.821	86.519	63.033	38.726
7.0	109.864	93.486	65.140	51.080
8.0	106.276	97.271	65.629	57.164
10.0	102.089	99.921	64.533	61.774
12.0	100.710	100.295	63.555	62.883
15.0	100.218	100.191	63.115	63.623
20.0	100.063	100.063	62.964	62.964
∞	99.998	99.998	62.835	62.835

Energies refer to stability relative to the dissociation limit
$K^+ + K^+ + e^-$

Figure 5.3:

Potential curves for NaK$^+$
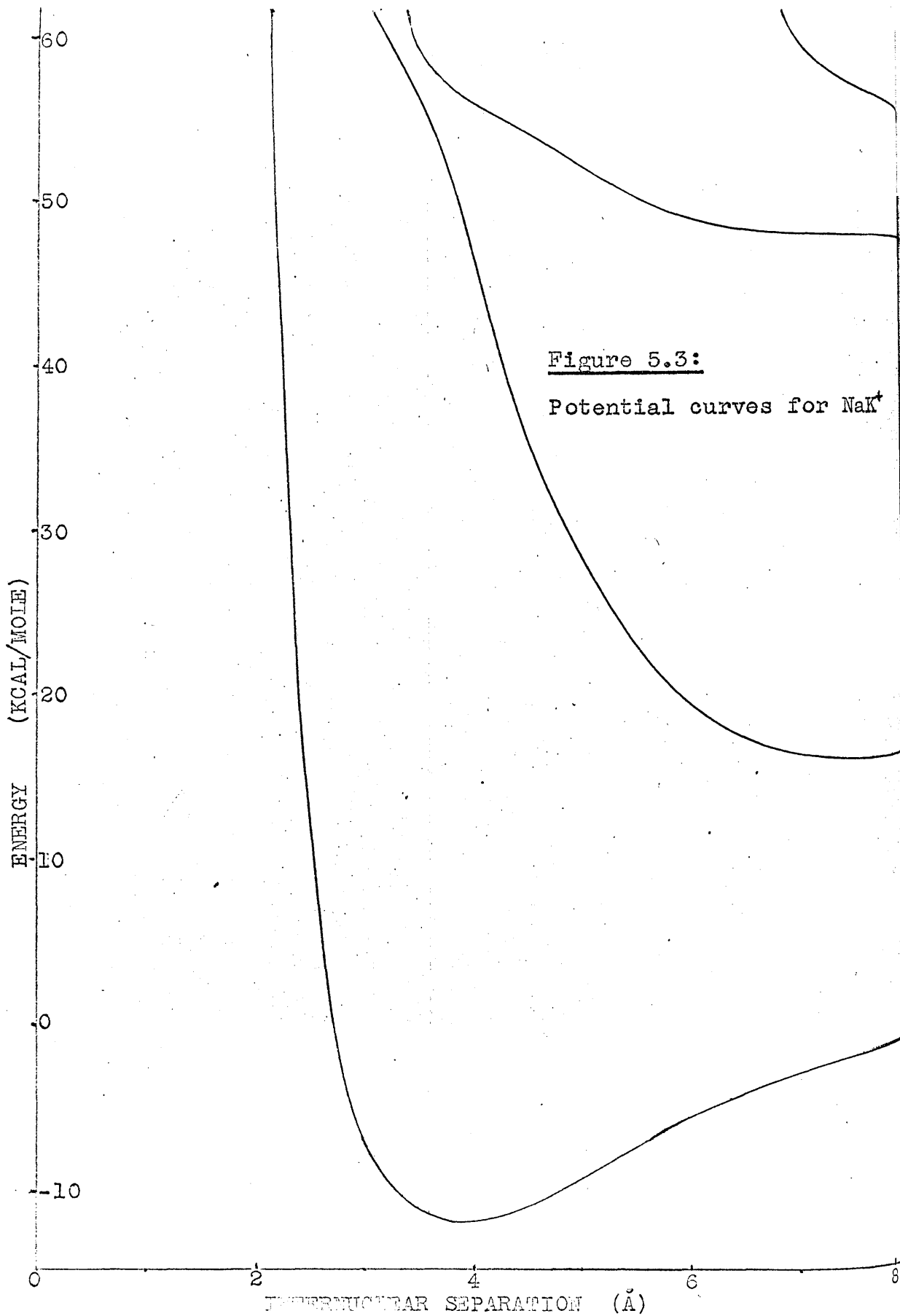
Table 5.4   Potential curves of NaK$^+$

r(Å)	VI (Kcal/mole)	V2	V3	V4
2.0	42.560	-I6.038	-50.799	-9'7.404
2.5	I04.325	32.864	2I.422	-36.275
3.0	I24.970	56.340	44.909	- 8.037
3.3	I29.I76	60.III	54.767	0.562
3.6	I30.62I	64.064	60.604	6.63I
3.8	I30.9I9	68.733	6I.394	I0.7ö4
3.9	I30.954	7I.0I4	6I.778	I3.053
4.0	I30.927	73.205	62.I92	I5.447
4.2	I30.708	77.30I	63.097	20.492
4.5	I30.020	82.752	64.535	28.I26
5.0	I28.I89	90.094	66.753	39.204
5.5	I25.977	95.4II	68.479	47.347
6.0	I23.843	98.935	69.659	52.976
7.0	I20.824	I0I.937	70.665	59.347
8.0	II9.506	I02.072	70.658	62.075
I0.0	II8.786	I0I.045	70.305	63.272
I2.0	II8.59I	I00.508	70.I66	63.230
I5.0	II8.487	I00.206	70.064	63.090
20.0	II8.438	I00.063	69.989	62.964
∞	II8.4I5	99.998	69.922	62.835

Energies refer to stability relative to the dissociation limit
Na$^+$ + K$^+$ + e$^-$

The calculated properties listed in table 5.1 are derived
from the ground state curves.   The agreement between
the experimental and calculated dissociation energies
for Na_2^+ and K_2^+ is striking.   The dissociation energy
predicted in the case of the heteroion NaK^+ suggests that it
is more conventional in its binding behaviour, being
marginally less strongly bound than the corresponding
neutral molecule.   The calculated vibrational frequencies
and anharmonicities are derived from the parameters of
Morse curves [55] fitted about the ground state minima.
In view of the uncertainties of 5 - 10% in the extrapolation
for experimental quantities, agreement is again very
satisfactory.   The correctness of the calculated bondlengths
is supported within about 4% by the values obtained from
the experimental extrapolated rotational constants.   The
expected trends in bondlength are followed among the three
calculated ionic values and the experimental figures for
neutral Na_2 and K_2, all of these distances being unusually
large by normal chemical standards.   The length of these
bonds underlines the relative insensitivity of the results to
the precise choice of M^+-N^+ exponential repulsion terms, as
these become significant only at considerably shorter range.

One final point of interest concerns the asymptotic
behaviour at large R.   At sufficiently large separations

Figure 5.4: Long range behaviour of potential curves

1. Dissociation limit $M^+ + K$

2. Dissociation limit $M^+ + Na$

KCAL/MOLE

(LOGARITHMIC SCALES)

ENERGY DEPRESSION of DISSOCIATION

INTERNUCLEAR SEPARATION (Å)
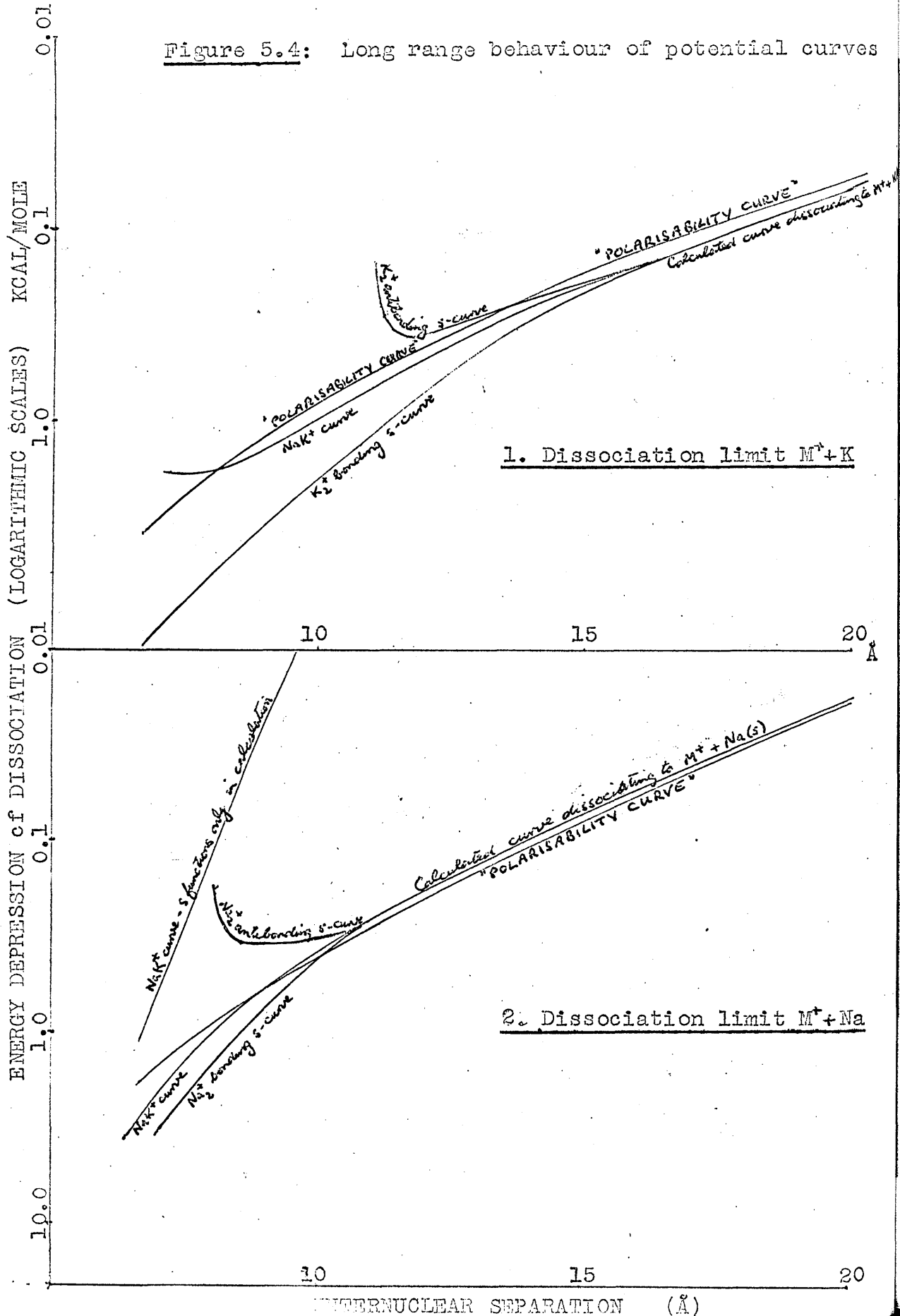
the interaction becomes principally that between an alkali ion and an alkali atom. The polarisabilities of the alkali atoms are of the order of a hundred times greater than those of their ions and values of 23$Å^3$ for Na and 44 $Å^3$ for K have been proposed for these parameters.[30] With the aid of these figures, therefore, the limiting ion - induced dipole interaction energy may be computed. Figure 5.4 demonstrates the agreement between these results and the calculated curves for the ground and first excited states of NaK^+ (corresponding to the dissociation limits Na + K^+ and K + Na^+ respectively) down to internuclear separations of around 8$Å$. In the homonuclear molecules, however, appreciable binding forces may be seen to operate at even larger separations. The correct form of asymptotic behaviour cannot be reproduced without the inclusion of p-atomic orbitals. It is important for any application to scattering experiments, that potential surfaces should be used which have the correct behaviour at large distances, because long range collisions predominate.

The success of these calculations provides encouraging evidence for the reliability of the model.

Before proceeding to outline and discuss the

results obtained for the system K + NaCl, however, it
is interesting to analyse the improvements to the
diatomic ion calculations resulting from the inclusion
first of the pseudopotentials of chapter 3.1, and
secondly of p-orbitals in the wavefunctions.

Table 5.5

Ground state minima of the diatomic ions

Calculation	NaK$^+$		Na$_2^+$		K$_2^+$	
	W(Kcal/mole)	R(Å)	W	R	W	R
Zs	34	2.18	70	1.5	150	2.2
			13	3.5	6	7.5
1s	6	4.0	16	3.3	7	7.0
1sp	74	2.4				
Hs	4	4.4	12.5	3.7	9	5.1
Hsp	14	3.8	25	3.3	17	4.5
ψsp	12.5	3.9	22.8	3.4	16.5	4.9
Experiment			22.9		17.5	

Table 5.5 lists the ground state potential curve
minima obtained in a variety of calculations. If the
electrostatic ion potentials (3.9) are employed within as
well as outside the ion cores and if the wavefunctions
contain only s-orbitals, the potential curves, labelled

INTERNUCLEAR SEPARATION (Å)

ENERGY (KCAL/MOLE)

Figure 5.5: Potential curve for NaK$^+$, from calculation Zs

INTERNUCLEAR SEPARATION (Å)

ENERGY (KCAL/MOLE)

Figure 5.6: Potential curve for Na$_2^+$, from calculation Zs

Zs, are obtained.   Figure 5.5 gives the relevant ground
state curve for NaK^+, showing unexpectedly high binding
energy and a correspondingly short bond.   (Furthermore
the curve shape in the range 3-6Å is unusual.)   The
spurious characteristics of this calculation are much more
clearly evidenced in the double minima recorded for
Na_2^+ and K_2^+ , the curve for the former of which is plotted
in figure 5.6.   There is ample evidence that these
disquieting features arise from interactions within the
ion cores.   In the first instance the ground state curves
for Na_2^+ and K_2^+ around their inner minima are those
corresponding to the antisymmetric molecular orbital.
The positions of these respective minima at 1.5Å and 2.2Å
may be compared with the radial maxima of the atomic
orbitals which occur at 1.2Å for Na and 2.0Å for K.
A simple calculation shows that under these circumstances
the antisymmetric molecular orbital concentrates more
charge within the ion cores than does the symmetric orbital.
Further evidence that a core effect causes this behaviour
is provided by the results labelled 1s where the electrostatic
potentials are replaced by simple point charge expressions
(throughout space) resulting in the disappearance of the
inner minima giving more plausible bonding parameters.
However, the reintroduction of p-orbitals leads again to

INTERNUCLEAR SEPARATION (Å)

ENERGY (KCAL/MOLE)
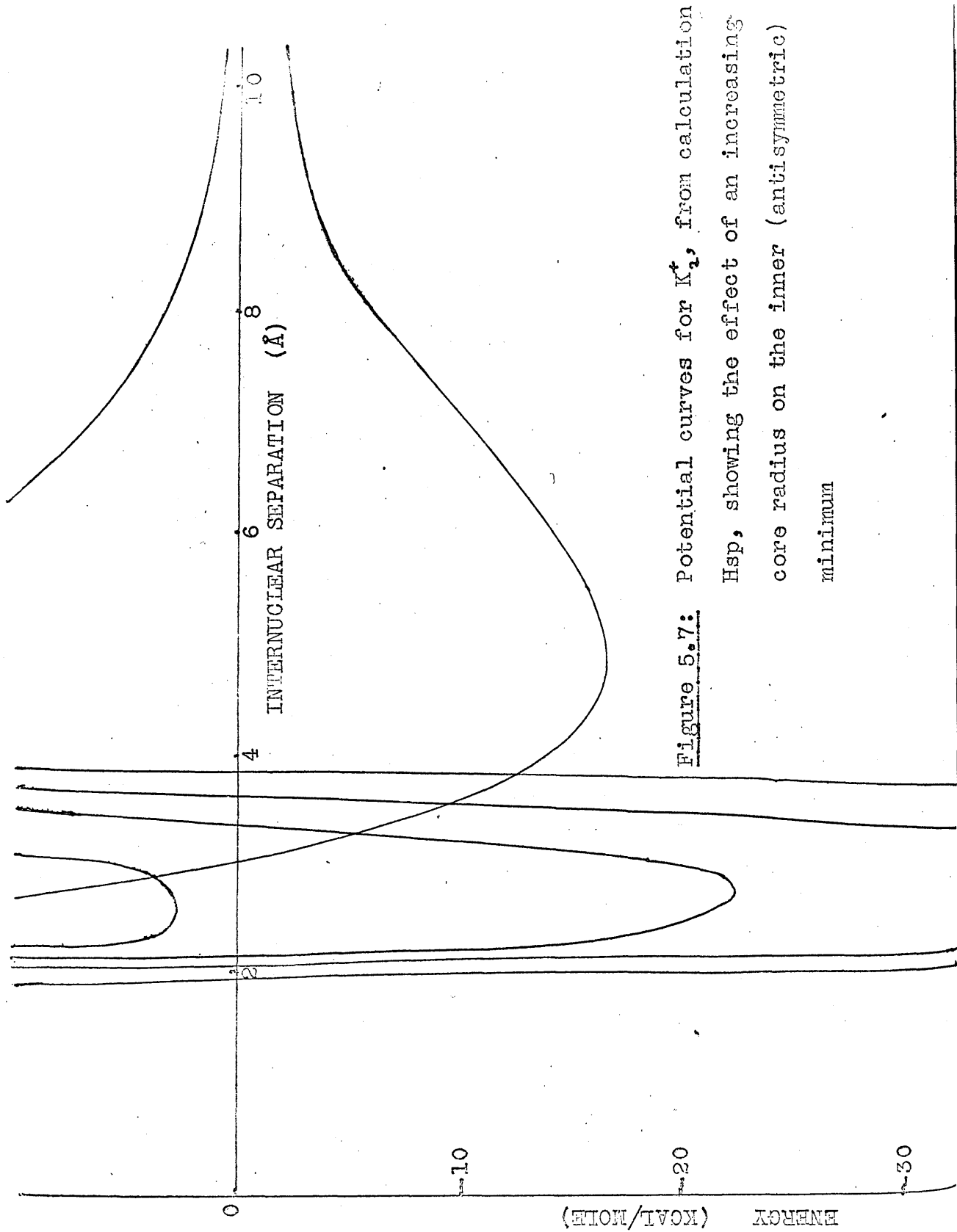
Figure 5.7: Potential curves for K_2^+, from calculation Hsp, showing the effect of an increasing core radius on the inner (antisymmetric) minimum

a deep minimum at very short range as exemplified
by the result 1sp for NaK$^+$.

In the calculations Hsp and Hs (respectively with and
without p-orbitals) the valence orbitals are made orthogonal
to foreign cores simply by setting them to be uniformly
zero within the core radius.   As is clear from table 5.5,
the results Hsp obtained for the diatomic ions with this
method are essentially the same as those from the adopted
pseudopotential model (labelled Ψsp).   They are recorded
here for two reasons.   In the first place comparison of
the two parallel sets demonstrates that only approximately
half of the total binding in the diatomic ions results
on the inclusion of s-orbitals alone in the valence basis
set.   Secondly, figure 5.7 shows the results of a series
of Hsp calculations on K_2^+ , steadily increasing the size
of the core radius from zero to the K^+ gaseous ionic
radius.   The inner curves demonstrate the successive
diminution of the antisymmetric curve at the inner minimum.
The symmetric curve is not so sensitive to core radius and
is shown only at its final position.

The procedure Hsp which involves cutting "holes" in
the valence orbitals within foreign cores is, for the
diatomic ions, nearly equivalent to the adopted procedure,
though on the basis of the discussion in chapter 3.1,

insufficient core penetration is allowed in such a
model.   This effect would become important in a system
containing a chloride ion.   There are also difficulties
inherent in such an approach in that the orbitals would
presumably be required to be renormalised, and also strict
orthogonality between s- and p- valence orbitals on a
particular centre is relaxed, with the result that a
suitable atomic combination assumes a larger "ionisation
potential."   The adopted procedure is clearly more
satisfactory.

The salient points from this discussion may be
summarised.   The use of electrostatic potentials leads
to spuriously strong and close range binding.   Using
pseudopotentials, however, as the core radius is
steadily increased from zero to the ionic radius, these
deep inner minima disappear, and the resulting longer
range binding is not rapidly altered.   The inclusion of
p-orbitals is essential both to obtain accurate dissociation
energies and to describe effectively the long range
behaviour.   As a result of these calculations it is
possible to proceed with some confidence to outline the
results for the reaction K + NaCl = KCl + Na.

Chapter 6   The potential surfaces for the reaction
                    K + NaCl = KCl + Na

In table 6.1 the energies of the two lowest

potential energy surfaces for the reaction K + NaCl = KCl + Na

are listed at all configurations for which they were

calculated.   The format in which these results are

presented requires some explanation.   For the reaction

M + NCl the nuclear configuration is specified in terms

of the coordinate system depicted in figure 6.1.
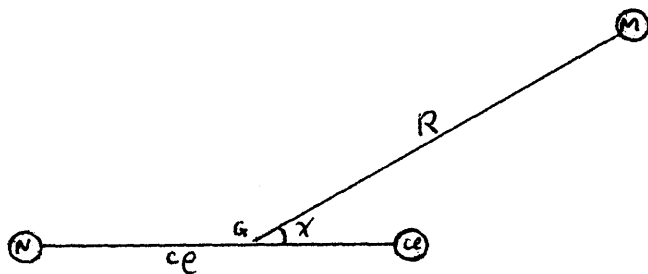
Figure 6.1

R is the distance from the reactant atom M to the centre

of mass, G, of the NCl molecule.   The dimensionless

constant c is defined in terms of the atomic masses as

$$c = \sqrt{\frac{m_M (m_N + m_{cl})^2}{m_N m_{cl}(m_M + m_N + m_{cl})}} \quad , \tag{6.1}$$

and the length of the N-Cl bond is given by $c\varrho$.

Finally, χ is the angle $\widehat{MGCl}$.   In this coordinate system

the classical energy for nuclear motion restricted to a

plane is given by

$$E = \tfrac{1}{2}m\left\{\dot{R}^2 + \dot{\varrho}^2 + (R^2 + \varrho^2)\dot{\chi}^2\right\} + V(R,\varrho,\chi), \tag{6.2}$$

where $m = \dfrac{m_M (m_N + m_{cl})}{m_M + m_N + m_{cl}} \quad ,$

so that any orthogonal transformation will preserve the
diagonalisation of the kinetic energy.   The results in
table 6.1 are divided into two parts, expressed in the
coordinate systems for K + NaCl and Na + KCl respectively;
the former is concerned principally with configurations in
the reactants region and the latter with the products
region.   For each part the results are broken down in the
first instance into separate sections for each angle χ ,
at 15° intervals.   These sections are further subdivided for
each R, the value of which is given at the head of each
subsection, together with an integer,n, indicating the
number of configurations listed for that (χ,R).   The data
for each point is then listed, giving first the relevant
ρ - value, and then the two lowest electronic eigenvalues
$E_1(R,\rho,\chi)$ and $E_2(R,\rho,\chi)$.   The format of each section may
be illustrated:

$$
\begin{aligned}
&M+NC\ell \quad angle = \chi\,deg;\\
&R_1; n_1;\\
&e_{11}; E_1(R_1,e_{11},\chi); E_2(R_1,e_{11},\chi);\\
&e_{12}; E_1(R_1,e_{12},\chi); E_2(R_1,e_{12},\chi);\\
&e_{1n_1}; E_1(R_1,e_{1n_1},\chi); E_2(R_1,e_{1n_1},\chi);\\
&R_2; n_2;\\
&e_{21}; E_1(R_2,e_{21},\chi); E_2(R_2,e_{21},\chi);\\
&ie.
\end{aligned}
\tag{6.3}
$$

Distances are given in Å and the energies, in Kcal/mole,
measure stability relative to the dissociation limit
$(Na^+ + K^+ + Cl^- + e^-)$.   The completion of the calculation at the
points listed in table 6.1 required some 30 hours of
computing time.

Table 6.1

K+NaCl   angle= ZERO;

3.5; 10;

1.85;	205.874;	197.709;
1.90;	207.529;	198.706;
1.95;	208.594;	198.380;
2.00;	209.007;	196.987;
2.05;	208.737;	194.726;
2.10;	207.786;	191.743;
2.30;	197.493;	174.195;
2.50;	176.769;	148.895;
2.70;	143.696;	114.935;
3.00;	61.500;	40.810;

3.8; 11;

1.80;	219.018;	208.777;
1.90;	222.922;	216.509;
1.95;	224.356;	218.358;
2.00;	225.774;	219.076;
2.05;	227.039;	218.891;
2.10;	228.007;	218.025;
2.15;	228.627;	216.650;
2.30;	228.473;	210.493;
2.50;	224.131;	199.182;
2.70;	215.039;	184.818;
3.00;	189.579;	155.395;

4.0; 13;

1.70;	213.957;	195.680;
1.80;	223.013;	209.929;
1.91;	226.947;	219.427;
1.95;	227.499;	221.555;
2.00;	228.153;	223.285;
2.05;	229.103;	224.042;
2.10;	230.213;	223.972;
2.15;	231.230;	223.290;
2.20;	232.044;	222.187;
2.30;	233.021;	219.189;
2.50;	232.791;	211.505;
2.70;	230.021;	202.427;
3.00;	220.082;	185.555;

4.5; 10;

1.70;	216.051;	191.100;
1.85;	227.580;	209.468;
1.90;	229.015;	213.359;
1.95;	229.660;	216.468;
2.00;	229.681;	218.935;

2.05;	229.192;	220.861;
2.10;	228.262;	222.300;
2.30;	227.212;	222.809;
2.70;	230.650;	212.136;
3.00;	232.250;	204.695;

5.0; 9;

1.70;	215.721;	185.329;
1.80;	224.420;	197.570;
1.85;	226.686;	195.465;
1.91;	228.110;	206.144;
1.93;	228.332;	207.278;
1.95;	228.449;	208.309;
2.00;	228.345;	210.488;
2.05;	227.785;	212.194;
2.50;	218.234;	214.836;

6.0; 9;

1.70;	215.018;	181.434;
1.80;	223.146;	189.328;
1.85;	225.132;	191.199;
1.91;	226.224;	193.873;
1.93;	226.337;	194.800;
1.95;	226.345;	195.626;
2.00;	225.971;	197.308;
2.05;	225.145;	198.537;
2.30;	217.7;	200.6;

8.0; 10;

1.70;	214.799;	178.817;
1.80;	222.554;	186.540;
1.85;	224.355;	188.325;
1.89;	225.069;	189.027;
1.91;	225.225;	189.176;
1.93;	225.264;	189.209;
1.96;	225.129;	189.064;
1.99;	224.791;	188.716;
2.15;	220.7;	184.5;
2.30;	216.5;	180.0;

12.0; 9;

1.70;	214.790;	177.858;
1.80;	222.451;	185.523;
1.85;	224.206;	187.279;
1.89;	224.821;	187.957;
1.91;	225.019;	188.095;
1.93;	225.039;	188.116;

Table 6.1 (cont.)

1.95;	224.954;	188.031;
2.15;	220.3;	183.4;
2.30;	214.442;	177.531;

K+NaCl   angle= 15 deg;

3.0;   6;

1.80;	106.440;	95.5073;
1.85;	102.220;	90.435;
1.90;	96.512;	82.001;
1.95;	89.311;	72.314;
2.00;	80.610;	60.766;
2.05;	70.405;	47.293;

3.5;   11;

1.80;	208.407;	199.188;
1.85;	210.708;	202.242;
1.90;	212.502;	203.756;
1.95;	213.827;	204.006;
2.00;	214.634;	203.237;
2.05;	214.887;	201.650;
2.10;	214.585;	199.396;
2.30;	208.224;	185.458;
2.50;	194.200;	165.261;
2.70;	171.432;	140.500;
3.00;	117.115;	89.666;

3.8;   12;

1.70;	213.229;	196.029;
1.80;	221.472;	210.005;
1.90;	225.107;	217.965;
1.95;	226.341;	220.037;
2.00;	227.588;	221.029;
2.05;	228.791;	221.139;
2.10;	229.805;	220.571;
2.15;	230.552;	219.498;
2.30;	231.143;	214.355;
2.50;	228.697;	204.903;
2.70;	222.944;	193.334;
3.00;	206.483;	171.924;

4.0;   14;

1.70;	215.930;	196.273;
1.80;	224.350;	210.379;
1.85;	227.003;	215.367;
1.90;	228.266;	219.218;
1.95;	228.871;	220.037;
2.00;	229.278;	223.889;

2.05;	229.919;	224.833;
2.10;	230.818;	224.977;
2.15;	231.746;	224.498;
2.20;	232.549;	223.579;
2.30;	233.637;	220.935;
2.50;	234.049;	214.114;
2.70;	232.636;	206.352;
3.00;	226.764;	193.108;

4.5;   13;

1.70;	216.693;	191.314;
1.80;	225.788;	204.554;
1.85;	228.222;	209.298;
1.90;	229.629;	213.099;
1.95;	230.228;	216.132;
2.00;	230.194;	218.533;
2.05;	229.660;	220.404;
2.10;	228.706;	221.806;
2.20;	226.328;	223.303;
2.30;	226.499;	222.690;
2.50;	228.196;	217.681;
2.70;	229.486;	212.291;
3.00;	231.196;	205.170;

5.0;   10;

1.70;	215.973;	185.132;
1.80;	224.646;	197.519;
1.85;	226.902;	201.868;
1.90;	228.159;	205.297;
1.93;	228.529;	206.990;
1.96;	228.660;	208.451;
1.99;	228.586;	209.711;
2.10;	227.016;	212.993;
2.30;	221.193;	215.630;
2.50;	217.189;	214.505;

6.0;   9;

1.70;	215.100;	181.295;
1.80;	223.203;	189.219;
1.85;	225.178;	191.094;
1.90;	226.158;	193.261;
1.93;	226.364;	194.660;
1.96;	226.332;	195.833;
1.99;	226.099;	196.811;
2.10;	223.969;	199.107;
2.30;	217.427;	200.273;

8.0;   10;

Table 6.1 (cont.)

1.70;	214.812;	178.801;	1.90;	223.170;	213.583;
1.80;	222.563;	186.522;	1.95;	224.722;	214.923;
1.85;	224.361;	188.305;	2.00;	225.925;	215.359;
1.89;	225.073;	189.001;	2.05;	226.804;	215.072;
1.91;	225.228;	189.135;	2.30;	226.696;	207.177;
1.93;	225.266;	188.853;	2.50;	222.329;	197.124;
1.95;	225.199;	189.000;	2.70;	215.058;	185.599;
2.05;	223.622;	187.507;	3.0;	199.003;	166.041;
2.15;	220.666;	184.523;			
2.30;	215.723;	179.097;	3.8;	12;	

12.0;	9;		1.70;	216.821;	198.856;
			1.80;	225.708;	212.281;
1.70;	214.790;	177.855;	1.90;	229.701;	220.243;
1.80;	222.451;	185.520;	1.95;	230.750;	222.598;
1.85;	224.205;	187.276;	2.00;	231.571;	224.045;
1.89;	224.882;	187.954;	2.05;	232.332;	224.318;
1.91;	225.018;	188.092;	2.10;	233.063;	224.357;
1.93;	225.039;	188.112;	2.15;	233.720;	224.299;
1.95;	224.953;	188.028;	2.30;	234.932;	221.056;
2.15;	220.239;	183.321;	2.50;	234.860;	214.732;
2.30;	214.439;	177.526;	2.70;	233.450;	207.894;
			3.00;	229.318;	197.297;

K+NaCl	angle= 30 deg;		4.0;	13;	
			1.70;	218.000;	197.896;
3.0;	6;		1.80;	227.051;	211.220;
			1.85;	229.453;	215.909;
1.80;	155.493;	143.615;	1.90;	230.865;	219.546;
1.85;	155.660;	143.118;	1.95;	231.555;	222.272;
1.90;	154.859;	141.116;	2.00;	231.802;	224.188;
1.95;	153.152;	137.856;	2.05;	231.908;	225.372;
2.00;	150.595;	133.544;	2.10;	232.108;	225.898;
2.05;	147.226;	128.348;	2.15;	232.466;	225.859;
			2.30;	233.725;	223.474;
3.25;	6;		2.50;	234.550;	218.111;
			2.70;	234.593;	212.363;
1.90;	204.710;	192.892;	3.00;	233.733;	204.170;
2.10;	204.910;	187.484;			
2.30;	197.299;	173.610;	4.5;	10;	
2.50;	183.466;	155.546;			
2.70;	164.160;	134.683;	1.70;	217.485;	191.979;
3.00;	125.187;	97.785;	1.80;	226.418;	204.480;
			1.90;	230.131;	212.373;
3.5;	11;		1.95;	230.686;	215.106;
			2.00;	230.624;	217.228;
1.70;	209.950;	194.860;	2.05;	230.084;	218.846;
1.80;	218.546;	207.357;	2.10;	229.171;	220.040;
1.85;	221.178;	211.134;			

Table 6.1 (cont.)

2.30; 224.860; 221.209;
2.50; 225.055; 217.062;
3.00; 226.761; 204.801;

5.0; 14;

1.70; 216.387; 185.655;
1.80; 224.924; 197.433;
1.85; 227.111; 201.515;
1.90; 228.300; 204.692;
1.93; 228.628; 206.239;
1.96; 228.717; 207.559;
1.99; 228.602; 208.621;
2.05; 227.879; 210.426;
2.10; 226.887; 211.476;
2.20; 224.200; 212.777;
2.30; 220.930; 213.337;
2.50; 214.591; 212.693;
2.70; 214.337; 207.741;
3.00; 214.880; 200.170;

6.0; 10;

1.70; 215.266; 180.772;
1.80; 223.302; 188.864;
1.85; 225.243; 190.767;
1.90; 226.190; 192.983;
1.93; 226.376; 194.290;
1.96; 226.324; 195.376;
1.99; 226.070; 196.270;
2.10; 223.864; 198.275;
2.20; 220.760; 198.928;
2.30; 217.174; 198.952;

8.0; 11;

1.70; 214.046; 178.761;
1.80; 222.589; 186.477;
1.85; 224.378; 188.257;
1.89; 225.082; 188.945;
1.91; 225.233; 189.073;
1.93; 225.267; 189.009;
1.95; 225.196; 188.843;
2.00; 224.625; 188.422;
2.10; 222.241; 186.067;
2.20; 218.843; 183.043;
2.30; 214.948; 182.474;

12.0; 11;

1.70; 214.791; 177.848;
1.80; 222.451; 185.512;

1.85; 224.204; 187.268;
1.89; 224.880; 187.946;
1.91; 225.017; 188.083;
1.93; 225.036; 188.104;
1.95; 224.951; 188.019;
2.00; 224.343; 186.619;
2.10; 221.883; 184.958;
2.20; 218.407; 181.486;
2.30; 214.432; 177.515;

K+NaCl   angle= 45 deg;

3.0; 10;

1.85; 201.254; 187.315;
1.90; 203.242; 188.769;
1.95; 204.577; 189.249;
2.00; 205.377; 188.945;
2.05; 205.734; 188.014;
2.10; 205.719; 186.563;
2.30; 202.907; 177.888;
2.50; 196.873; 168.577;
2.70; 189.167; 159.724;
3.00; 176.962; 147.145;

3.3; 12;

1.70; 213.957; 195.876;
1.80; 222.669; 208.161;
1.90; 227.684; 214.397;
1.95; 229.293; 215.951;
2.00; 230.477; 216.730;
2.05; 231.321; 216.890;
2.10; 231.885; 216.564;
2.15; 232.216; 215.856;
2.30; 232.136; 212.230;
2.50; 230.381; 205.772;
2.70; 227.520; 199.341;
3.00; 222.422; 190.744;

3.5; 14;

1.70; 220.053; 199.832;
1.80; 228.297; 212.764;
1.85; 230.735; 216.914;
1.90; 232.613; 219.844;
1.95; 233.956; 221.788;
2.00; 234.946; 222.938;
2.05; 235.677; 223.451;
2.10; 236.209; 223.459;

Table 6.1 (cont.)

2.15;	236.580;	223.071;
2.20;	236.815;	222.378;
2.30;	236.951;	220.356;
2.50;	236.292;	215.056;
2.70;	234.957;	209.444;
3.00;	232.421;	202.005;

4.0;　13;

1.70;	220.187;	199.374;
1.80;	229.532;	211.174;
1.85;	232.117;	215.176;
1.90;	233.617;	218.275;
1.95;	234.198;	220.678;
2.00;	234.160;	222.443;
2.05;	233.811;	223.599;
2.10;	233.348;	224.215;
2.20;	232.511;	224.152;
2.30;	232.010;	222.845;
2.50;	231.473;	218.398;
2.70;	231.055;	213.388;
3.00;	230.691;	206.605;

4.5;　12;

1.70;	218.190;	192.919;
1.80;	226.914;	204.273;
1.90;	230.474;	211.139;
1.95;	230.981;	213.393;
2.00;	230.891;	215.062;
2.05;	230.344;	216.262;
2.10;	229.437;	217.091;
2.20;	224.231;	212.432;
2.30;	223.853;	217.650;
2.50;	220.702;	214.465;
2.70;	219.759;	209.389;
3.00;	219.230;	202.091;

5.0;　9;

1.70;	216.737;	186.616;
1.80;	225.091;	197.420;
1.85;	227.186;	201.083;
1.90;	228.285;	203.874;
1.93;	228.560;	205.201;
1.96;	228.597;	206.307;
1.99;	228.431;	207.221;
2.05;	227.609;	208.569;
2.50;	213.026;	208.832;

6.0;　9;

1.70;	215.392;	179.551;
1.80;	223.350;	188.129;
1.85;	225.249;	190.219;
1.90;	226.154;	192.701;
1.93;	226.313;	193.859;
1.96;	226.235;	194.805;
1.99;	225.955;	195.566;
2.10;	223.649;	197.131;
2.30;	216.771;	197.105;

8.0;　10;

1.70;	214.863;	178.713;
1.80;	222.581;	186.418;
1.85;	224.364;	188.189;
1.89;	225.063;	188.363;
1.91;	225.211;	188.980;
1.93;	225.242;	188.935;
1.95;	225.168;	188.591;
2.05;	223.558;	187.255;
2.15;	220.568;	184.342;
2.30;	214.854;	181.713;

12.0;　11;

1.70;	214.792;	177.839;
1.80;	222.450;	185.503;
1.85;	224.202;	187.258;
1.89;	224.877;	187.935;
1.91;	225.013;	188.073;
1.93;	225.033;	188.093;
1.95;	224.947;	188.008;
2.0;	224.338;	187.402;
2.10;	221.876;	184.945;
2.20;	218.398;	181.473;
2.30;	214.422;	177.501;

K+NaCl　　　angle= 60 deg;

2.80;　7;

1.80;	207.237;	190.950;
1.90;	214.219;	196.587;
2.10;	220.539;	198.798;
2.30;	222.311;	194.950;
2.50;	222.448;	190.566;
2.70;	221.363;	190.666;
3.00;	220.537;	188.959;

Table 6.1 (cont.)

3.0; 13;

1.70;	212.618;	194.657;
1.80;	223.567;	205.396;
1.85;	227.138;	209.282;
1.90;	229.818;	211.718;
1.95;	231.807;	213.311;
2.00;	233.257;	214.232;
2.05;	234.288;	214.626;
2.10;	234.993;	214.609;
2.15;	235.445;	214.275;
2.30;	235.809;	212.038;
2.50;	235.200;	207.517;
2.70;	234.060;	203.899;
3.00;	232.246;	200.850;

3.3; 13;

1.60;	203.676;	184.751;
1.70;	221.985;	203.045;
1.80;	232.103;	213.886;
1.90;	237.337;	219.792;
1.95;	238.824;	221.439;
2.00;	239.807;	222.433;
2.05;	240.416;	222.901;
2.10;	240.748;	222.954;
2.15;	240.872;	222.683;
2.30;	240.477;	220.600;
2.50;	239.151;	216.451;
2.70;	237.677;	212.111;
3.00;	235.713;	206.605;

3.5; 15;

1.60;	205.202;	186.047;
1.70;	223.185;	204.040;
1.80;	232.909;	214.720;
1.85;	235.736;	218.126;
1.90;	237.623;	220.561;
1.95;	238.811;	222.208;
2.00;	239.487;	223.215;
2.05;	239.799;	223.707;
2.10;	239.856;	223.785;
2.15;	239.734;	223.534;
2.20;	239.491;	223.027;
2.30;	238.786;	221.470;
2.50;	237.055;	217.270;
2.70;	235.370;	212.783;
3.00;	233.334;	206.674;
4		

4.0; 13;

1.70;	221.152;	200.302;
1.80;	230.127;	210.668;
1.85;	232.534;	214.027;
1.90;	233.950;	216.471;
1.95;	234.606;	218.174;
2.00;	234.692;	219.274;
2.05;	234.363;	219.885;
2.10;	233.748;	220.096;
2.20;	232.063;	219.601;
2.30;	230.234;	218.233;
2.50;	227.109;	214.067;
2.70;	224.818;	209.263;
3.00;	222.451;	202.456;

4.5; 8;

1.70;	218.554;	194.124;
1.80;	227.039;	204.088;
1.90;	230.359;	209.743;
2.00;	230.537;	212.297;
2.10;	228.877;	213.654;
2.30;	223.203;	212.686;
2.50;	217.729;	209.410;
2.70;	214.274;	204.873;

5.0; 10;

1.70;	216.909;	188.298;
1.80;	225.083;	197.807;
1.85;	227.090;	200.920;
1.90;	228.101;	203.210;
1.93;	228.324;	204.258;
1.96;	228.309;	205.098;
1.99;	228.091;	205.756;
2.10;	226.013;	206.974;
2.30;	219.538;	206.334;
2.50;	212.257;	204.067;

6.0; 9;

1.70;	215.517;	180.165;
1.80;	223.355;	188.040;
1.85;	225.203;	190.772;
1.90;	226.059;	192.809;
1.93;	226.191;	193.741;
1.96;	226.085;	194.482;

Table 6.1 (cont.)

1.99;	225.778;	195.056;	3.00;	232.561;	196.527;
2.10;	223.375;	196.036;			
2.30;	216.324;	195.164;	2.8;	15;	

8.0; 10;

1.70;	214.870;	178.689;
1.80;	222.571;	186.384;
1.85;	224.344;	188.143;
1.89;	225.036;	188.802;
1.91;	225.181;	188.909;
1.93;	225.209;	188.867;
1.95;	225.131;	188.639;
2.05;	223.505;	186.502;
2.15;	220.493;	184.175;
2.30;	214.751;	180.920;

2.8; 15;

1.60;	195.818;	172.239;
1.70;	216.726;	192.975;
1.80;	228.981;	204.922;
1.90;	235.986;	211.112;
1.95;	238.200;	212.780;
2.00;	239.799;	213.769;
2.05;	240.918;	214.233;
2.10;	241.664;	214.295;
2.15;	242.121;	214.053;
2.20;	242.356;	213.585;
2.30;	242.360;	212.199;
2.40;	241.979;	210.471;
2.50;	241.403;	208.575;
2.75;	239.651;	204.366;
3.00;	237.781;	202.264;

12.0; 10;

1.70;	214.791;	177.833;
1.80;	222.447;	185.496;
1.85;	224.199;	187.251;
1.89;	224.873;	187.928;
1.91;	225.009;	188.066;
1.93;	225.028;	188.086;
1.95;	224.942;	188.001;
2.05;	223.270;	186.336;
2.15;	220.217;	183.289;
2.30;	214.410;	177.491;

3.0; 16;

1.60;	203.447;	180.152;
1.70;	222.881;	197.778;
1.80;	234.189;	209.215;
1.85;	237.713;	212.805;
1.90;	240.237;	215.274;
1.95;	241.994;	216.859;
2.00;	243.162;	217.756;
2.05;	243.877;	218.122;
2.10;	244.244;	218.080;
2.15;	244.346;	217.729;
2.20;	244.247;	217.147;
2.30;	243.641;	215.524;
2.40;	242.709;	213.568;
2.50;	241.628;	211.494;
2.75;	238.843;	206.443;
3.00;	236.286;	202.441;

K+NaCl   angle= 75 deg;

3.5; 15;

1.60;	207.003;	186.714;
1.70;	224.912;	203.093;
1.80;	234.609;	211.989;
1.85;	237.396;	214.555;
1.90;	239.189;	216.271;
1.95;	240.207;	217.366;
2.00;	240.635;	217.972;
2.05;	240.628;	218.156;
2.10;	240.313;	217.976;
2.15;	239.780;	217.499;

2.25; 5;

2.10;	183.745;	151.887;
2.30;	194.090;	161.182;
2.50;	200.845;	171.674;
2.70;	206.722;	176.162;
3.00;	214.715;	180.980;

2.5; 8;

1.90;	214.898;	193.047;
2.00;	220.723;	195.914;
2.10;	224.480;	196.691;
2.20;	226.977;	196.024;
2.30;	228.742;	193.948;
2.40;	229.994;	191.419;
2.70;	231.408;	196.172;

Table 6.1 (cont.)

2.20;	239.097;	216.789;	1.70;	215.410;	182.602;
2.30;	237.469;	214.893;	1.80;	223.242;	190.114;
2.50;	233.906;	210.237;	1.90;	225.918;	193.849;
2.70;	230.577;	205.479;	1.93;	226.038;	194.492;
3.00;	226.436;	199.144;	1.96;	225.921;	194.964;
			1.99;	225.601;	195.289;
4.0;	15;		2.10;	223.148;	195.498;
			2.30;	216.003;	193.594;
1.60;	204.377;	184.122;			
1.70;	221.511;	200.028;	8.0;	10;	
1.80;	230.367;	208.925;			
1.85;	232.729;	211.553;	1.70;	214.863;	178.740;
1.90;	234.111;	213.285;	1.80;	222.549;	186.419;
1.95;	234.736;	214.303;	1.85;	224.316;	188.159;
2.00;	234.784;	214.760;	1.89;	225.002;	188.787;
2.05;	234.396;	214.780;	1.91;	225.144;	188.874;
2.10;	233.684;	214.467;	1.93;	225.169;	188.811;
2.15;	232.738;	213.905;	1.95;	225.088;	188.587;
2.20;	231.631;	213.158;	2.05;	223.446;	184.415;
2.30;	229.174;	211.273;	2.15;	220.423;	183.678;
2.50;	224.309;	206.620;	2.30;	214.659;	180.374;
2.70;	220.201;	201.692;			
3.00;	215.529;	194.881;	12.0;	10;	
4.5;	10;		1.70;	214.790;	177.838;
			1.80;	222.445;	185.501;
1.60;	201.980;	179.989;	1.85;	224.196;	187.256;
1.70;	218.657;	195.308;	1.89;	224.870;	187.933;
1.80;	227.027;	203.950;	1.91;	225.005;	188.070;
1.90;	230.244;	208.335;	1.93;	225.024;	188.090;
1.95;	230.590;	209.437;	1.95;	224.937;	188.005;
2.00;	230.348;	210.009;	2.05;	223.264;	186.340;
2.05;	229.664;	210.162;	2.15;	220.210;	183.293;
2.10;	228.651;	209.989;	2.30;	214.400;	177.495;
2.30;	222.908;	207.281;			
2.50;	216.705;	203.112;	K+NaCl	angle= 90 deg;	
5.0;	9;		2.0;	7;	
1.70;	216.905;	190.485;	1.70;	151.949;	131.517;
1.80;	225.003;	198.822;	1.90;	169.354;	167.852;
1.90;	227.933;	203.084;	2.10;	188.488;	176.105;
1.93;	228.130;	203.814;	2.30;	201.366;	179.572;
1.96;	228.089;	204.348;	2.50;	210.045;	180.440;
1.99;	227.847;	204.712;	2.70;	216.658;	177.230;
2.10;	225.692;	204.937;	3.00;	224.265;	176.781;
2.30;	219.149;	202.754;			
2.50;	211.914;	199.264;	2.3;	7;	
6.0;	8;				

Table 6.1 (cont.)

1.70;	197.095;	185.312;
1.90;	220.752;	198.471;
2.10;	229.997;	199.775;
2.30;	233.536;	196.434;
2.50;	234.672;	195.577;
2.70;	235.103;	196.262;
3.00;	235.253;	192.405;

2.5;   16;

1.60;	193.893;	167.823;
1.70;	214.840;	187.207;
1.80;	227.331;	198.494;
1.85;	231.441;	201.752;
1.90;	234.532;	203.893;
1.95;	236.821;	205.167;
2.00;	238.483;	205.774;
2.05;	239.652;	205.872;
2.10;	240.437;	205.589;
2.15;	240.923;	205.022;
2.20;	241.177;	204.250;
2.30;	241.196;	202.307;
2.40;	240.797;	200.049;
2.50;	240.165;	197.597;
2.75;	238.267;	195.032;
3.0;	236.367;	193.021;

2.8;   16;

1.60;	206.302;	176.514;
1.70;	224.892;	189.608;
1.80;	235.615;	197.621;
1.85;	238.974;	201.669;
1.90;	241.336;	204.857;
1.95;	242.927;	206.945;
2.00;	243.925;	208.109;
2.05;	244.467;	208.574;
2.10;	244.657;	208.523;
2.15;	244.578;	208.088;
2.20;	244.295;	207.372;
2.30;	243.312;	205.404;
2.40;	242.002;	203.067;
2.50;	240.545;	200.626;
2.75;	236.853;	194.874;
3.0;	233.482;	190.423;

3.0;   16;

1.60;	208.303;	180.353;
1.70;	226.421;	195.821;
1.80;	236.589;	202.916;

1.85;	239.652;	204.622;
1.91;	242.056;	206.286;
1.95;	243.052;	207.357;
2.00;	243.771;	208.398;
2.05;	244.041;	208.907;
2.10;	243.974;	208.894;
2.15;	243.655;	208.469;
2.20;	243.149;	207.742;
2.30;	241.761;	205.701;
2.40;	240.095;	203.244;
2.50;	238.320;	200.650;
2.75;	233.967;	194.472;
3.00;	230.103;	189.327;

3.2;   13;

1.60;	208.447;	182.122;
1.70;	226.217;	198.132;
1.80;	235.967;	206.199;
1.90;	240.726;	209.166;
1.95;	241.859;	209.465;
2.00;	242.396;	209.398;
2.05;	242.472;	209.201;
2.10;	242.203;	208.878;
2.20;	240.993;	207.552;
2.30;	239.276;	205.411;
2.50;	235.322;	200.150;
2.70;	231.433;	194.901;
3.00;	226.342;	188.223;

3.5;   15;

1.60;	207.130;	183.110;
1.70;	224.640;	198.907;
1.80;	233.938;	207.104;
1.91;	238.423;	210.608;
1.95;	239.083;	210.924;
2.00;	239.398;	210.808;
2.02;	239.394;	210.632;
2.05;	239.271;	210.253;
2.07;	239.122;	209.935;
2.10;	238.809;	209.380;
2.15;	238.095;	208.304;
2.30;	235.064;	204.626;
2.50;	230.451;	199.140;
2.70;	226.123;	193.696;
3.00;	220.640;	186.689;

4.0;   13;

Table 6.1 (cont.)

1.60;	204.114;	182.720;		2.30;	216.061;	192.712;
1.70;	221.322;	197.810;				
1.80;	230.147;	205.723;		8.0;	9;	
1.91;	233.988;	209.219;				
1.95;	234.399;	209.584;		1.70;	214.856;	178.947;
2.00;	234.401;	209.556;		1.80;	222.538;	186.608;
2.05;	233.967;	209.105;		1.89;	224.987;	188.927;
2.10;	233.210;	208.332;		1.91;	225.128;	189.003;
2.20;	231.060;	206.133;		1.93;	225.152;	188.936;
2.3;	228.454;	203.433;		1.95;	225.071;	188.738;
2.5;	222.949;	197.642;		1.98;	224.774;	188.197;
2.70;	217.939;	192.124;		2.10;	222.035;	184.459;
3.00;	211.906;	184.907;		2.30;	214.628;	180.432;

4.5;   10;   12.0;   8;

1.70;	218.669;	195.440;		1.70;	214.789;	177.860;
1.80;	227.111;	203.135;		1.80;	222.444;	185.524;
1.85;	229.241;	205.228;		1.89;	224.868;	187.957;
1.90;	230.377;	206.470;		1.91;	225.003;	188.094;
1.95;	230.744;	207.044;		1.93;	225.022;	188.114;
2.00;	230.523;	207.099;		2.05;	223.262;	186.365;
2.05;	229.860;	206.748;		2.15;	220.207;	183.319;
2.15;	227.645;	205.196;		2.30;	214.397;	177.521;
2.30;	223.202;	201.665;				
2.50;	216.916;	196.220;				

K+NaCl   angle= 105 deg;

5.0;   11;   2.0;   7;

1.70;	216.960;	192.266;		1.70;	169.509;	159.071;
1.80;	225.114;	199.830;		1.90;	189.961;	180.389;
1.91;	228.180;	203.318;		2.10;	204.351;	182.638;
1.93;	228.290;	203.587;		2.30;	212.108;	181.536;
1.95;	228.296;	203.770;		2.50;	216.595;	178.415;
1.98;	228.132;	203.899;		2.70;	219.379;	175.192;
2.00;	227.920;	203.900;		3.00;	222.219;	169.494;
2.05;	227.098;	203.651;				
2.15;	224.546;	202.353;		2.25;	8;	
2.30;	219.561;	199.268;				
2.5;	212.523;	194.407;		1.70;	198.850;	194.292;

			1.80;	212.506;	198.192;

6.0;   10;

				1.90;	220.442;	198.415;
1.70;	215.390;	185.037;		2.10;	226.728;	195.073;
1.80;	223.228;	192.579;		2.30;	227.860;	189.733;
1.91;	225.989;	195.904;		2.50;	227.348;	185.048;
1.93;	226.044;	196.158;		2.70;	226.457;	179.653;
1.95;	225.993;	196.331;		3.00;	225.410;	168.521;
1.98;	225.742;	196.462;				
2.00;	225.471;	196.473;		2.5;	13;	
2.05;	224.495;	196.282;				
2.15;	221.610;	195.226;		1.60;	201.709;	180.604;

Table 6.1 (cont.)

1.70;	218.660;	193.341;	2.00;	237.891;	199.418;
1.80;	228.248;	198.803;	2.05;	237.738;	198.533;
1.90;	233.255;	199.611;	2.10;	237.270;	197.314;
1.95;	234.627;	199.398;	2.15;	236.569;	195.861;
2.00;	235.424;	198.943;	2.20;	235.699;	194.253;
2.05;	235.778;	198.100;	2.30;	233.643;	190.807;
2.10;	235.806;	196.929;	2.50;	229.139;	184.243
2.20;	235.211;	193.978;	2.70;	224.876;	178.411
2.30;	234.107;	190.658;	3.00;	219.411;	170.737;
2.50;	231.389;	184.160;			
2.70;	228.786;	179.848;			
3.00;	225.692;	166.950;			

3.5;   15;

2.8;   12;

			1.60;	206.582;	173.450;
1.70;	224.224;	189.675;	1.70;	223.373;	189.872;
1.80;	233.100;	196.011;	1.80;	231.931;	198.130;
1.90;	237.358;	197.307;	1.85;	234.217;	200.196;
1.95;	238.334;	196.685;	1.90;	235.576;	201.261;
2.00;	238.764;	195.446;	1.95;	236.225;	201.545;
2.05;	238.773;	193.755;	2.00;	236.331;	201.227;
2.10;	238.468;	192.008;	2.05;	236.027;	200.450;
2.20;	237.281;	190.232;	2.10;	235.415;	199.331;
2.30;	235.647;	188.563;	2.15;	234.577;	197.961;
2.50;	231.889;	182.884;	2.20;	233.574;	196.415;
2.70;	228.284;	176.942;	2.30;	231.267;	193.013;
3.00;	223.790;	170.085;	2.50;	226.275;	185.967;
			2.70;	221.585;	179.530;
			3.00;	215.726;	171.482;

3.0;   14;

4.0;   13;

1.70;	224.643;	188.608;	1.70;	220.469;	192.575;
1.80;	233.332;	196.086;	1.80;	229.414;	200.105;
1.85;	235.819;	197.751;	1.85;	231.735;	201.982;
1.90;	237.412;	198.420;	1.90;	233.046;	202.927;
1.95;	238.303;	198.318;	1.95;	233.586;	203.145;
2.00;	238.650;	197.629;	2.00;	233.538;	202.804;
2.05;	238.580;	196.508;	2.05;	233.051;	202.033;
2.10;	238.193;	195.083;	2.10;	232.240;	200.938;
2.15;	237.572;	193.452;	2.20;	229.993;	198.090;
2.20;	236.781;	191.714;	2.30;	227.301;	194.753;
2.30;	234.910;	188.584;	2.50;	221.644;	187.737;
2.50;	230.810;	183.380;	2.70;	216.402;	181.177;
2.70;	226.825;	177.632;	3.00;	209.882;	172.937;
3.00;	221.748;	170.307;			

4.5;   9;

3.2;   14;

1.60;	208.345;	171.995;	1.70;	213.495;	193.749;
1.70;	224.419;	188.596;	1.80;	227.132;	200.770;
1.80;	232.941;	196.766;	1.90;	230.599;	203.300;
1.90;	236.829;	199.681;	2.00;	230.868;	203.156;
1.95;	237.630;	199.850;	2.10;	229.299;	201.300;
			2.30;	223.754;	195.489;

Table 6.1 (cont.)

2.50; 217.516; 188.767;
2.70; 211.800; 182.413;
3.00; 204.755; 174.316;

5.0; 11;

1.70; 217.031; 192.554;
1.80; 225.335; 199.776;
1.85; 227.416; 201.554;
1.90; 228.509; 202.461;
1.93; 228.785; 202.671;
1.96; 228.826; 202.675;
1.99; 228.665; 202.503;
2.05; 227.855; 201.742;
2.15; 225.478; 199.624;
2.30; 220.714; 195.385;
2.50; 213.945; 189.154;

6.0; 9;

1.70; 215.517; 187.224;
1.80; 223.412; 194.750;
1.85; 225.286; 196.642;
1.90; 226.167; 197.672;
1.93; 226.314; 197.966;
1.96; 226.225; 198.062;
1.99; 225.935; 197.992;
2.10; 223.604; 196.714;
2.30; 216.735; 192.295;

8.0; 10;

1.70; 214.875; 179.444;
1.80; 222.565; 187.108;
1.85; 224.334; 188.830;
1.89; 225.021; 189.455;
1.91; 225.164; 189.556;
1.93; 225.190; 189.532;
1.95; 225.111; 189.398;
2.05; 223.474; 187.533;
2.15; 220.457; 184.930;
2.30; 214.704; 181.401;

12.0; 10;

1.70; 214.790; 177.904;
1.80; 222.445; 185.569;
1.85; 224.196; 187.326;
1.89; 224.870; 188.003;
1.91; 225.006; 188.141;
1.93; 225.024; 188.162;

1.95; 224.938; 188.077;
2.05; 223.265; 186.414;
2.15; 220.211; 183.370;
2.30; 214.402; 177.575;

K+NaCl   angle= 120 deg;

2.8; 9;

1.70; 216.115; 181.489;
1.80; 222.654; 185.803;
1.90; 224.895; 185.855;
1.95; 224.998; 184.863;
2.05; 223.939; 181.632;
2.10; 222.994; 179.615;
2.20; 220.655; 175.160;
2.30; 218.055; 170.436;
2.40; 215.450; 165.682;

3.0; 13;

1.70; 220.329; 175.986;
1.80; 226.745; 184.167;
1.85; 228.264; 185.592;
1.90; 228.989; 185.915;
1.95; 229.101; 185.428;
2.00; 228.746; 184.344;
2.05; 228.041; 182.823;
2.10; 227.079; 180.985;
2.20; 224.667; 176.700;
2.30; 221.942; 171.971;
2.50; 216.505; 161.664;
2.70; 211.853; 154.244;
3.00; 206.698; 145.084;

3.3; 12;

1.60; 207.668; 162.445;
1.70; 221.762; 175.450;
1.80; 228.811; 180.766;
1.95; 231.578; 186.005;
2.00; 231.344; 185.741;
2.05; 230.746; 184.852;
2.10; 229.874; 183.516;
2.20; 227.591; 179.996;
2.30; 224.923; 175.888;
2.50; 219.412; 167.370;
2.70; 214.444; 159.762;
3.00; 208.549; 151.035;

Table 6.1 (cont.)

3.5; 15;

1.60;	207.236;	165.424;
1.70;	221.740;	179.482;
1.80;	229.030;	185.743;
1.85;	230.883;	186.795;
1.90;	231.852;	187.242;
1.95;	232.120;	187.657;
2.00;	231.894;	187.655;
2.05;	231.313;	187.017;
2.10;	230.462;	185.882;
2.15;	229.413;	184.399;
2.20;	228.221;	182.675;
2.30;	225.584;	178.800;
2.50;	220.069;	170.601;
2.70;	214.997;	163.020;
3.00;	208.832;	154.128;

4.0; 13;

1.70;	220.018;	186.853;
1.80;	228.153;	193.425;
1.85;	230.218;	194.829;
1.90;	231.337;	195.334;
1.95;	231.729;	195.139;
2.00;	231.569;	194.401;
2.05;	230.998;	193.240;
2.10;	230.122;	191.763;
2.20;	227.737;	188.319;
2.30;	224.895;	184.572;
2.50;	219.077;	176.542;
2.70;	213.747;	168.878;
3.00;	207.119;	159.049;

4.5; 7;

1.70;	218.187;	190.632;
1.80;	226.728;	197.173;
1.90;	230.127;	199.112;
2.00;	230.424;	198.242;
2.10;	228.919;	195.726;
2.30;	223.481;	188.457;
2.50;	217.274;	180.511;

5.0; 10;

1.70;	217.240;	191.653;
1.80;	225.661;	198.392;
1.85;	227.796;	199.904;
1.90;	228.942;	200.529;
1.93;	229.249;	200.563;
1.96;	229.320;	200.386;

1.99;	229.192;	200.028;
2.10;	227.465;	197.581;
2.30;	221.724;	190.750;
2.50;	215.217;	183.188;

6.0; 9;

1.70;	215.918;	189.056;
1.80;	223.936;	196.354;
1.85;	225.871;	198.105;
1.90;	226.820;	198.971;
1.93;	227.009;	199.153;
1.96;	226.964;	199.129;
1.99;	226.719;	198.928;
2.10;	224.568;	197.097;
2.30;	218.068;	191.488;

8.0; 10;

1.70;	214.938;	180.257;
1.80;	222.652;	187.994;
1.85;	224.433;	189.780;
1.89;	225.131;	190.482;
1.91;	225.280;	190.635;
1.93;	225.311;	190.675;
1.95;	225.237;	190.615;
2.05;	223.629;	189.233;
2.15;	220.643;	186.907;
2.30;	214.943;	183.083;

12.0; 10;

1.70;	214.795;	177.963;
1.80;	222.451;	185.632;
1.85;	224.203;	187.389;
1.89;	224.878;	188.068;
1.91;	225.014;	188.206;
1.93;	225.033;	188.228;
1.95;	224.946;	188.143;
2.05;	223.275;	186.483;
2.15;	220.223;	183.442;
2.30;	214.417;	177.651;

K+NaCl   angle= 135 deg;

3.0; 7;

1.70;	202.308;	165.630;
1.80;	205.122;	167.972;
1.85;	204.865;	167.391;

Table 6.1 (cont.)

1.90;   203.857;   165.952;
1.95;   202.326;   163.801;
2.00;   200.419;   161.099;
2.05;   198.216;   158.034;

3.5;   10;

1.60;   208.369;   158.078;
1.70;   219.786;   171.572;
1.80;   224.706;   177.003;
1.85;   225.520;   177.702;
1.90;   225.543;   177.437;
1.95;   224.950;   176.424;
2.00;   223.882;   174.837;
2.05;   222.454;   172.814;
2.15;   218.869;   167.895;
2.30;   212.579;   159.722;

4.0;   11;

1.60;   207.320;   165.523;
1.70;   221.670;   179.282;
1.80;   228.211;   185.636;
1.85;   229.637;   186.808;
1.90;   230.216;   187.020;
1.95;   230.148;   186.488;
2.00;   229.590;   185.384;
2.05;   228.663;   183.844;
2.10;   227.461;   181.978;
2.30;   221.166;   172.767;
2.50;   214.204;   162.888;

4.2;   12;

1.70;   220.228;   182.466;
1.80;   227.750;   188.599;
1.85;   229.469;   189.803;
1.90;   230.256;   190.067;
1.95;   230.342;   189.598;
2.00;   229.904;   188.566;
2.10;   227.965;   185.323;
2.20;   225.191;   181.121;
2.30;   222.025;   176.459;
2.50;   215.450;   166.802;
2.70;   209.263;   157.870;
3.00;   201.275;   145.968;

4.5;   13;

1.70;   218.304;   186.330;
1.80;   226.640;   192.277;
1.85;   228.703;   193.398;

1.90;   229.757;   193.656;
1.95;   230.032;   193.229;
2.00;   229.727;   192.257;
2.05;   228.991;   190.866;
2.10;   227.943;   189.161;
2.20;   225.247;   185.124;
2.30;   222.141;   180.631;
2.50;   215.740;   171.355;
2.70;   209.819;   162.574;
3.00;   202.311;   151.029;

5.0;   10;

1.70;   217.320;   189.761;
1.80;   225.857;   195.927;
1.85;   228.020;   197.159;
1.90;   229.181;   197.502;
1.93;   229.495;   197.365;
1.96;   229.573;   197.013;
1.99;   229.451;   196.480;
2.10;   227.716;   193.385;
2.30;   221.683;   185.364;
2.50;   215.304;   176.571;

6.0;   9;

1.70;   216.369;   189.843;
1.80;   224.567;   196.918;
1.85;   226.599;   198.530;
1.90;   227.644;   199.229;
1.93;   227.892;   199.300;
1.96;   227.906;   199.154;
1.99;   227.720;   198.826;
2.10;   225.786;   196.467;
2.30;   219.651;   189.758;

8.0;   10;

1.70;   215.053;   181.392;
1.80;   222.807;   189.227;
1.85;   224.610;   191.089;
1.89;   225.326;   191.872;
1.91;   225.483;   192.071;
1.93;   225.524;   192.161;
1.95;   225.460;   192.154;
2.05;   223.903;   191.041;
2.15;   220.974;   188.867;
2.30;   215.372;   184.925;

12.0;   10;

1.70;   214.802;   178.028;

Table 6.1 (cont.)

1.80;	222.461;	185.700;		1.60;	209.593;	167.262;
1.85;	224.214;	187.458;		1.70;	223.559;	179.610;
1.89;	224.890;	188.138;		1.80;	229.578;	184.640;
1.91;	225.026;	188.278;		1.85;	230.691;	185.278;
1.93;	225.046;	188.299;		1.90;	230.931;	185.003;
1.95;	224.960;	188.216;		1.95;	230.505;	184.010;
2.05;	223.292;	186.559;		2.05;	228.252;	180.466;
2.15;	220.243;	183.521;		2.15;	224.808;	175.573;
2.30;	214.441;	177.734;		2.30;	218.476;	166.940;
				2.50;	209.144;	154.490;

K+NaCl   angle= 150 deg;

4.5; 10;

3.0; 6;

				1.60;	205.174;	170.356;
				1.70;	221.031;	182.785;
1.80;	140.867;	116.724;		1.80;	228.452;	187.966;
1.85;	134.129;	109.899;		1.85;	230.092;	188.709;
1.90;	127.096;	102.393;		1.90;	230.768;	188.558;
1.95;	119.708;	94.450;		1.95;	230.711;	187.706;
2.00;	111.102;	85.122;		2.00;	230.102;	186.310;
2.05;	101.227;	74.563;		2.10;	227.750;	182.356;
				2.30;	220.724;	171.989;
				2.50;	212.666;	160.523;

3.5; 9;

4.7; 8;

1.60;	203.586;	150.969;		1.70;	218.841;	185.254;
1.70;	210.838;	161.511;		1.85;	228.962;	191.397;
1.75;	211.844;	163.728;		1.90;	229.926;	191.332;
1.80;	211.547;	164.497;		1.95;	230.122;	190.574;
1.85;	210.224;	164.084;		2.00;	229.736;	189.281;
1.90;	208.075;	162.647;		2.10;	227.770;	185.564;
1.95;	205.245;	160.364;		2.30;	221.479;	175.768;
2.00;	201.853;	157.424;		2.50;	214.298;	165.047;
2.05;	197.992;	153.989;				

4.0; 13;

5.0; 11;

1.60;	213.320;	161.309;		1.70;	217.466;	187.800;
1.70;	223.951;	173.423;		1.80;	225.913;	193.410;
1.75;	226.624;	176.454;		1.85;	228.036;	194.357;
1.80;	228.029;	177.988;		1.90;	229.154;	194.414;
1.85;	228.435;	178.325;		1.93;	229.437;	194.104;
1.90;	228.052;	177.712;		1.96;	229.482;	193.582;
1.95;	227.046;	176.350;		1.99;	229.323;	192.879;
2.00;	225.549;	174.412;		2.05;	228.516;	191.032;
2.05;	223.664;	172.052;		2.15;	226.170;	187.039;
2.10;	221.475;	169.382;		2.30;	221.482;	179.924;
2.20;	216.440;	163.348;		2.50;	214.766;	169.879;
2.30;	210.830;	156.658;				
2.50;	198.737;	142.493;		6.0; 10;		

4.3; 10;

1.70; 216.839; 190.074;

Table 6.1 (cont.)

1.80;	225.161;	196.808;
1.85;	227.253;	198.242;
1.90;	228.358;	198.756;
1.93;	228.640;	198.711;
1.96;	228.688;	198.447;
1.99;	228.535;	197.997;
2.05;	227.748;	196.646;
2.15;	225.443;	193.458;
2.30;	220.791;	187.512;

8.0; 10;

1.70;	215.204;	182.629;
1.80;	223.006;	190.524;
1.85;	224.836;	192.431;
1.89;	225.575;	193.258;
1.91;	225.744;	193.482;
1.93;	225.796;	193.596;
1.95;	225.744;	193.615;
2.00;	225.224;	193.303;
2.10;	222.951;	191.637;
2.30;	215.936;	186.398;

12.0; 10;

1.70;	214.810;	178.086;
1.80;	222.472;	185.760;
1.85;	224.227;	187.520;
1.89;	224.904;	188.202;
1.91;	225.041;	188.341;
1.93;	225.061;	188.364;
1.95;	224.976;	188.281;
2.05;	223.311;	186.627;
2.15;	220.265;	183.593;
2.30;	214.469;	177.811;

K+NaCl   angle= 165 deg;

3.5; 6;

1.80;	185.528;	146.992;
1.85;	180.673;	143.182;
1.90;	174.494;	138.031;
1.95;	167.320;	131.706;
2.00;	159.589;	124.288;
2.05;	151.084;	115.892;

4.0; 9;

1.60;	215.750;	156.473;

1.70;	223.558;	167.256;
1.75;	225.025;	169.105;
1.80;	225.218;	169.515;
1.85;	224.278;	170.176;
1.90;	222.552;	169.193;
1.95;	220.156;	167.183;
2.00;	217.188;	164.437;
2.05;	213.724;	161.128;

4.3; 10;

1.60;	215.908;	164.213;
1.70;	227.102;	175.700;
1.80;	230.959;	179.799;
1.85;	231.158;	179.850;
1.90;	230.566;	178.790;
1.95;	229.270;	177.303;
2.00;	227.431;	175.378;
2.10;	222.669;	169.824;
2.30;	210.149;	155.138;
2.50;	194.855;	138.358;

4.5; 10;

1.60;	210.790;	168.166;
1.70;	225.316;	179.878;
1.80;	231.298;	184.356;
1.85;	232.245;	184.725;
1.90;	232.258;	184.166;
1.95;	231.570;	182.834;
2.00;	230.357;	180.869;
2.10;	226.675;	176.064;
2.30;	216.657;	163.093;
2.50;	204.626;	148.112;

4.7; 10;

1.60;	205.275;	171.117;
1.70;	221.721;	183.067;
1.80;	229.466;	187.798;
1.85;	231.165;	188.329;
1.90;	231.834;	187.967;
1.95;	231.714;	186.897;
2.00;	230.995;	185.264;
2.10;	228.330;	180.740;
2.30;	220.182;	169.173;
2.50;	210.416;	155.837;

5.0; 12;

1.70;	218.272;	186.353;
1.80;	226.749;	191.471;

Table 6.1 (cont.)

1.85; 228.862; 192.183;
1.90; 229.956; 192.006;
1.93; 230.220; 191.558;
1.96; 230.241; 190.896;
1.99; 230.056; 190.053;
2.05; 229.190; 187.918;
2.10; 228.084; 185.785;
2.20; 225.204; 180.843;
2.30; 221.755; 175.424;
2.50; 214.204; 163.890;

6.0; 10;

1.70; 217.152; 190.002;
1.80; 225.549; 196.464;
1.85; 227.676; 197.759;
1.90; 228.812; 198.130;
1.93; 229.113; 197.996;
1.96; 229.177; 197.643;
1.99; 229.041; 197.102;
2.05; 228.281; 195.564;
2.15; 226.007; 192.052;
2.30; 221.368; 185.597;

8.0; 10;

1.70; 215.332; 183.523;
1.80; 223.178; 191.447;
1.85; 225.031; 193.377;
1.89; 225.791; 194.222;
1.91; 225.970; 194.455;
1.93; 226.034; 194.578;
1.95; 225.993; 194.604;
2.00; 225.502; 194.313;
2.10; 223.294; 192.643;
2.30; 216.439; 187.246;

12.0; 10;

1.70; 214.817; 178.126;
1.80; 222.482; 185.802;
1.85; 224.237; 187.564;
1.89; 224.915; 188.246;
1.91; 225.053; 188.386;
1.93; 225.074; 188.409;
1.95; 224.989; 188.327;
2.05; 223.326; 186.676;
2.15; 220.284; 183.645;
2.30; 214.492; 177.866;

K+NaCl   angle= 180 deg;

4.0; 4;

1.91; 218.245; 165.475;
1.95; 215.657; 163.260;
2.00; 211.816; 159.876;
2.20; 190.705; 141.330;

4.25; 7;

1.60; 218.618; 162.611;
1.70; 227.584; 173.547;
1.80; 230.023; 176.985;
1.90; 228.399; 175.527;
2.10; 217.967; 164.192;
2.30; 201.661; 147.120;
2.50; 180.338; 126.990;

4.5; 11;

1.60; 214.136; 167.799;
1.70; 227.338; 179.193;
1.80; 232.266; 183.300;
1.89; 232.563; 182.908;
1.92; 232.085; 182.159;
1.95; 231.386; 181.166;
2.00; 229.812; 179.046;
2.10; 225.488; 173.469;
2.30; 213.779; 159.029;
2.50; 199.253; 142.289;
2.70; 181.723; 124.134;

4.7; 6;

1.60; 207.578; 170.819;
1.70; 223.652; 182.516;
1.80; 230.887; 186.995;
1.90; 232.712; 186.864;
2.00; 231.355; 183.817;
2.10; 228.156; 178.942;

5.0; 13;

1.70; 218.863; 185.938;
1.80; 227.352; 190.872;
1.85; 229.456; 191.493;
1.91; 230.646; 191.081;
1.93; 230.782; 190.717;
1.95; 230.810; 190.257;
1.98; 230.670; 189.409;
2.01; 230.343; 188.392;
2.05; 229.662; 186.818;
2.10; 228.498; 184.564;

Table 6.1 (cont.)

2.20;	225.434;	179.369;		3.0;	225.093;	218.056;
2.30;	221.755;	173.589;		3.1;	225.322;	215.527;
2.50;	213.435;	161.142;		3.3;	222.753;	206.453;
				3.5;	215.513;	193.228;

6.0; 10;

4.5; 13;

1.70;	217.216;	189.920;		2.5;	217.176;	191.475;
1.80;	225.634;	196.289;		2.6;	225.304;	202.099;
1.85;	227.770;	197.535;		2.7;	230.077;	209.703;
1.91;	229.044;	197.827;		2.8;	232.490;	215.144;
1.93;	229.218;	197.691;		2.90;	233.257;	219.037;
1.95;	229.287;	197.457;		3.0;	232.889;	221.809;
1.97;	229.261;	197.134;		3.1;	231.751;	223.732;
2.00;	229.067;	196.504;		3.3;	228.454;	225.139;
2.10;	227.304;	193.433;		3.5;	228.614;	222.117;
2.30;	221.474;	184.858;		3.7;	229.404;	216.739;
				3.8;	229.290;	213.616;

8.0; 11;

4.0;	227.982;	206.506;
4.2;	224.710;	197.824;

1.70;	215.384;	183.851;		5.0;	10;	
1.80;	223.247;	191.778;				
1.85;	225.110;	193.711;		2.5;	218.206;	185.525;
1.89;	225.877;	194.559;		2.6;	226.174;	195.127;
1.91;	226.061;	194.793;		2.7;	230.813;	201.871;
1.93;	226.129;	194.918;		2.8;	233.127;	206.594;
1.95;	226.092;	194.945;		2.9;	233.837;	209.905;
1.97;	225.962;	194.885;		3.0;	233.460;	212.245;
2.05;	224.688;	193.961;		3.1;	232.367;	213.931;
2.15;	221.934;	191.779;		3.3;	228.996;	216.176;
2.30;	216.642;	187.506;		3.5;	225.000;	217.717;
				3.7;	221.004;	218.715;

12.0; 10;

6.0; 10;

1.70;	214.820;	178.140;		2.5;	218.022;	175.947;
1.80;	222.485;	185.817;		2.6;	225.674;	184.082;
1.85;	224.241;	187.579;		2.7;	229.995;	189.493;
1.89;	224.920;	188.262;		2.75;	231.232;	191.438;
1.91;	225.057;	188.402;		2.8;	231.988;	192.986;
1.93;	225.078;	188.425;		2.85;	232.345;	194.203;
1.95;	224.994;	188.343;		2.9;	232.373;	195.148;
2.05;	223.333;	186.693;		3.0;	231.670;	196.404;
2.15;	220.291;	183.663;		3.2;	228.374;	197.332;
2.30;	214.501;	177.886;		3.5;	221.623;	197.191;

→

Na+KCl   zero angle;

4.0; 8;

8.0; 8;

2.6;	217.520;	205.131;		2.5;	217.811;	169.983;
2.7;	221.774;	212.407;		2.6;	225.289;	177.456;
2.8;	223.720;	216.799;		2.7;	229.427;	181.592;
2.9;	224.502;	218.620;				

Table 6.1 (cont.)

2.8;	231.231;	183.391;
2.9;	231.421;	183.576;
3.1;	228.883;	181.025;
3.3;	224.413;	177.644;
3.5;	219.313;	175.716;

12.0; 9;

2.5;	217.760;	169.394;
2.60;	225.201;	176.838;
2.70;	229.304;	180.944;
2.8;	231.071;	182.713;
2.85;	231.312;	182.955;
2.95;	230.860;	182.505;
3.1;	228.601;	180.250;
3.3;	224.042;	175.697;
3.5;	218.845;	170.504;

Na+KCl   angle=15 deg;

4.0; 9;

2.6;	220.371;	206.227;
2.7;	224.941;	213.767;
2.8;	227.166;	218.646;
2.9;	227.968;	221.332;
3.0;	228.293;	222.039;
3.1;	228.771;	220.967;
3.3;	229.131;	214.933;
3.5;	226.772;	205.579;
3.7;	218.879;	194.520;

4.5; 13;

2.5;	217.975;	191.101;
2.6;	226.063;	201.679;
2.7;	230.821;	209.179;
2.8;	233.249;	214.487;
2.9;	234.059;	218.245;
3.0;	233.761;	220.905;
3.1;	232.720;	222.770;
3.3;	229.453;	224.671;
3.5;	227.498;	223.386;
3.7;	229.033;	219.371;
3.8;	229.637;	216.939;
4.0;	229.593;	211.658;
4.2;	228.539;	205.896;

5.0; 10;

2.5;	218.494;	185.213;

2.6;	226.446;	194.664;
2.7;	231.053;	201.270;
2.8;	233.320;	205.852;
2.9;	233.982;	209.006;
3.0;	233.564;	211.175;
3.1;	232.435;	212.681;
3.3;	229.012;	214.553;
3.5;	224.993;	215.742;
3.7;	220.989;	216.675;

6.0; 10;

2.5;	218.066;	175.898;
2.6;	225.706;	183.923;
2.7;	230.016;	189.224;
2.75;	231.246;	191.114;
2.8;	231.995;	192.606;
2.85;	232.346;	193.769;
2.9;	232.367;	194.657;
3.0;	231.649;	195.801;
3.2;	228.312;	196.502;
3.5;	221.468;	195.990;

8.0; 8;

2.5;	217.814;	169.967;
2.6;	225.289;	177.439;
2.7;	229.426;	181.573;
2.8;	231.227;	183.370;
2.9;	231.414;	183.551;
3.1;	228.869;	180.989;
3.3;	224.392;	177.294;
3.5;	219.284;	175.270;

12.0; 9;

2.5;	217.760;	169.394;
2.60;	225.201;	176.838;
2.70;	229.304;	180.944;
2.8;	231.071;	182.713;
2.85;	231.312;	182.955;
2.95;	230.860;	182.505;
3.1;	228.601;	180.250;
3.3;	224.042;	175.697;
3.5;	218.845;	170.504;

Na+KCl   angle=30 deg;

3.0; 6;

2.8;	145.641;	124.555;

Table6.1 (cont.)

2.9;	137.360;	118.367;
3.0;	126.620;	110.322;
3.1;	114.051;	100.718;
3.3;	84.636;	78.061;
3.5;	52.073;	50.737;

3.5;   8;

2.4;	190.572;	176.827;
2.5;	204.110;	191.713;
2.6;	212.941;	201.448;
2.8;	221.846;	210.225;
3.0;	224.072;	209.847;
3.2;	222.077;	204.340;
3.4;	216.670;	196.215;
3.7;	204.087;	181.300;

4.0;   12;

2.5;	217.166;	196.130;
2.6;	225.499;	206.957;
2.7;	230.490;	214.474;
2.8;	233.152;	219.585;
2.9;	234.234;	222.920;
3.0;	234.308;	224.908;
3.1;	233.849;	225.821;
3.3;	232.632;	225.072;
3.5;	232.497;	221.852;
3.7;	231.981;	217.403;
4.0;	230.063;	210.003;
4.3;	226.956;	202.265;

4.5;   13;

2.5;	219.091;	190.443;
2.6;	227.172;	200.406;
2.7;	231.920;	207.340;
2.8;	234.339;	212.114;
2.9;	235.150;	215.362;
3.0;	234.871;	217.539;
3.1;	233.871;	218.972;
3.3;	230.697;	220.430;
3.5;	227.026;	220.694;
3.7;	224.105;	219.725;
3.8;	223.569;	218.653;
4.0;	224.023;	215.006;
4.2;	224.691;	212.608;

5.0;   10;

2.5;	218.801;	184.667;
2.6;	226.663;	193.646;

2.7;	231.190;	199.760;
2.8;	233.385;	203.843;
2.9;	233.971;	206.501;
3.0;	233.468;	208.174;
3.1;	232.246;	209.180;
3.3;	228.623;	210.035;
3.5;	224.400;	210.192;
3.7;	220.201;	210.182;

6.0;   10;

2.5;	218.130;	175.768;
2.6;	225.732;	183.505;
2.7;	229.999;	188.513;
2.75;	231.207;	190.257;
2.8;	231.933;	191.603;
2.85;	232.260;	192.618;
2.9;	232.256;	193.360;
3.0;	231.485;	194.208;
3.2;	228.036;	194.304;
3.5;	221.000;	192.842;

8.0;   8;

2.5;	217.819;	169.927;
2.6;	225.287;	177.394;
2.7;	229.417;	181.524;
2.8;	231.211;	183.316;
2.9;	231.391;	183.492;
3.1;	228.829;	180.400;
3.3;	224.334;	176.413;
3.5;	219.203;	174.076;

12.0;   9;

2.5;	217.758;	169.378;
2.60;	225.198;	176.821;
2.7;	229.300;	180.926;
2.8;	231.065;	182.694;
2.85;	231.305;	182.935;
2.95;	230.852;	182.484;
3.1;	228.590;	180.227;
3.3;	224.028;	175.671;
3.5;	218.828;	170.475;

Na+KCl   angle=45 deg;

3.0;   6;

2.8;	217.622;	200.024;
2.9;	219.948;	201.664;

Table 6.1 (cont.)

3.0;	220.956;	202.081;
3.1;	221.041;	201.724;
3.3;	219.563;	199.719;
3.5;	217.142;	196.985;

3.5; 9;

2.4;	202.983;	182.592;
2.5;	216.865;	198.165;
2.6;	226.023;	208.680;
2.8;	235.375;	220.047;
3.0;	238.233;	223.938;
3.2;	238.288;	224.023;
3.4;	237.262;	222.251;
3.7;	235.115;	218.271;
4.0;	232.930;	214.099;

4.0; 13;

2.4;	208.045;	176.995;
2.5;	220.713;	193.333;
2.6;	228.765;	204.342;
2.7;	233.634;	211.451;
2.8;	236.230;	216.047;
2.9;	237.246;	218.926;
3.0;	237.192;	220.608;
3.1;	236.441;	221.449;
3.3;	233.863;	221.522;
3.5;	230.933;	220.338;
3.7;	228.410;	218.456;
4.0;	225.893;	214.955;
4.3;	224.443;	211.244;

4.5; 11;

2.5;	219.908;	188.664;
2.6;	227.913;	197.575;
2.7;	232.575;	203.565;
2.8;	234.745;	207.858;
2.9;	235.316;	210.535;
3.0;	234.840;	212.029;
3.1;	233.660;	212.753;
3.3;	230.130;	212.852;
3.5;	225.997;	212.060;
3.7;	221.903;	210.926;
4.0;	216.538;	208.947;

5.0; 10;

2.5;	218.980;	183.823;
2.6;	226.728;	192.132;
2.7;	231.144;	197.567;

2.8;	233.232;	200.968;
2.9;	233.720;	202.944;
3.0;	233.108;	203.967;
3.1;	231.702;	204.396;
3.3;	227.707;	204.039;
3.5;	223.128;	202.934;
3.7;	218.553;	201.660;

6.0; 10;

2.5;	218.150;	175.694;
2.6;	225.703;	183.073;
2.7;	229.919;	187.670;
2.75;	231.100;	189.207;
2.8;	231.800;	190.347;
2.85;	232.098;	191.158;
2.9;	232.067;	191.698;
3.0;	231.238;	192.147;
3.2;	227.665;	191.458;
3.5;	220.431;	188.831;

8.0; 8;

2.5;	217.817;	169.881;
2.6;	225.277;	177.343;
2.7;	229.398;	181.468;
2.8;	231.184;	183.255;
2.9;	231.354;	183.426;
3.1;	228.772;	180.779;
3.3;	224.255;	176.193;
3.5;	219.100;	172.505;

12.0; 9;

2.5;	217.758;	169.378;
2.60;	225.198;	176.821;
2.7;	229.300;	180.926;
2.8;	231.065;	182.694;
2.85;	231.305;	182.935;
2.95;	230.852;	182.484;
3.1;	228.590;	180.227;
3.3;	224.028;	175.671;
3.5;	218.828;	170.475;

Na+KCl   angle= 60 deg;

2.5; 8;

2.8;	214.408;	190.060;
2.9;	218.922;	193.313;
3.0;	222.120;	195.760;
3.1;	224.380;	197.662;

Table 6.1 (cont.)

3.3;	227.120;	200.217;
3.5;	228.631;	201.517;
3.7;	229.660;	202.172;
4.0;	230.835;	202.653;

3.0; 13;

2.4;	202.475;	182.241;
2.5;	217.732;	196.903;
2.6;	227.986;	206.562;
2.7;	234.701;	212.728;
2.8;	238.928;	216.447;
2.9;	241.417;	218.463;
3.0;	242.705;	219.316;
3.1;	243.170;	219.410;
3.3;	242.610;	218.387;
3.5;	241.022;	216.622;
3.7;	239.047;	214.572;
4.0;	235.980;	211.402;
4.3;	233.107;	208.294;

3.5; 9;

2.4;	209.112;	181.728;
2.5;	222.508;	195.920;
2.6;	231.147;	205.713;
2.8;	239.449;	215.964;
3.0;	241.086;	218.984;
3.2;	239.652;	218.570;
3.4;	236.973;	216.619;
3.7;	232.437;	212.737;
4.0;	228.204;	208.773;

4.0; 12;

2.4;	208.752;	179.176;
2.5;	221.520;	192.250;
2.6;	229.568;	200.983;
2.7;	234.275;	206.626;
2.8;	236.635;	210.102;
2.9;	237.371;	212.061;
3.0;	237.012;	212.930;
3.1;	235.936;	213.023;
3.3;	232.597;	211.794;
3.5;	228.630;	209.640;
3.7;	224.650;	207.179;
4.0;	219.208;	203.485;

4.5; 11;

2.5;	219.948;	187.683;
2.6;	227.716;	195.822;
2.7;	232.148;	200.996;

2.8;	234.245;	204.075;
2.9;	234.726;	205.691;
3.0;	234.108;	206.298;
3.1;	232.759;	206.222;
3.3;	228.843;	204.877;
3.5;	224.290;	202.771;
3.7;	219.726;	200.454;
4.0;	213.405;	197.109;

5.0; 10;

2.5;	218.943;	183.372;
2.6;	226.572;	191.018;
2.7;	230.864;	195.777;
2.8;	232.820;	198.516;
2.9;	233.161;	199.854;
3.0;	232.404;	200.235;
3.1;	230.918;	199.974;
3.3;	226.735;	198.357;
3.5;	221.906;	196.109;
3.7;	217.055;	193.751;

6.0; 10;

2.5;	218.119;	175.852;
2.6;	225.628;	183.103;
2.7;	229.800;	187.330;
2.75;	230.959;	188.645;
2.8;	231.635;	189.556;
2.85;	231.911;	190.136;
2.9;	231.856;	190.447;
3.0;	230.979;	190.448;
3.2;	227.304;	188.922;
3.5;	219.897;	185.147;

8.0; 8;

2.5;	217.807;	169.861;
2.6;	225.260;	177.320;
2.7;	229.374;	181.442;
2.8;	231.152;	183.226;
2.9;	231.314;	183.395;
3.1;	228.715;	180.792;
3.3;	224.179;	175.792;
3.5;	219.004;	171.149;

12.0; 9;

2.5;	217.758;	169.378;
2.60;	225.198;	176.821;
2.7;	229.300;	180.926;
2.8;	231.065;	182.694;
2.85;	231.305;	182.935;

Table 6.1 (cont.)

2.95; 230.852; 182.484;
3.1;   228.590; 180.227;
3.3;   224.028; 175.671;
3.5;   218.828; 170.475;

Na+KCl   angle= 75 deg;

2.5;   13;

2.4;   201.394; 182.057;
2.5;   217.197; 193.737;
2.6;   227.878; 201.062;
2.7;   234.919; 205.316;
2.8;   239.377; 207.424;
2.9;   242.009; 208.074;
3.0;   243.356; 207.787;
3.1;   243.806; 206.935;
3.3;   243.048; 204.464;
3.5;   241.100; 202.870;
3.7;   238.669; 201.523;
4.0;   234.811; 198.199;
4.3;   230.976; 194.477;

3.0;   13;

2.4;   210.922; 180.460;
2.5;   224.749; 193.175;
2.6;   233.713; 201.868;
2.7;   239.254; 207.289;
2.8;   242.397; 210.240;
2.9;   243.863; 211.477;
3.0;   244.168; 211.559;
3.1;   243.679; 210.876;
3.3;   241.299; 208.218;
3.5;   238.032; 204.831;
3.7;   234.516; 201.345;
4.0;   229.368; 196.425;
4.3;   224.640; 192.072;

3.5;   9;

2.4;   210.908; 180.342;
2.5;   223.834; 192.444;
2.6;   232.034; 200.239;
2.8;   239.399; 207.528;
3.0;   240.032; 208.705;
3.2;   237.595; 206.931;
3.4;   233.920; 203.832;
3.7;   227.870; 198.555;
4.0;   222.133; 193.537;

4.0;   12;

2.4;   209.088; 178.220;
2.5;   221.632; 190.015;
2.6;   229.466; 197.552;
2.7;   233.971; 202.078;
2.8;   236.142; 204.493;
2.9;   236.700; 205.440;
3.0;   236.159; 205.381;
3.1;   234.889; 204.645;
3.3;   231.126; 202.021;
3.5;   226.707; 198.730;
3.7;   222.251; 195.315;
4.0;   216.027; 190.491;

4.5;   10;

2.5;   219.935; 186.947;
2.6;   227.588; 194.262;
2.7;   231.911; 198.608;
2.8;   233.902; 200.882;
2.9;   234.280; 201.723;
3.0;   233.562; 201.598;
3.1;   232.116; 200.827;
3.3;   228.013; 198.201;
3.5;   223.266; 194.975;
3.7;   218.495; 191.686;

5.0;   9;

2.5;   218.922; 183.603;
2.6;   226.481; 190.743;
2.7;   230.707; 194.926;
2.8;   232.599; 197.061;
2.9;   232.878; 197.794;
3.0;   232.061; 197.582;
3.1;   230.516; 196.750;
3.3;   226.216; 194.066;
3.5;   221.274; 190.850;

6.0;   10;

2.5;   218.088; 176.588;
2.6;   225.573; 183.858;
2.7;   229.719; 187.941;
2.75; 230.866; 189.124;
2.8;   231.530; 189.872;
2.85; 231.793; 190.269;
2.9;   231.725; 190.381;
3.0;   230.822; 189.965;
3.2;   227.097; 187.606;
3.5;   219.614; 182.717;

8.0;   8;

Table 6.1 (cont.)

2.5;	217.96;	169.923;	4.0;	222.308;	177.759;
2.6;	225.243;	177.382;	4.3;	217.143;	172.929;
2.7;	229.353;	181.504;			
2.8;	231.125;	183.291;	3.5;	9;	
2.9;	231.282;	183.463;			
3.1;	228.673;	180.884;	2.4;	210.332;	178.276;
3.3;	224.126;	176.319;	2.5;	222.935;	188.782;
3.5;	218.941;	171.121;	2.6;	230.855;	195.053;
			2.8;	237.736;	199.642;
12.0;	9;		3.0;	237.966;	198.511;
			3.2;	235.149;	194.908;
2.5;	217.755;	169.382;	3.4;	231.092;	190.631;
2.6;	225.194;	176.825;	3.7;	224.545;	184.178;
2.7;	229.295;	180.929;	4.0;	218.415;	178.287;
2.8;	231.059;	182.696;			
2.85;	231.298;	182.938;	4.0;	12;	
2.95;	230.843;	182.486;			
3.1;	228.580;	180.228;	2.4;	209.087;	176.579;
3.3;	224.015;	175.670;	2.5;	221.494;	187.516;
3.5;	218.811;	170.473;	2.6;	229.210;	194.167;
			2.7;	233.611;	197.607;
			2.8;	235.691;	199.358;
Na+KCl	angle= 90 deg;		2.9;	236.166;	199.481;
			3.0;	235.547;	198.649;
2.5;	13;		3.1;	234.201;	197.197;
			3.3;	230.295;	193.307;
2.4;	205.928;	182.784;	3.5;	225.732;	188.960;
2.5;	219.799;	192.031;	3.7;	221.124;	184.693;
2.6;	228.806;	197.293;	4.0;	214.697;	178.879;
2.7;	234.404;	199.691;			
2.8;	237.596;	200.182;	4.5;	10;	
2.9;	239.106;	199.409;			
3.0;	239.454;	197.814;	2.5;	220.107;	186.077;
3.1;	239.011;	195.704;	2.6;	227.715;	192.852;
3.3;	236.734;	190.758;	2.7;	231.998;	196.609;
3.5;	233.586;	185.695;	2.8;	233.954;	198.274;
3.7;	230.215;	181.442;	2.9;	234.304;	198.507;
4.0;	225.370;	177.035;	3.0;	233.562;	197.779;
4.3;	220.913;	173.115;	3.1;	232.096;	196.426;
			3.3;	227.958;	192.716;
3.0;	13;		3.5;	223.180;	188.529;
			3.7;	218.379;	184.402;
2.4;	210.462;	180.998;			
2.5;	223.440;	190.217;	5.0;	9;	
2.6;	231.704;	195.203;			
2.7;	236.624;	197.069;	2.5;	219.097;	184.011;
2.8;	239.189;	197.047;	2.6;	226.641;	190.862;
2.9;	240.132;	197.182;	2.7;	230.855;	194.673;
3.0;	239.966;	196.984;	2.8;	232.738;	196.382;
3.1;	239.050;	195.836;	2.9;	233.009;	196.660;
3.3;	235.935;	192.072;	3.0;	232.185;	195.982;
3.5;	232.063;	187.731;	3.1;	230.637;	194.683;
3.7;	228.048;	183.483;	3.3;	226.335;	191.095;

Table 6.1 (cont.)

3.5; 221.398; 187.039;   3.0; 12;

6.0; 10;

    2.4; 204.347; 164.886;
2.5; 218.139; 178.176;   2.5; 216.824; 175.331;
2.6; 225.619; 185.343;   2.6; 224.694; 181.228;
2.7; 229.762; 189.318;   2.7; 229.310; 183.902;
2.75; 230.906; 190.432;   2.8; 231.649; 184.268;
2.8; 231.569; 191.099;   2.9; 232.416; 182.941;
2.85; 231.830; 191.398;   3.0; 232.118; 180.317;
2.9; 231.761; 191.399;   3.1; 231.115; 176.749;
3.0; 230.857; 190.724;   3.3; 227.942; 170.086;
3.2; 227.130; 187.755;   3.5; 224.104; 167.490;
3.5; 219.646; 181.909;   3.7; 220.187; 166.462;
    4.0; 214.736; 156.514;

8.0; 8;   3.5; 8;

2.5; 217.793; 170.183;   2.4; 207.484; 169.307;
2.6; 225.239; 177.647;   2.5; 219.998; 180.519;
2.7; 229.347; 181.779;   2.6; 227.831; 187.086;
2.8; 231.118; 183.579;   2.8; 234.571; 191.503;
2.9; 231.274; 183.769;   3.0; 234.706; 189.625;
3.1; 228.662; 181.249;   3.2; 231.837; 185.000;
3.3; 224.112; 176.835;   3.4; 227.780; 179.384;
3.5; 218.924; 171.909;   3.7; 221.266; 170.831;

12.0; 9;   4.0; 12;

2.5; 217.755; 169.382;   2.4; 208.476; 172.605;
2.6; 225.194; 176.825;   2.5; 220.873; 183.403;
2.7; 229.295; 180.929;   2.6; 228.581; 189.767;
2.8; 231.059; 182.696;   2.7; 232.967; 193.010;
2.85; 231.298; 182.938;   2.8; 235.023; 194.090;
2.95; 230.843; 182.486;   2.9; 235.475; 193.701;
3.1; 228.580; 180.228;   3.0; 234.840; 192.333;
3.3; 224.015; 175.670;   3.1; 233.482; 190.335;
3.5; 218.811; 170.473;   3.3; 229.562; 185.357;
    3.5; 224.995; 179.974;
    3.7; 220.393; 174.355;
Na+KCl   angle= 105 deg;   4.0; 213.968; 167.719;

2.5; 8;   4.5; 10;

2.6; 216.740; 183.786;   2.5; 220.372; 184.093;
2.7; 221.596; 185.539;   2.6; 227.990; 190.602;
2.8; 224.138; 185.340;   2.7; 232.287; 194.023;
2.9; 225.083; 183.685;   2.8; 234.261; 195.300;
3.0; 224.967; 181.234;   2.9; 234.630; 195.112;
3.1; 224.162; 178.382;   3.0; 233.906; 193.945;
3.3; 221.431; 172.202;   3.1; 232.456; 192.144;
3.5; 218.143; 165.981;   3.3; 228.354; 187.545;
    3.5; 223.618; 182.501;

Table6.1 (cont.)

3.7; 218.862; 177.571;

5.0; 9;

2.5; 219.529; 183.822;
2.6; 227.094; 190.475;
2.7; 231.332; 194.037;
2.8; 233.241; 195.456;
2.9; 233.541; 195.412;
3.0; 232.750; 194.390;
3.1; 231.234; 192.732;
3.3; 227.002; 188.411;
3.5; 222.135; 183.631;

6.0; 10;

2.5; 218.346; 180.227;
2.6; 225.841; 187.211;
2.7; 230.001; 191.031;
2.75; 231.155; 192.071;
2.8; 231.826; 192.661;
2.85; 232.097; 192.883;
2.9; 232.036; 192.802;
3.0; 231.154; 191.949;
3.2; 227.471; 188.572;
3.5; 220.059; 182.026;

8.0; 8;

2.5; 217.808; 170.827;
2.6; 225.256; 178.305;
2.7; 229.367; 182.458;
2.8; 231.140; 184.289;
2.9; 231.298; 184.519;
3.1; 228.691; 182.108;
3.3; 224.147; 177.858;
3.5; 218.964; 173.126;

12.0; 9;

2.5; 217.755; 169.382;
2.6; 225.194; 176.825;
2.7; 229.295; 180.929;
2.8; 231.059; 182.696;
2.85; 231.298; 182.938;
2.95; 230.843; 182.486;
3.1; 228.580; 180.228;
3.3; 224.015; 175.670;
3.5; 218.811; 170.473;
Na+KCl   angle= 120 deg;

2.5; 6;

2.8; 196.129; 149.999;
2.9; 196.100; 149.227;
3.0; 195.143; 147463;
3.1; 193.614; 145.079;
3.3; 189.768; 139.470;
3.5; 185.787; 134.084;

3.0; 6;

2.8; 219.086; 167.889;
2.9; 219.297; 167.000;
3.0; 218.483; 165.059;
3.1; 217.005; 162.405;
3.3; 213.006; 155.851;
3.5; 208.556; 148.626;

3.5; 7;

2.4; 202.249; 152.702;
2.5; 214.611; 164.137;
2.6; 222.319; 170.903;
2.8; 228.853; 175.833;
3.0; 228.788; 174.660;
3.2; 225.703; 170.590;
3.4; 221.454; 165.380;

4.0; 10;

2.5; 219.003; 175.406;
2.6; 226.705; 182.025;
2.7; 231.093; 185.413;
2.8; 233.160; 186.550;
2.9; 233.622; 186.138;
3.0; 232.992; 184.685;
3.1; 231.637; 182.551;
3.3; 227.713; 177.187;
3.5; 223.122; 171.314;
3.7; 218.499; 165.505;

4.5; 10;

2.5; 220.331; 180.432;
2.6; 227.961; 186.900;
2.7; 232.273; 190.205;
2.8; 234.262; 191.309;
2.9; 234.646; 190.901;
3.0; 233.940; 189.476;
3.1; 232.510; 187.388;
3.3; 228.447; 182.145;
3.5; 223.743; 176.400;
3.7; 219.015; 170.737;

Table 6.1 (cont.)

5.0; 10;

2.5;	220.090;	182.540;	Na+KCl	angle= 135 deg;
2.6;	227.682;	189.036;		
2.7;	231.950;	192.407;	3.5; 6;	
2.8;	233.893;	193.605;		
2.9;	234.229;	193.313;	2.5;	206.970;	157.637;
3.0;	233.475;	192.020;	2.6;	214.064;	164.222;
3.1;	231.997;	190.074;	2.8;	219.282;	168.370;
3.3;	227.842;	185.135;	3.0;	217.839;	165.855;
3.5;	223.054;	179.703;	3.2;	213.357;	160.270;
3.7;	218.250;	174.348;	3.4;	207.679;	153.403;

6.0; 10;   4.0; 10;

2.5;	218.750;	182.120;
2.6;	226.275;	188.865;
2.7;	230.468;	192.400;
2.75;	231.640;	193.425;
2.8;	232.330;	193.923;
2.85;	232.620;	194.053;
2.9;	232.580;	193.882;
3.0;	231.737;	192.847;
3.2;	228.139;	189.089;
3.5;	220.866;	181.919;

2.5;	215.671;	169.774;
2.6;	223.359;	173.577;
2.7;	227.508;	177.064;
2.8;	229.415;	178.233;
2.9;	229.698;	177.809;
3.0;	228.873;	176.309;
3.1;	227.306;	174.106;
3.3;	222.922;	168.566;
3.5;	217.843;	162.484;
3.7;	212.694;	156.470;

8.0; 8;   4.5; 9;

2.5;	217.847;	172.048;
2.6;	225.301;	179.540;
2.7;	229.418;	183.719;
2.8;	231.198;	185.586;
2.9;	231.362;	185.862;
3.1;	228.769;	183.570;
3.3;	224.240;	179.464;
3.5;	219.074;	174.865;

2.5;	219.530;	175.296;
2.6;	227.149;	181.838;
2.7;	231.434;	185.148;
2.8;	233.391;	186.200;
2.9;	233.740;	185.698;
3.0;	232.993;	184.144;
3.1;	231.517;	181.898;
3.3;	227.347;	176.277;
3.5;	222.519;	170.094;

12.0; 9;   5.0; 10;

2.5;	217.761;	169.459;
2.6;	225.201;	176.903;
2.7;	229.302;	181.010;
2.8;	231.067;	182.779;
2.85;	231.307;	183.022;
2.95;	230.854;	182.572;
3.1;	228.592;	180.317;
3.3;	224.030;	175.764;
3.5;	218.829;	170.572;

2.5;	220.454;	180.132;
2.6;	228.055;	186.537;
2.7;	232.336;	189.782;
2.8;	234.292;	190.823;
2.9;	234.640;	190.346;
3.0;	233.892;	188.843;
3.1;	232.421;	186.668;
3.3;	228.273;	181.227;
3.5;	223.485;	175.247;
3.7;	218.670;	169.310;

Table 6.1 (cont.)

6.0; 10;

2.5;	219.299;	183.251;
2.6;	226.363;	189.767;
2.7;	231.098;	193.171;
2.75;	232.291;	194.015;
2.8;	233.004;	194.413;
2.85;	233.317;	194.445;
2.9;	233.300;	194.174;
3.0;	232.505;	192.941;
3.2;	229.010;	188.770;
3.5;	221.899;	180.929;

8.0; 8;

2.5;	217.911;	173.852;
2.6;	225.374;	181.331;
2.7;	229.500;	185.507;
2.8;	231.291;	183.379;
2.9;	231.466;	183.668;
3.1;	228.897;	185.422;
3.3;	224.395;	181.377;
3.5;	219.258;	176.831;

12.0; 9;

2.5;	217.761;	169.459;
2.6;	225.201;	176.903;
2.7;	229.302;	181.010;
2.8;	231.067;	182.779;
2.85;	231.307;	183.022;
2.95;	230.854;	182.572;
3.1;	228.592;	180.317;
3.3;	224.030;	175.764;
3.5;	218.829;	170.572;

Na+KCl   angle= 150 deg;

4.0; 8;

2.6;	218.413;	168.069;
2.7;	222.234;	171.108;
2.8;	223.657;	171.799;
2.9;	223.400;	170.918;
3.0;	221.975;	169.322;
3.1;	219.750;	167.138;
3.3;	213.872;	160.877;
3.5;	207.072;	154.112;

4.5; 9;

2.5;	217.916;	170.534;

2.6;	225.448;	177.137;
2.7;	229.639;	180.450;
2.8;	231.483;	181.462;
2.9;	231.695;	180.883;
3.0;	230.790;	179.226;
3.1;	229.131;	176.856;
3.3;	224.518;	170.943;
3.5;	219.128;	164.422;

5.0; 10;

2.5;	220.353;	177.165;
2.6;	227.930;	183.543;
2.7;	232.181;	186.724;
2.8;	234.104;	187.670;
2.9;	234.415;	187.074;
3.0;	233.627;	185.434;
3.1;	232.110;	183.106;
3.3;	227.848;	177.317;
3.5;	222.912;	170.948;
3.7;	217.914;	164.595;

6.0; 10;

2.5;	219.862;	183.556;
2.6;	227.455;	189.875;
2.7;	231.722;	193.093;
2.75;	232.932;	193.845;
2.8;	233.662;	194.153;
2.85;	233.993;	194.093;
2.9;	233.995;	193.730;
3.0;	233.237;	192.309;
3.2;	229.817;	187.743;
3.5;	222.817;	179.251;

8.0; 8;

2.5;	217.989;	175.850;
2.6;	225.463;	183.266;
2.7;	229.601;	187.389;
2.8;	231.404;	189.218;
2.9;	231.594;	189.473;
3.1;	229.056;	183.182;
3.3;	224.589;	183.111;
3.5;	219.493;	178.538;

12.0; 9;

2.5;	217.761;	169.459;
2.6;	225.201;	176.903;
2.7;	229.302;	181.010;
2.8;	231.067;	182.779;
2.65;	231.307;	183.022;

Table 6.1 (cont.)

2.95; 230.854; 182.572;
3.1;   228.592; 180.317;
3.3;   224.030; 175.764;
3.5;   218.829; 170.572;

Na+KCl   angle= 165 deg;

4.0;   8;

2.6;   213.840; 164.422;
2.7;   217.082; 167.685;
2.8;   217.859; 168.570;
2.9;   216.384; 167.705;
3.0;   214.666; 165.837;
3.1;   211.569; 163.087;
3.3;   203.666; 156.105;
3.5;   194.296; 148.022;

4.5;   9;

2.5;   216.294; 168.109;
2.6;   223.691; 174.682;
2.7;   227.717; 177.914;
2.8;   229.363; 178.796;
2.9;   229.338; 178.043;
3.0;   228.145; 176.162;
3.1;   226.153; 173.515;
3.3;   220.721; 166.847;
3.5;   214.283; 159.252;

5.0;   10;

2.5;   219.978; 174.819;
2.6;   227.511; 181.204;
2.7;   231.714; 184.354;
2.8;   233.579; 185.267;
2.9;   233.825; 184.610;
3.0;   232.963; 182.893;
3.1;   231.359; 180.476;
3.3;   226.882; 174.476;
3.5;   221.660; 167.867;
3.7;   216.288; 161.256;

6.0;   10;

2.5;   220.266; 183.394;
2.6;   227.373; 189.586;
2.7;   232.156; 192.680;
2.75; 233.374; 193.370;
2.8;   234.111; 193.614;
2.85; 234.451; 193.491;
2.9;   234.460; 193.063;

3.0;   233.718; 191.508;
3.2;   230.326; 186.656;
3.5;   223.353; 177.689;

8.0;   8;

2.5;   218.056; 177.395;
2.6;   225.540; 184.733;
2.7;   229.688; 188.787;
2.8;   231.503; 190.556;
2.9;   231.705; 190.761;
3.1;   229.194; 186.392;
3.3;   224.360; 184.261;
3.5;   219.702; 179.627;

12.0; 9;

2.5;   217.767; 169.510;
2.6;   225.208; 176.956;
2.7;   229.311; 181.064;
2.8;   231.077; 182.836;
2.85; 231.318; 183.079;
2.95; 230.865; 182.632;
3.1;   228.606; 180.382;
3.3;   224.047; 175.835;
3.5;   218.849; 170.650;

Na+KCl   angle= 180 deg;

4.0;   8;

2.6;   211.891; 163.323;
2.7;   214.885; 166.517;
2.8;   215.377; 167.295;
2.9;   214.076; 166.366;
3.0;   211.485; 164.234;
3.1;   207.959; 161.253;
3.3;   198.996; 153.634;
3.5;   188.291; 144.580;

4.5;   9;

2.5;   215.574; 167.478;
2.6;   222.898; 173.985;
2.7;   226.832; 177.126;
2.8;   228.365; 177.891;
2.9;   228.205; 176.992;
3.0;   226.862; 174.937;
3.1;   224.693; 172.080;
3.3;   218.815; 164.873;
3.5;   211.794; 157.787;

Table 6.1 (cont.)

5.0; 10;

2.5;	219.753;	173.950;
2.6;	227.270;	180.347;
2.7;	231.448;	183.509;
2.8;	233.285;	184.404;
2.9;	233.497;	183.733;
3.0;	232.594;	181.995;
3.1;	230.943;	179.550;
3.3;	226.344;	173.484;
3.5;	220.957;	166.788;
3.7;	215.352;	160.048;

6.0; 10;

2.5;	220.407;	183.261;
2.6;	228.017;	189.410;
2.7;	232.303;	192.461;
2.75;	233.523;	193.128;
2.8;	234.262;	193.351;
2.85;	234.603;	193.204;
2.9;	234.614;	192.753;
3.0;	233.874;	191.150;
3.2;	230.485;	186.195;
3.5;	223.506;	177.057;

8.0; 8;

2.5;	218.083;	177.971;
2.6;	225.571;	185.273;
2.7;	229.723;	189.296;
2.8;	231.542;	191.039;
2.9;	231.749;	191.221;
3.1;	229.250;	188.815;
3.3;	224.829;	184.654;
3.5;	219.787;	179.990;

12.0; 9;

2.5;	217.767;	169.510;
2.6;	225.208;	176.956;
2.7;	229.311;	181.064;
2.8;	231.077;	182.836;
2.85;	231.318;	183.079;
2.95;	230.865;	182.632;
3.1;	228.606;	180.382;
3.3;	224.047;	175.835;
3.5;	218.849;	170.650;

→

Figure 6.3a: First excited potential surface

θ = 180°
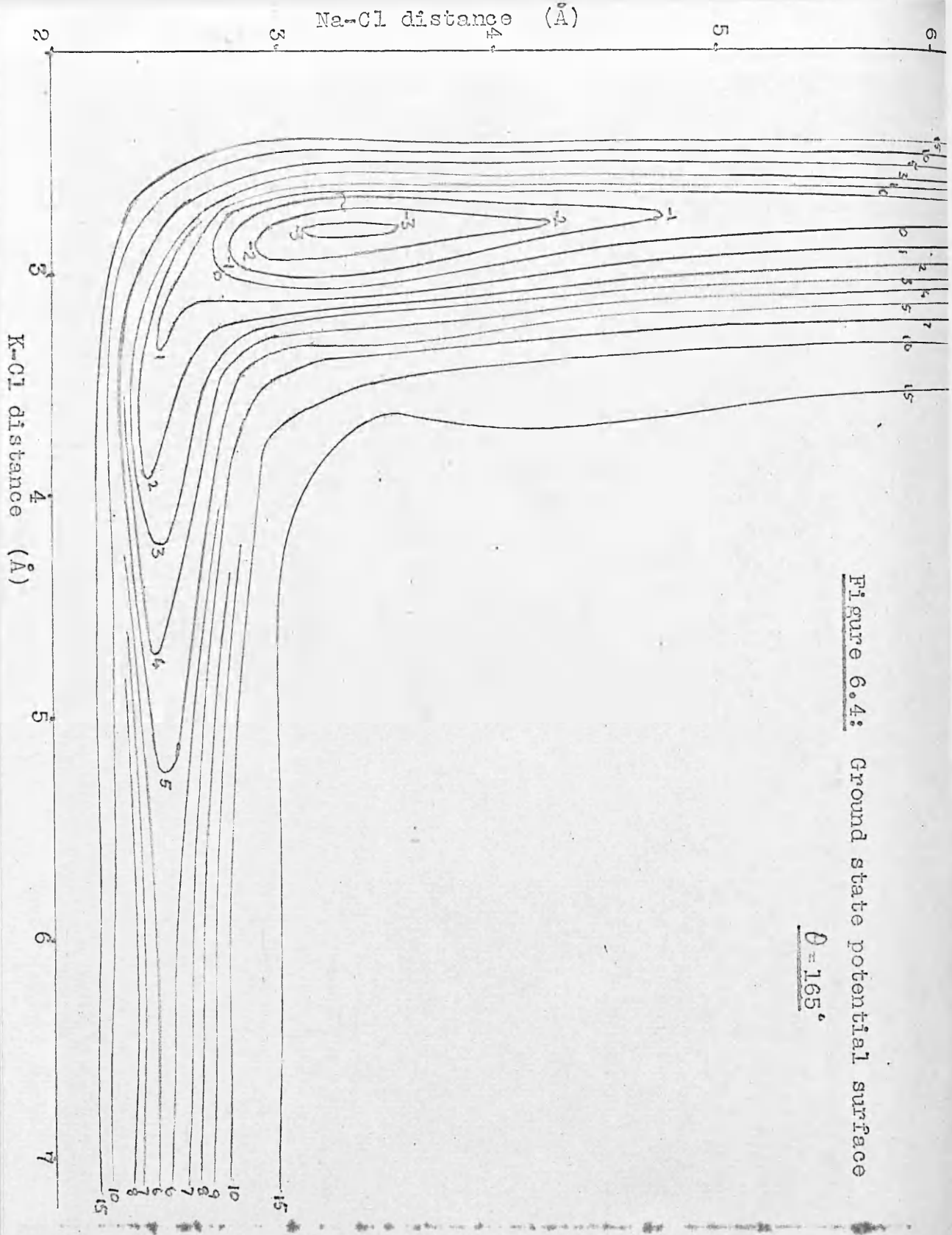
Figure 6.4: Ground state potential surface

$\theta = 165°$

I.6
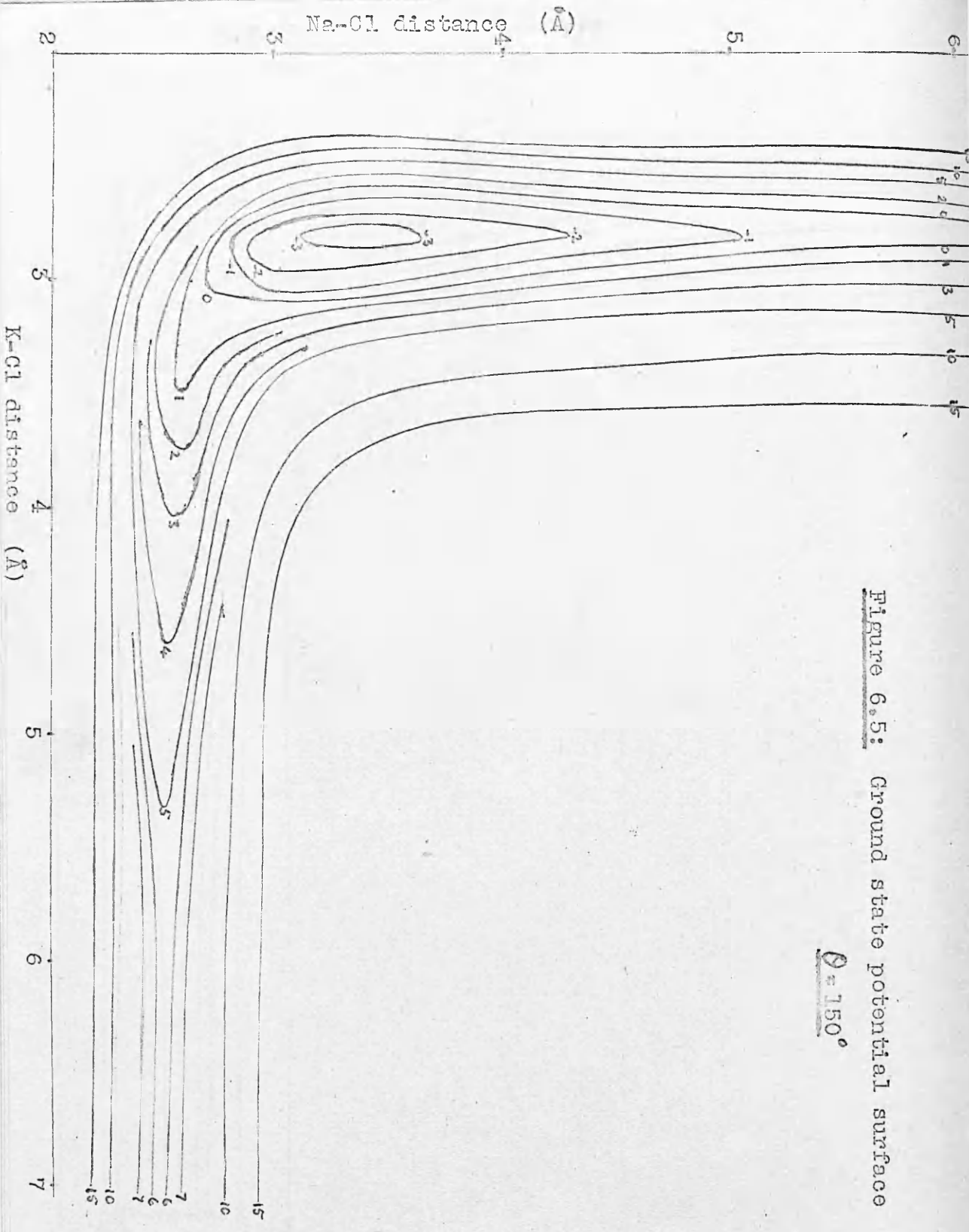
Figure 6.5: Ground state potential surface $\theta = 150°$

I.6
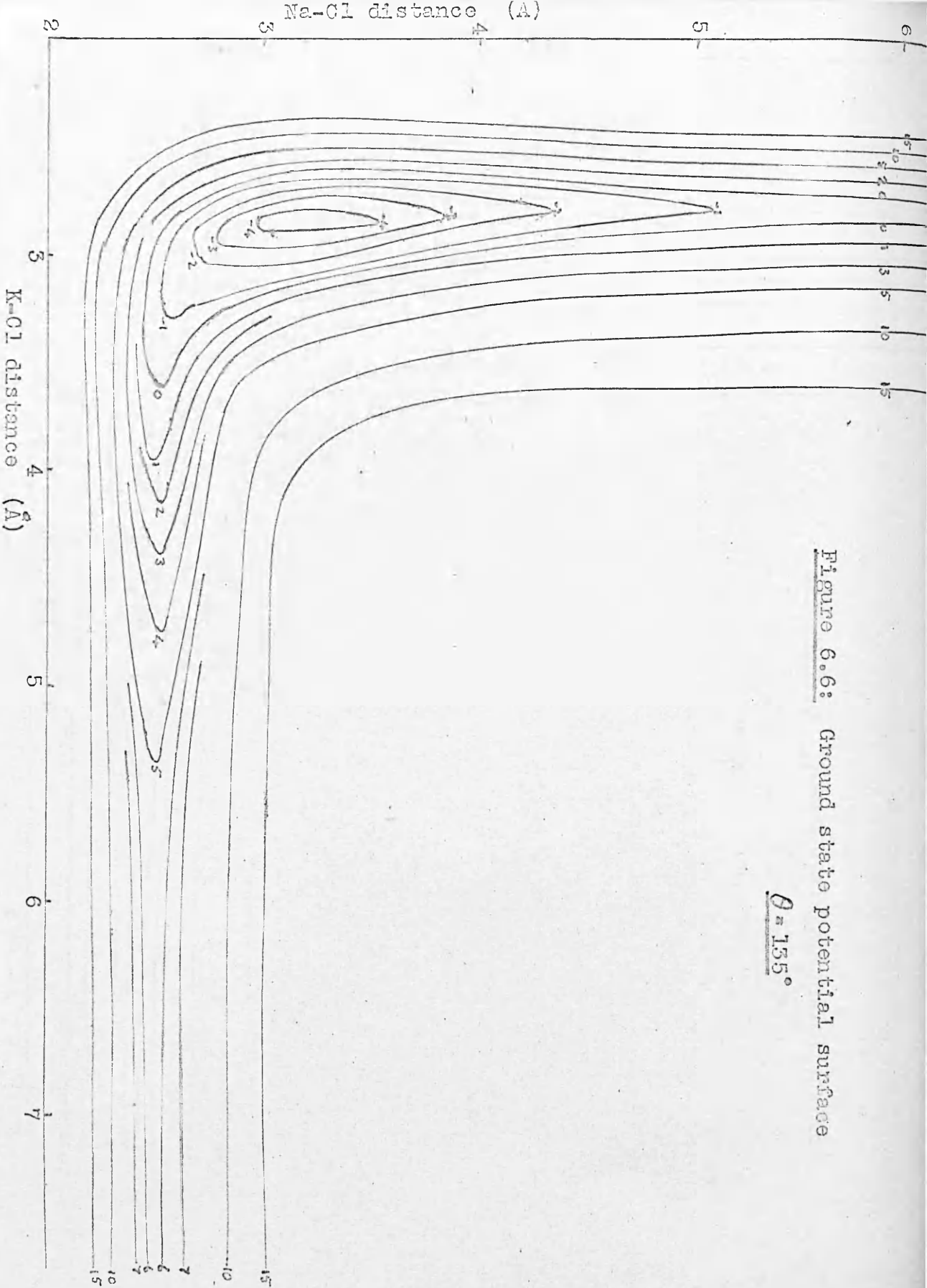
Figure 6.6: Ground state potential surface

$\theta = 155°$

I.6
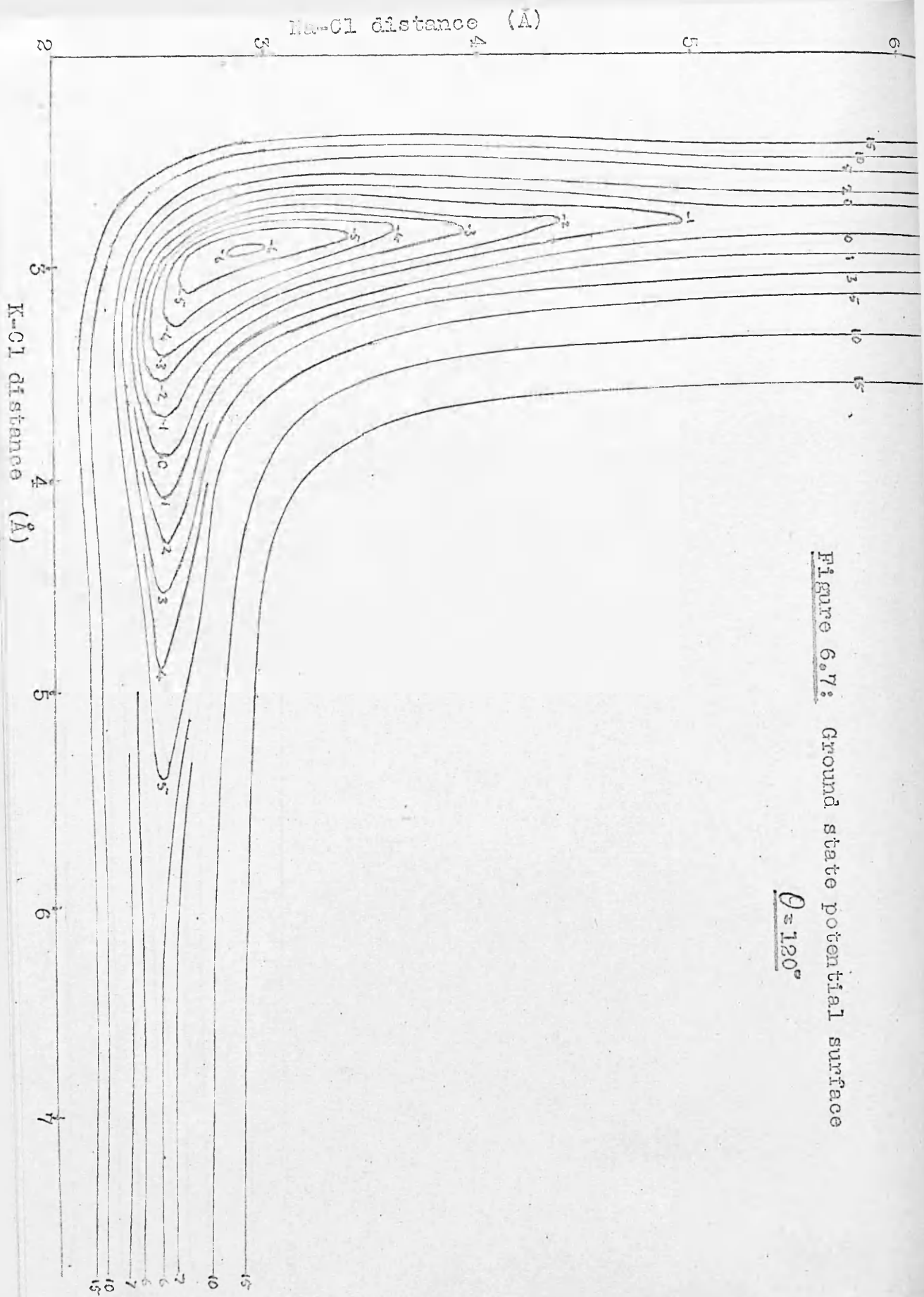
Figure 6.7: Ground state potential surface

$\theta = 120°$

I.6
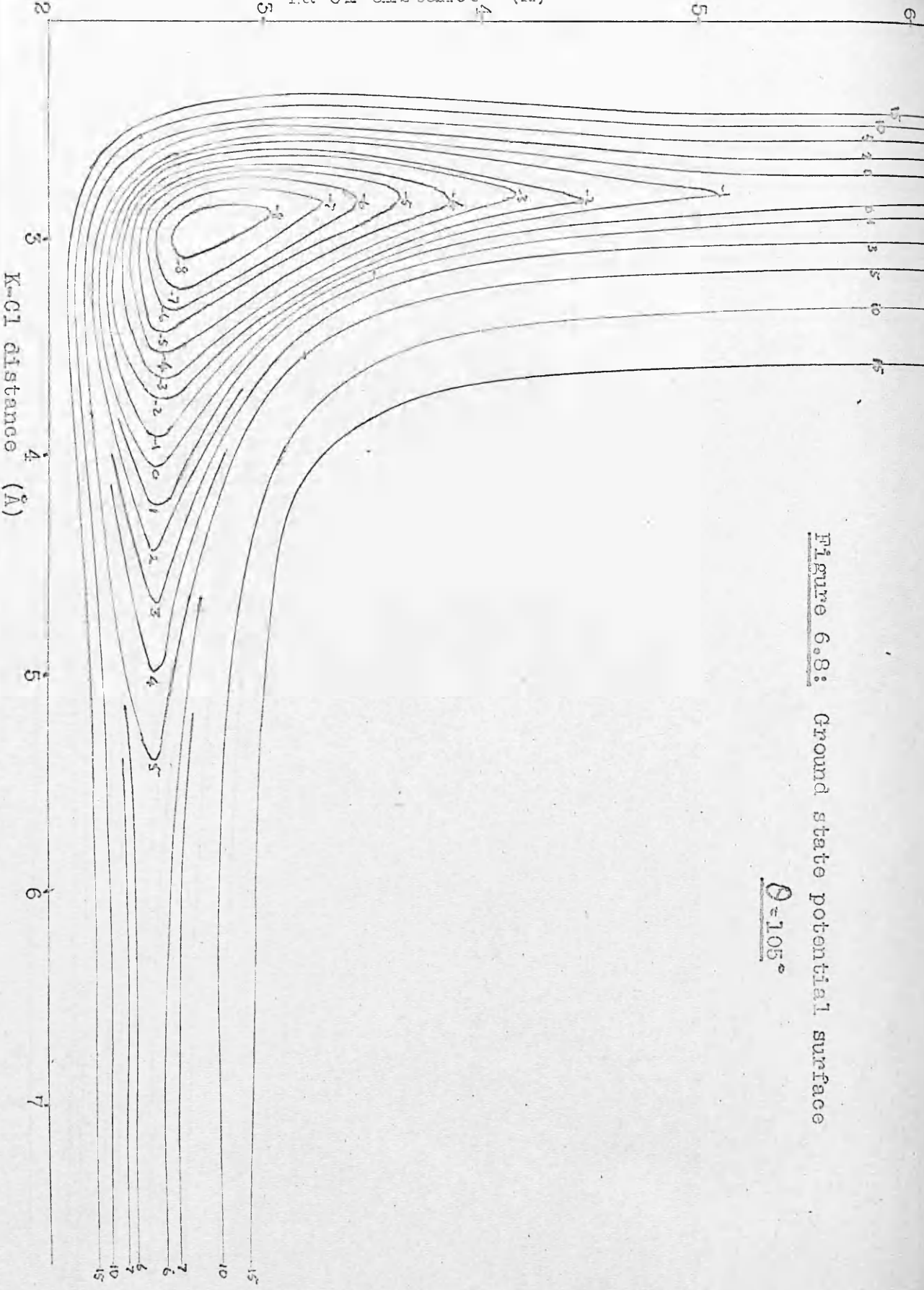
Figure 6.8: Ground state potential surface

$\theta = 105°$
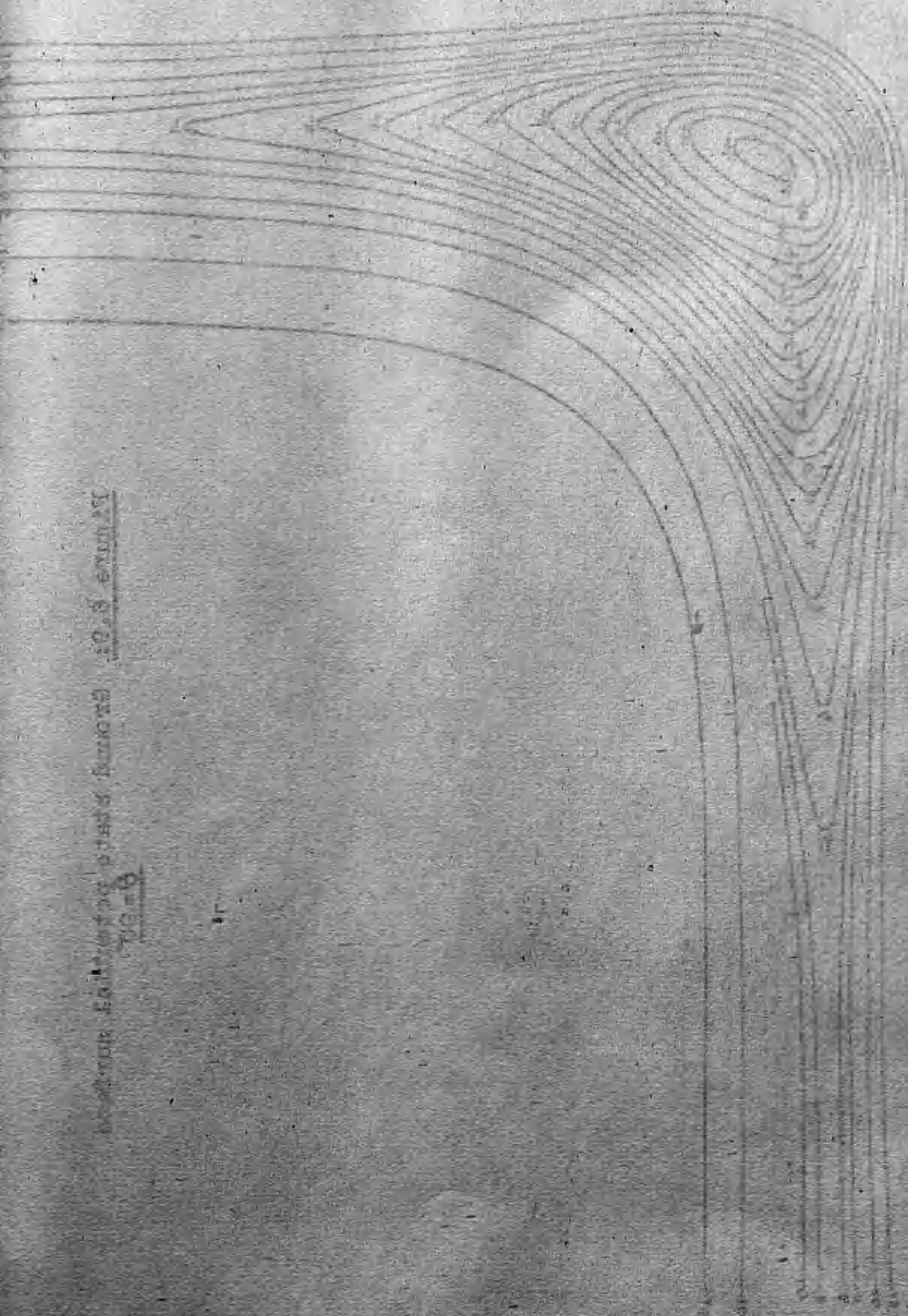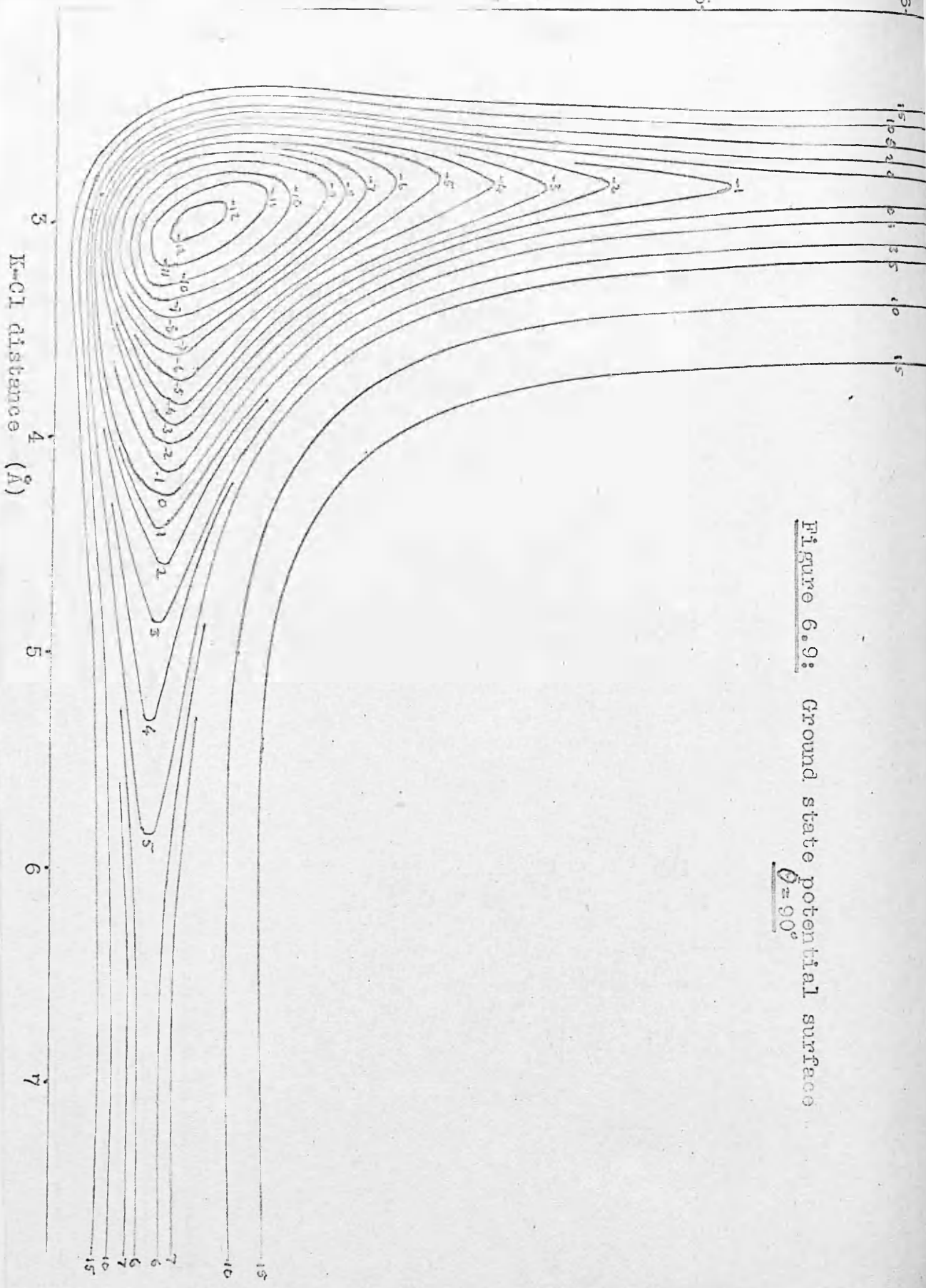
Figure 6.9: Ground state potential surface.
$\theta = 90°$
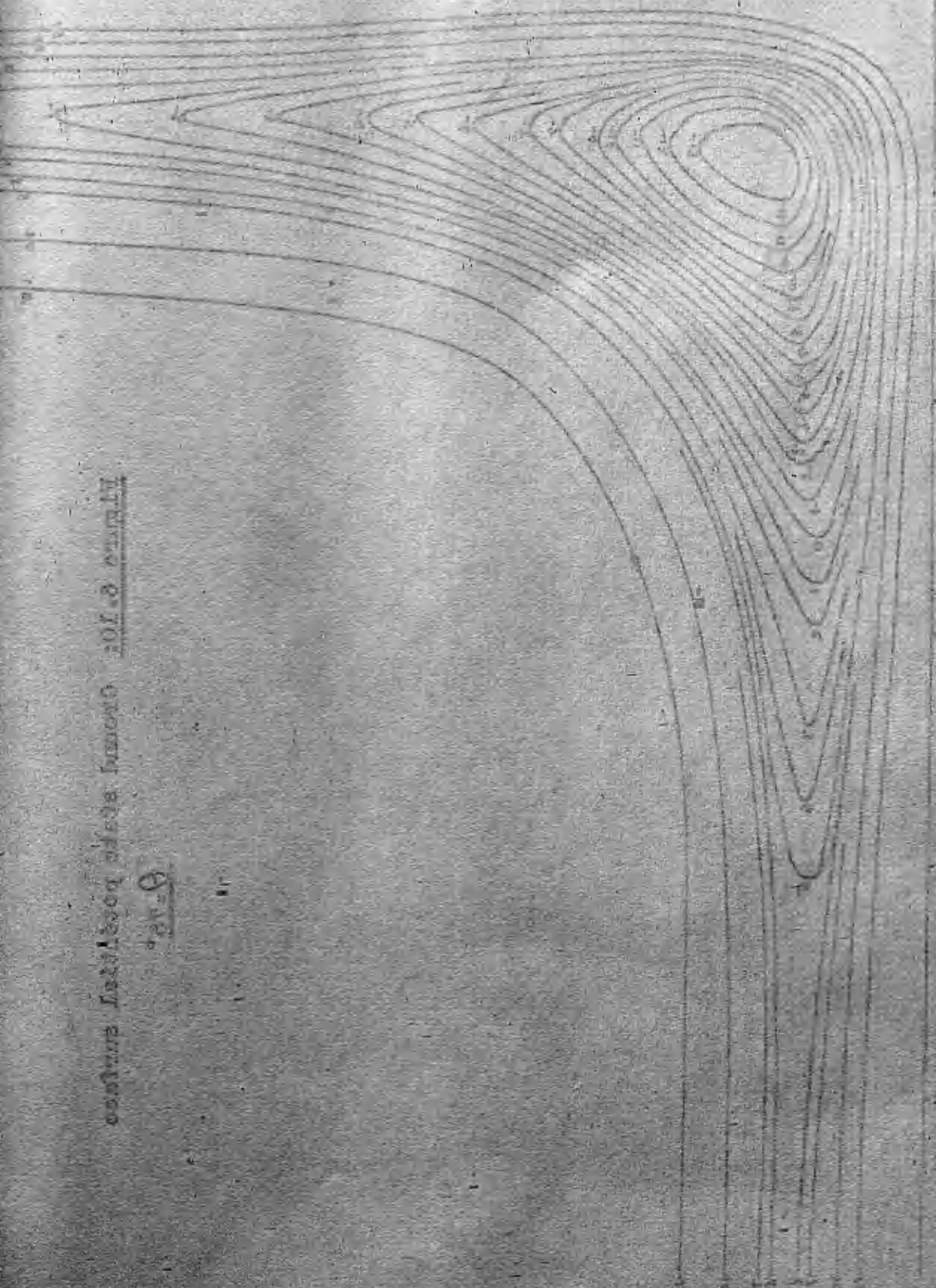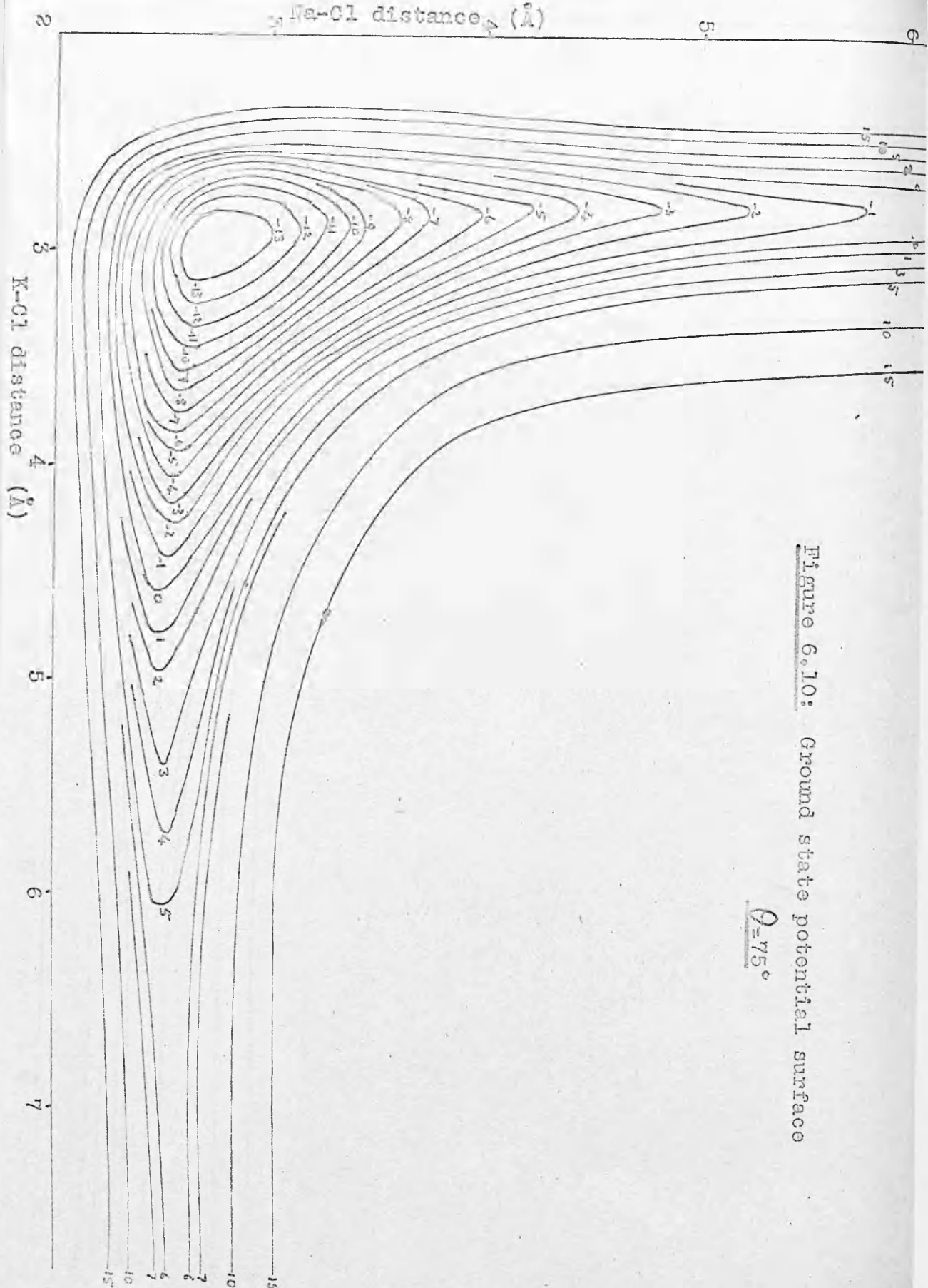
Figure 6.10: Ground state potential surface

$\theta = 75°$

Figure 6.11: Ground state potential energy surface
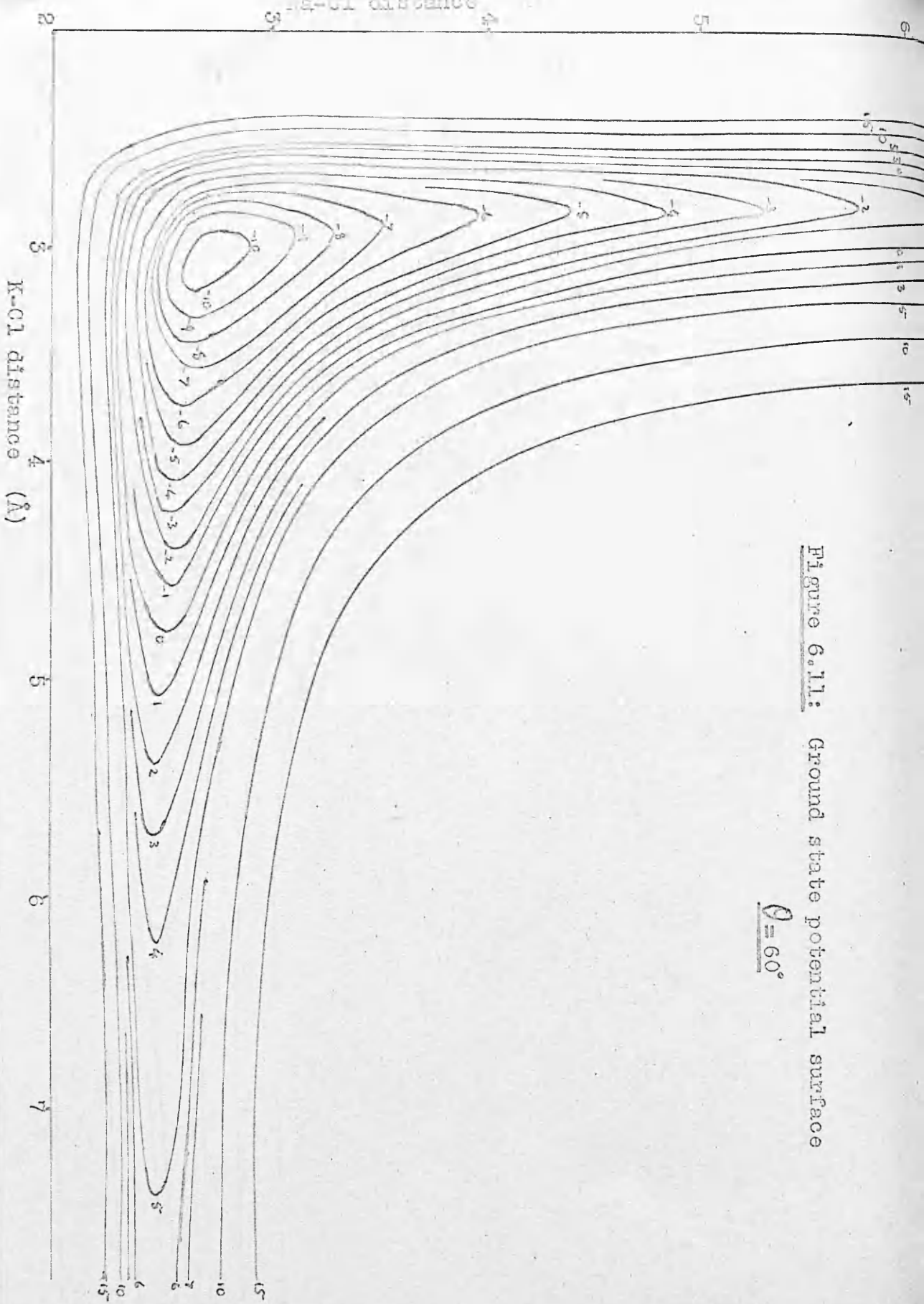
$HO_2 = \Theta$

Figure 6.11: Ground state potential surface

$\theta = 60°$
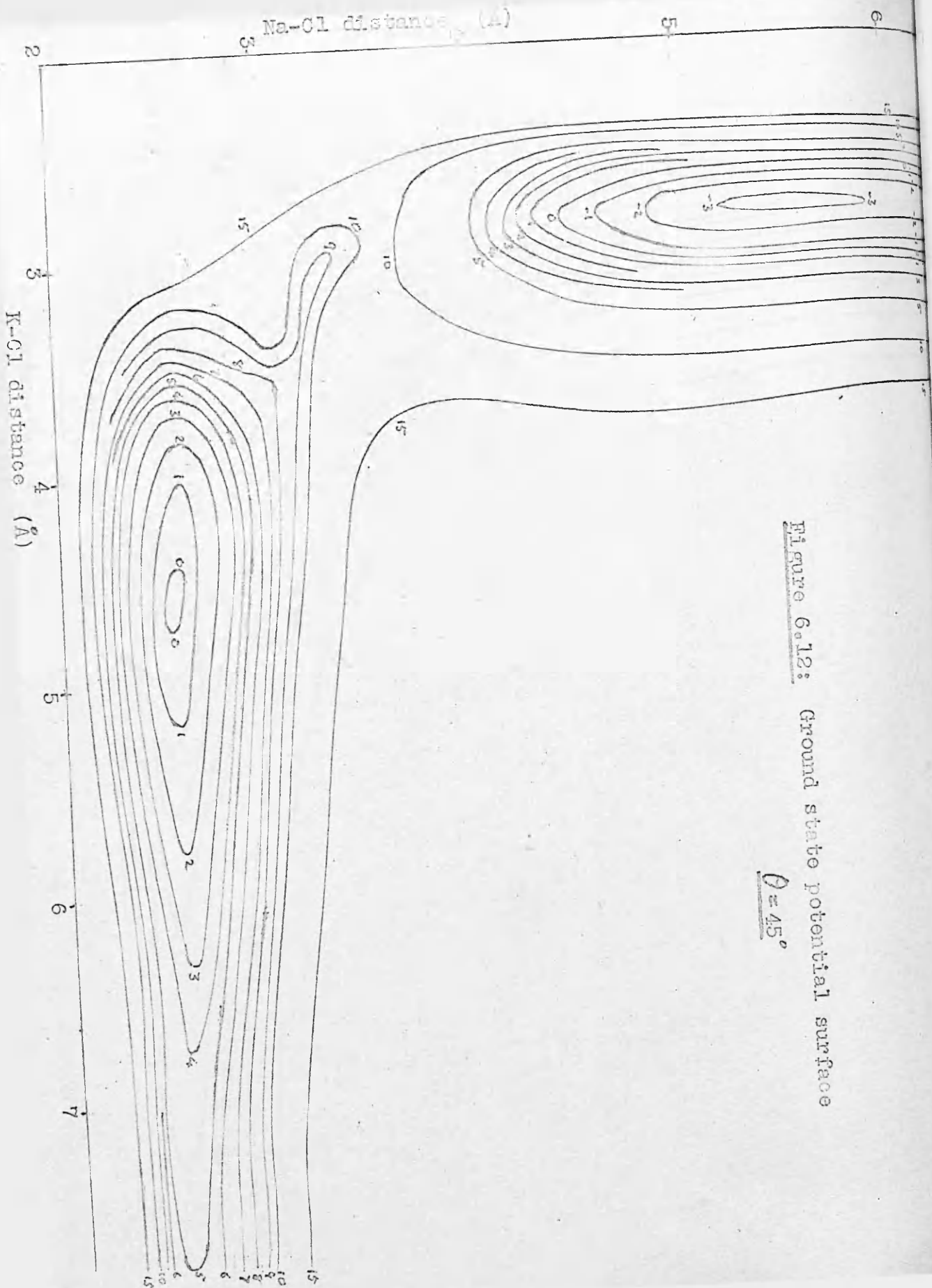
Figure 6.12: Ground state potential surface

$\theta = 45°$
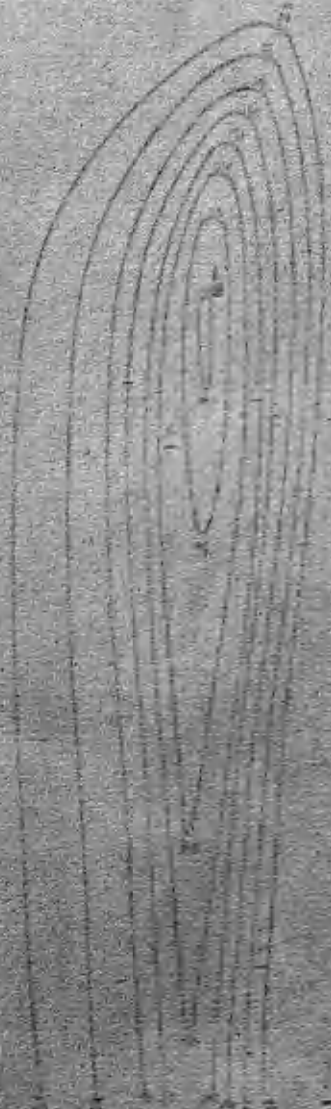
Na-Cl distance (Å)

K-Cl distance (Å)
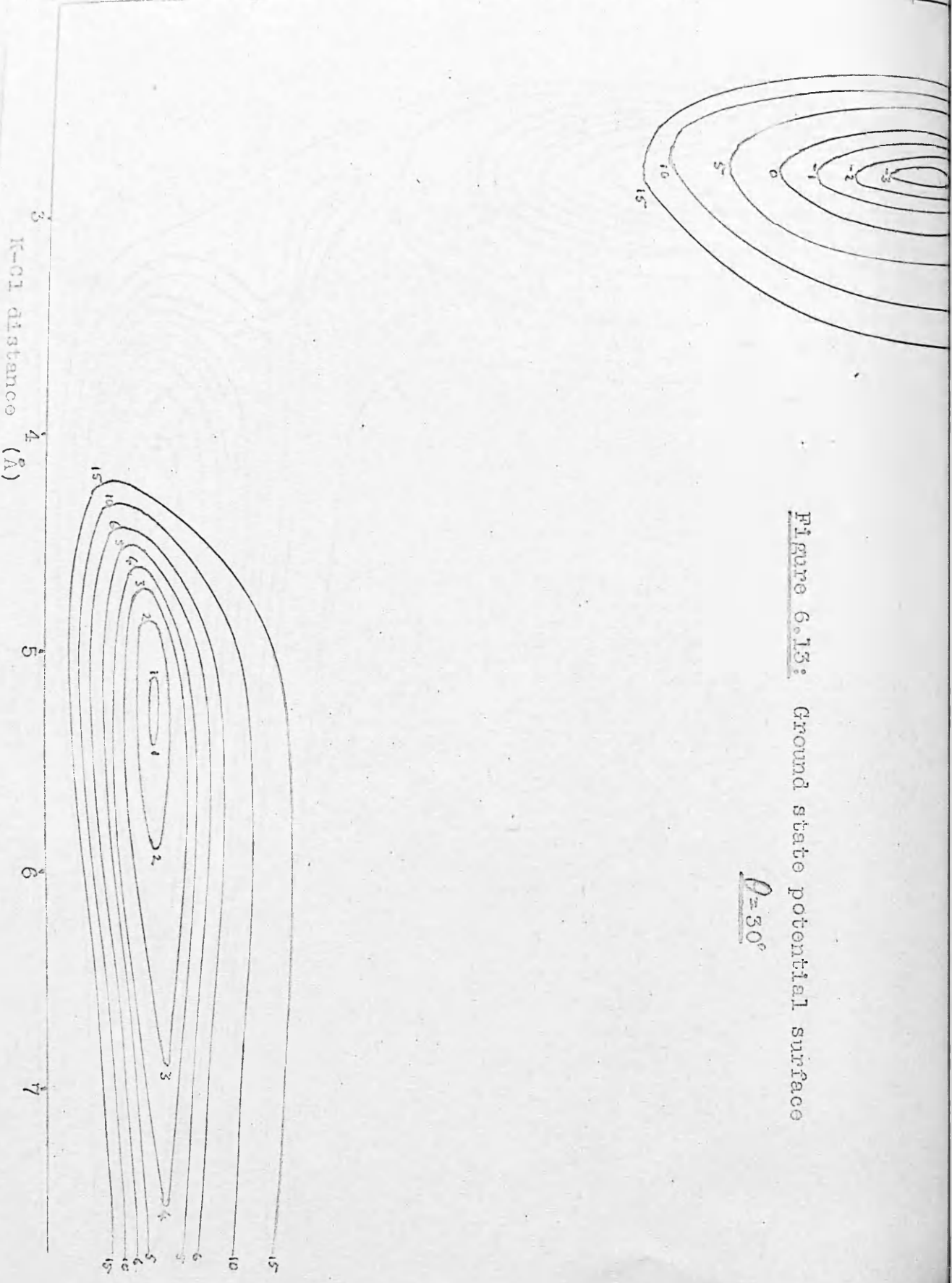
Figure 6.13: Ground state potential surface

$\theta = 30°$
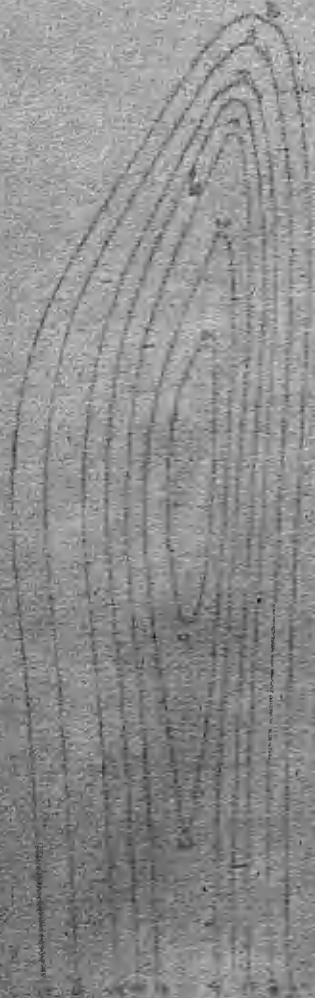
Figure 6.14: Ground state potential surface

$\theta = 15°$

The results as listed could form the basis for an
investigation of the nuclear motions.   For the purposes of
a discussion of the surfaces, however, it is more
convenient to document them in terms of a visually more
straightforward coordinate system, composed of the lengths
R_{NaCl} and R_{KCl} of the two alkali halide bonds and the
angle θ between them.

Figure 6.2

This latter system forms the basis of figures 6.3 and 6.4
in which the lowest potential surface is plotted at 10°
intervals in θ.   These contour diagrams were obtained
from the results of table 6.1 by 4 – point Lagrangian
interpolation in three dimensions, and they are referred to
an energy zero corresponding to the minimum surface energy
for the separated products.   Figure 6.3a gives the lowest
electronic surface for the collinear ($\theta = 180°$) case.

The asymptotic surface minima corresponding to
infinitely separated reactants and products respectively
taken together with estimated zero-point vibrational energies
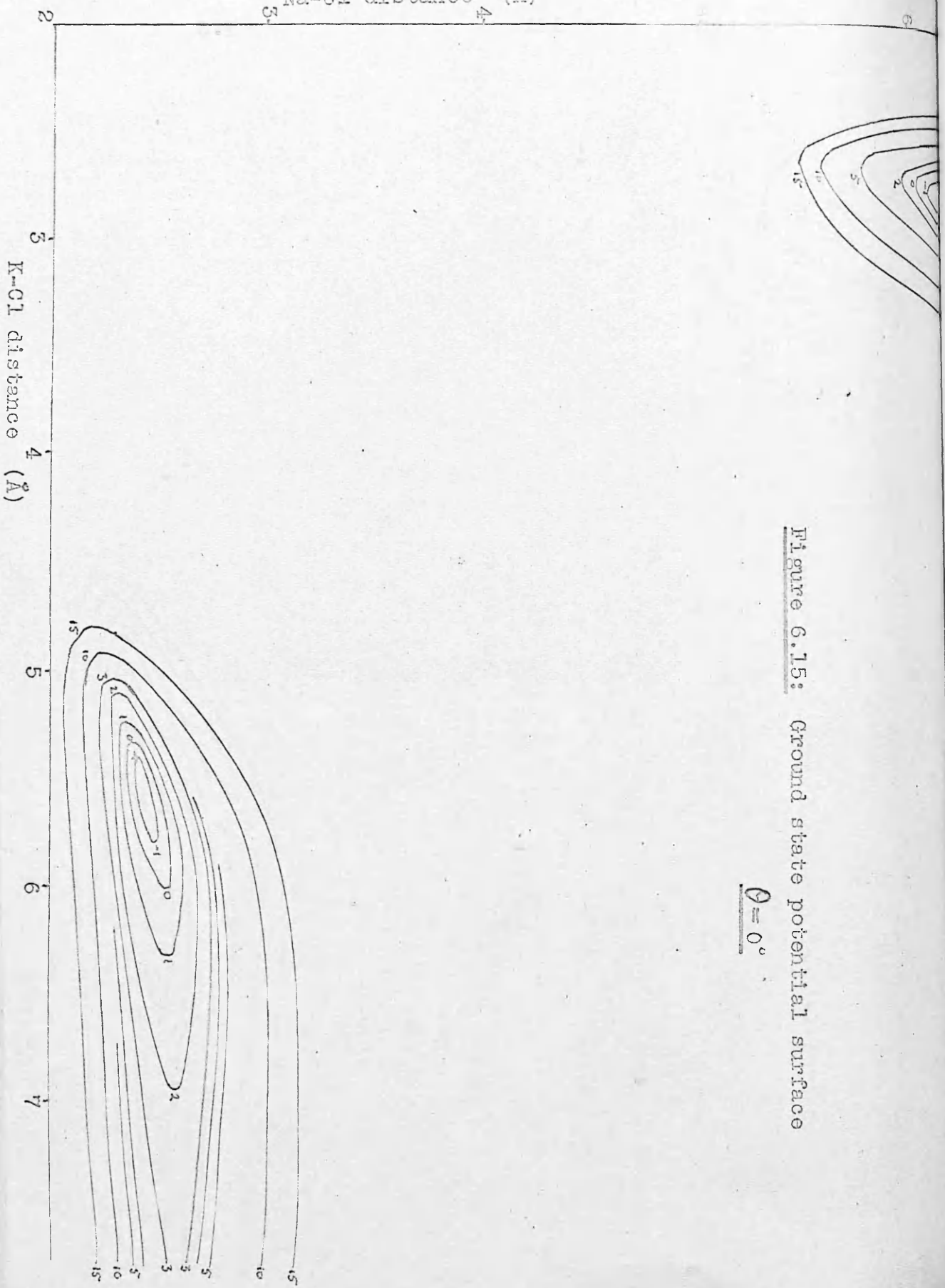
Figure 6.15: Ground state potential surface

$\theta = 0°$

Na-Cl distance (Å)

K-Cl distance (Å)

The results as listed could form the basis for an
investigation of the nuclear motions.   For the purposes of
a discussion of the surfaces, however, it is more
convenient to document them in terms of a visually more
straightforward coordinate system, composed of the lengths
R_{NaCl} and R_{KCl} of the two alkali halide bonds and the
angle θ between them.
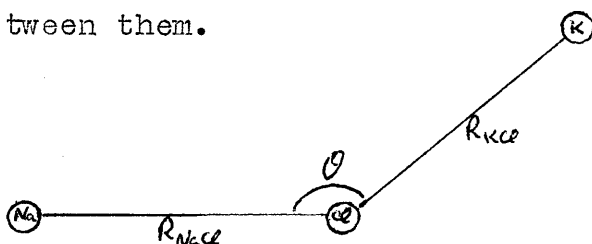
Figure 6.2

This latter system forms the basis of figures 6.3 - 6.15
in which the lowest potential surface is plotted at $15°$
intervals in θ.   These contour diagrams were obtained
from the results of table 6.1 by 4 - point Lagrangian
interpolation in three dimensions, and they are referred to
an energy zero corresponding to the minimum surface energy
for the separated products.   Figure 6.3a gives the first
excited electronic surface for the collinear ($\theta \approx 180°$) case.

The asymptotic surface minima corresponding to
infinitely separated reactants and products respectively,
taken together with estimated zero-point vibrational energies

for Na Cl and KCl of 0.52 and 0.40 Kcal/mole respectively[47],
leads to a calculated reaction exothermicity of just over
6 Kcal/mole.   This figure must be compared with the
accepted value of 4 Kcal/mole, derived from the experimental
dissociation energies of NaCl and KCl.[56]   The overestimate
is the result of small discrepancies in the asymptotic
Rittner treatments of the binding energies of NaCl and
KCl and does not constitute a serious defect in the
calculation.

A distinctive feature of the surfaces is the absence of
any activation barrier.   This is not unexpected as in the
course of the reaction the only substantial electronic
rearrangement concerns the non bonding valence electron;the
main binding forces in the system are electrostatic rather
than covalent and are as such subject to no valency
restriction that one bond should be partially broken
before another can be formed.   Furthermore, there is a
relatively strong long range dipole - induced dipole
attraction between the K atom and the NaCl molecule.   This
interaction may contribute up to 1 Kcal/mole to the binding
when the K atom is around 7 $\overset{o}{A}$ from the NaCl molecule.

At close distances directions of approach in the range
$0 \leq \theta \leq 45°$ are energetically unfavourable.   The crucial
stages of reaction cannot occur along such paths simply

because the approaching K atom is obstructed by the Na^+
ion before coming within bonding range of the Cl^- ion.
At long range, however, $\theta = 0$ is the most energetically
favourable direction of approach as the asymptotic dipole-
induced dipole interaction may become supplemented by a
certain degree of bonding between the alkali centres.
Thus, for example, the configuration,

$$\text{Ⓚ} \underset{4\cdot5\text{Å}}{\rule{3cm}{0.4pt}} \text{Ⓝⓐ} \underset{2\cdot5\text{Å}}{\rule{2cm}{0.4pt}} \text{Ⓒⓛ} \qquad\qquad (6.4)$$

is 4 Kcal/mole more stable than the reactants and 2 Kcal/mole
more stable than the corresponding $\theta = 180°$ configuration
in which the Na and Cl positions are reversed.   Similarly,
at long range $\theta = 0$ is the energetically most favourable
exit surface.   Thus the configuration

$$\text{Ⓝⓐ} \underset{4\cdot5\text{Å}}{\rule{3cm}{0.4pt}} \text{Ⓚ} \underset{2\cdot9\text{Å}}{\rule{2cm}{0.4pt}} \text{Ⓒⓛ} \qquad\qquad (6.5)$$

is 3 Kcal/mole more stable than the products and 2 Kcal/mole
more stable than the corresponding exit configuration in
which the K and Cl positions are interchanged.

All stages of reaction can occur quite smoothly in the
range $45° < \theta \leq 180°$.   If a "reaction path" is defined for each
value of θ, in this range, to follow the line of least
energy from reactants to products, then along this path,
the reaction may be envisaged as occurring in three stages.

First the K atom approaches from infinity to within
about 3.5 Å of the Cl⁻ ion, without appreciably
influencing the length of the NaCl bond.   In this stage
most or all of the reaction exothermicity is released.
In the second phase the K-Cl distance decreases to the
diatomic bond length while the Na-Cl bond increases to
approximately 3Å.   During this stage the energy
typically falls to its lowest value.   Finally, reaction
is completed by the departure of the Na atom, the KCl bond
length remaining constant,and the energy climbs to that of
the products (the transition complex is more stable than
either the reactants or the products).   The potential
surface is thus of the "attractive" classification, and
classical Monte Carlo calculations[57] suggest that much
of the exothermicity may be expected to appear in
vibrational excitation of the product KCl molecule.   Since
there is no activation barrier the precise course of the
"reaction path" is not of outstanding significance as a
great variety of routes leading to reaction are energetically
accessible, though the minimum energy path is still
favoured.

The prediction of a reaction complex NaKCl which is
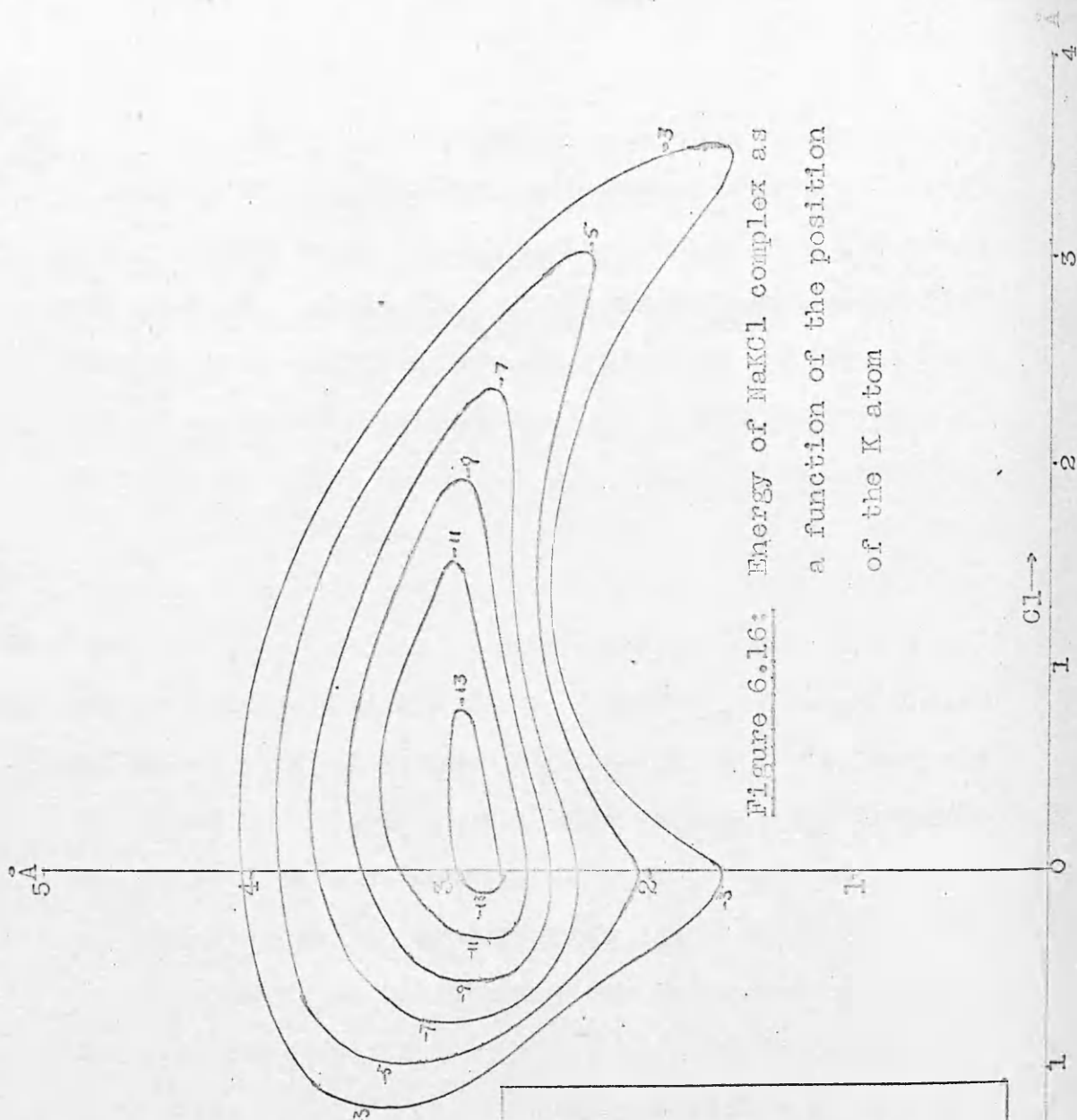
Figure 6.16: Energy of NaKCl complex as a function of the position of the K atom
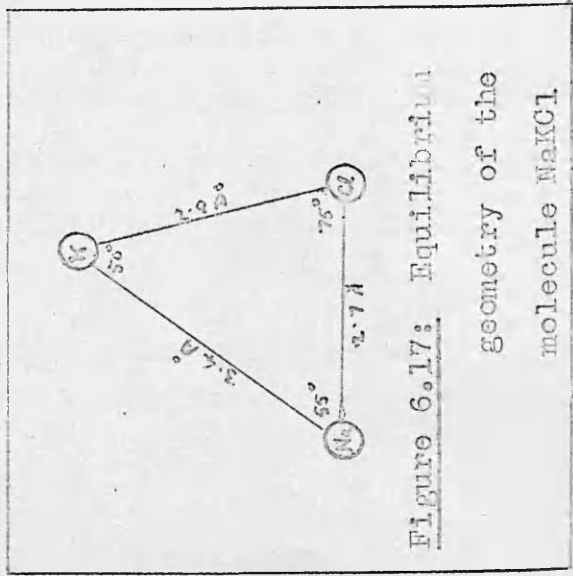
Figure 6.17: Equilibrium geometry of the molecule NaKCl

more stable than both the reactants and the products is
of considerable interest. For a collinear collision
($\theta = 180°$) this complex is only about 2 Kcal/mole more
stable than the products. As θ decreases, however, the
potential well becomes steadily more pronounced, reaching
a maximum depth of 13.5 Kcal/mole for $\theta = 75°$. If, therefore,
excess internal energy were removed (by collision at a
wall or with a third body) the molecule NaKCl would be
formed, with a dissociation energy, D_o^o, of 13.5 Kcal/mole
into the reaction products Na + KCl. As might be
expected the Na-K bond is the weakest of the three in
NaKCl as evidenced in figure 6.16 where energy contours
are plotted for the complex as a function of the position
of the K atom with respect to the centre of mass of the
NaCl bond. The NaCl bond is allowed to take up its
optimum length for each position of the K atom, so that the
minimum energy of the complex is selected at each point.
It is apparent that the largest vibrational amplitude of
the molecule will involve the deformation of the angle
$\theta = Na\widehat{C}lK$. The predicted equilibrium geometry is given
in figure 6.17.

The prediction of a stable molecule NaKCl is not

altogether surprising.   No covalent bonds need to be
broken in its formation, and there is a relatively strong
long range dipole-induced dipole attraction between Na
and KCl.   Also the stability of NaK$^+$ indicates that the
complex NaKCl may possess three positive bonds.   In
addition the positive ion NaKCl$^+$ has been observed in a
mass spectrometer, as have the symmetrical ions Na$_2$Cl$^+$,
K$_2$Cl$^+$ and Rb$_2$Cl$^+$; these latter have been assigned
experimental dissociation energies of 42, 41 and 28 Kcal/mole
respectively.[58]   The same author reported that a
Rittner calculation on Rb$_2$Cl$^+$ gave a value for the
dissociation energy in close agreement with his
experimental measurement (which success incidentally provides
direct evidence for the applicability of the Rittner
approach to an assembly of three ions).   A similar Rittner
calculation on NaKCl$^+$ (equivalent entirely to the
K + NaCl calculation with the omission of the valence
electron), gives rise to a calculated dissociation energy
of 30.7 Kcal/mole (for NaKCl$^+ \longrightarrow$ NaCl + K$^+$), so that the
positive ion appears to be about twice as stable to
dissociation as the neutral NaKCl molecule.

One further point of interest arising from this
latter calculation is the equilibrium geometry of the ion

Figure 6.18: Equilibrium
geometry of the
ion NaKCl[+]
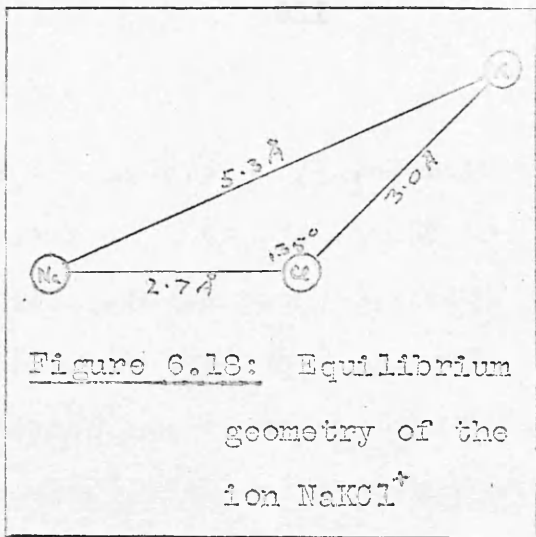
Figure 6.19: Energy of the ion
NaKCl[+] as a function of angle θ

NaKCl$^+$.   The Na-Cl and K-Cl bond lengths at 2.7Å and

3.0Å respectively are very little different from those

suggested for neutral NaKCl.   For totally unpolarisable

ions, however, the repulsion between the alkali ions would

dictate that θ ($\doteq$ NaĈlK) would take a value of 180°.   The

weaker polarisation interactions, however, favour a non-

linear arrangement.   In fact the calculation predicts

that $\theta \sim 135^\circ$, a surprisingly large deviation from linearity.

Figure 6.18 gives the calculated equilibrium geometry for

the ion. Figure 6.19 gives the energy of NaKCl$^+$ as a

function of the angle θ, showing a shallow double minimum

on either side of the linear configuration, the central

barrier having a height of only 0.6 Kcal/mole.   The ion

might thus be expected to exhibit an anomalous vibrational

spectrum, analogous to that of PH$_2$.   The spacing between

successive levels should at first decrease until an

energy close to the barrier height is attained whereupon

higher levels should appear at increasing energy intervals.[59]

The experimental confirmation of a bent equilibrium

geometry or of this type of vibrational spectrum would

provide extremely direct evidence of the importance of

polarisation interactions in gaseous ionic molecules.

The discussion thus far has assumed that the system

is confined to the lowest electronic potential surface.

In support of this assumption the results in table 6.1

show that for most configurations the lowest surface

is well separated from the excited electronic levels. For

a restricted range of configurations near the turning

point of the "reaction paths" for near collinear collisions

($\theta \geq 135°$), however the first excited electronic energy

surface may come within 2 Kcal/mole of the ground state.

Figure 6.3a gives the first excited electronic surface for

$\theta = 180°$.   This raises the possibility of a non-adiabatic,

electron jump, reaction mechanism.

In order of magnitude the probability of a non-adiabatic

transition may be determined by the Landau-Zener formula[5];

$$P = exp\left\{ -\frac{\pi}{2\hbar v} \frac{\Delta^2}{|\frac{\partial}{\partial a_s}(U_a - U_b)|} \right\} , \qquad (6.6)$$

using the notation of the introduction, equation (13).

For the collinear case ($\theta = 180°$), figure 6.20 gives a plot

of the four sigma energy levels along the path which is

drawn across the surface plotted in figure 6.3. (This

path is deliberately chosen to pass through the point of

closest collinear approach of the two surfaces and

therefore does not follow precisely the defined "reaction

path" for $\theta = 180°$.)   The labels on the energy curves in

Figure 6.20
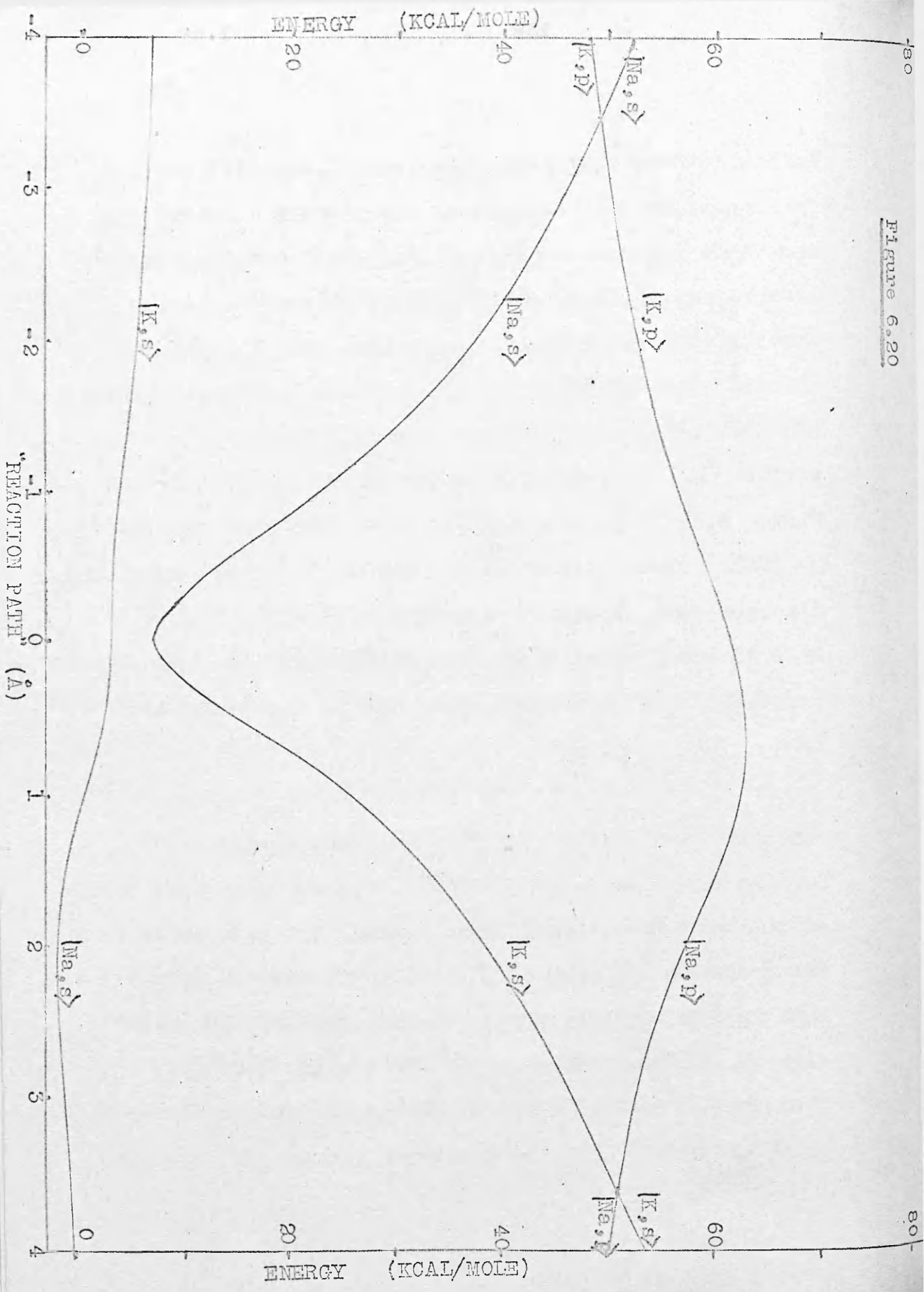
figure 6.20 indicate the predominant atomic orbital

contribution to the state in a given region.   The lowest

curves come within 3 Kcal/mole of each other at the

arbitrarily chosen origin of the path and around this

region in the lowest surface the valence electron is

transferred from an orbital of predominantly K 4s-form to

one of principally Na 3s-disposition.   This "electron jump"

takes place in regions where the atomic states $|Na,s\rangle$ and

$|K,s\rangle$ are of similar energy but where bonding between the

alkali centres is inhibited by the interposition of the

Cl^- ion.

From the figure it appears that the difference in

slopes between the states $|Na,s\rangle$ and $|K,s\rangle$ at the

"crossing point" is of the order of 20 Kcal/mole/$\overset{\circ}{A}$.   The

reduced mass associated with motion along the path may

be taken as 20 A.M.U. which is of the order of both the

reduced mass for the motion of a K atom relative to an

NaCl molecule and of an Na atom relative to a KCl molecule.

The classical velocity, v, of passage through the

crossing point may be obtained from the estimated relative

kinetic energy.   The closest separation, Δ , in this case

is 3 Kcal/mole.

In the first instance consider a thermal collision

where the initial relative kinetic energy of the reactants
is of the order of 0.5 Kcal/mole. If the exothermicity
released up to the crossing point appears as additional
kinetic energy along the reaction path, then the net
kinetic energy at the crossing is of the order of 3.5
Kcal/mole, $v = 1.2 \times 10^5$ cm/sec and $P \sim 0.03$, a very
small probability.

P is very dependent on the separation Δ . For $\Delta = 2$ Kcal/
mole, as it is for some, not quite collinear, paths,
$P \sim 0.2$, whereas for $\Delta = 1$ Kcal/mole, $P \sim 0.6$.   On the
other hand, for $\Delta = 5$ Kcal/mole, $P \sim 10^{-5}$.   Bearing in
mind that only a small proportion of collisions will pass
through regions in which $\Delta < 5$ Kcal/mole, it seems that
any non-adiabatic effects will be slight.   In any event
for thermal collisions there is no prospect of non-adiabatic
effects resulting in excited product states as there is
insufficient energy available, so that a second transition,
returning to the ground state, must precede dissociation.
The main effect of a non-adiabatic collision in this
case is therefore in extending the lifetime of the
collision complex, leading to randomisation in the angular
distribution of the small proportion of the total products
which arise by this mechanism.

Moulton and Herschbach[60] have, however, observed
experimentally that, for vibrationally excited KBr, the
reaction

$$Na + KBr = NaBr + K(p),   (6.7)$$
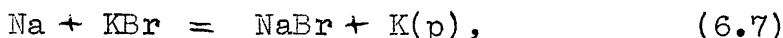
leading to a K atom in an excited p-electronic state,
occurs with a considerable cross section ($> 10\text{Å}^2$). In
these experiments the KBr is formed from a primary beam
reaction $K + Br_2 = KBr + Br$.   This primary reaction has
an exothermicity of 45 Kcal/mole which is almost entirely
produced as vibrational excitation; approximately half of
the KBr molecules possess over the 41 Kcal/mole threshold
energy necessary for the reaction (6.7) to proceed.

In the present example both of the reactions

$$K + NaCl = KCl + Na(p);   (6.8a)$$
$$and Na + KCl = NaCl + K(p),   (6.8b)$$

are approximately 43 Kcal/mole endothermic.   If the
crossing point of figure 6.20 is traversed with a relative
kinetic energy of 50 Kcal/mole, the probability of
transition given by the Landau-Zener formula is increased
to $P \sim 0.35$. (For a separation $\Delta = 1$ Kcal/mole the
probability would be further increased to $P \sim 0.9$.)
Nonetheless it is to be noted again that relatively few
collisions will follow paths passing through the calculated

range of configurations where the lowest surfaces are
close.   To such energetic collisions, however, there is
accessible a much wider range of nuclear paths traversing
regions of considerably higher energy than have been
documented here.   Typically the configurations passed
through, in which the atomic states $|Na,s\rangle$ and $|K,s\rangle$
become of similar energy, will correspond to rather longer
Na-K separations and hence the interaction between the states
will be smaller, so that Δ may be considerably reduced.   It
is quite possible that a reasonable proportion of collisions,
at least for $135° \leq \theta \leq 180°$ may lead to non-adiabatic
transitions to the second surface.

The occurrence of this transition does not, however,
automatically lead to the production of an electronically
excited product atom.   For the reaction K + NaCl, occurring
along a path similar to that of figure 6.20, after transition
the electron remains essentially in a K 4s-orbital as the
Na centre moves away. If no further crossing occurred
this surface would lead to the dissociation limit $Na^+ + KCl^-$.
When the Na-Cl distance has increased to around 6-7 Å,
however, a crossing with a predominantly Na 3p-state occurs.
The interaction between these surfaces at this large separation
is rather small ($\Delta < 0.1$ Kcal/mole) and it would seem on this

ground unlikely that an electron jump to the p-state
would occur. (Note that for reaction (6.8a) to be completed
this second crossing has to be passed adiabatically.)
On the other hand the available kinetic energy is reduced
by more than 40 Kcal/mole by this second crossing and the
corresponding reduction in nuclear velocity improves the
probability of the jump occurring, to yield an electronically
excited Na atom.   It must be noted that dissociation into
either of the ion pairs $Na^+ + KCl^-$ or $K^+ + NaCl^-$ is of the
order of 90 Kcal/mole endothermic and thus can be witnessed
only for extremely energetic collisions.   In the light of
this picture it is significant that in the observation
of excited product K atoms from the reaction $Na + KBr$[60]
none of the reactant KBr molecules contained more than
4 Kcal/mole energy in excess of the threshold required for
the electron excitation reaction to occur.   Thus if the
potential surfaces for this latter reaction are similar
to those for $K + NaCl$, the second crossing point would
indeed be traversed relatively slowly.   It is a prediction of
this work, therefore, that the yield of excited K atoms
in that experiment would be diminished on any further
increase in the vibrational excitation of the reactant KBr.

A serious treatment of the possible non-adiabatic
effects would require detailed information about the
electronic wavefunctions for the two lowest states.   Table
6.2 presents a list of the atomic orbital coefficients for

the two lowest eigenstates for all configurations of
table 6.1 in which they lie within 10 Kcal/mole of each
other.

Table 6.2:   Eigenfunctions of the two lowest potential
surfaces at the configurations of table 6.1 at which
their energies are less than 10 Kcal/mole separate.

$|e\rangle = c_1|Na,s\rangle + c_2|Na,p_1\rangle + c_3|Na,p_2\rangle + c_4|K,s\rangle + c_5|K,p_1\rangle + c_6|K,p_2\rangle.$

(Note: The p-orbitals point towards the alternative
 alkali centre and the p-orbitals are perpendicular to
 the NaK bond, with their positive lobes nearer the chloride
 centre.)

A: Reactant coordinates K + NaCl

χ	R	ϱ	Energy	c_1	c_2	c_3	c_4	c_5	c_6
0°	3.5	1.85	205.874	.698	-.353		.541	-.156	
			197.709	.568	-.216		-.783	.308	
		1.90	207.529	.760	-.367		.453	-.131	
			198.706	.493	-.177		-.833	.323	
	3.8	1.90	222.922	.610	-.310		.657	-.218	
			216.509	-.671	.270		.680	-.272	
		1.95	224.356	.708	-.340		.546	-.183	
			218.358	.574	-.219		-.769	.302	
		2.00	225.774	.781	-.358		.439	-.149	
			219.076	.478	-.172		-.832	.325	
		2.05	227.039	.830	-.367		.351	-.122	
			218.891	.396	-.134		-.870	.341	
		2.10	228.007	.862	-.368		.283	-.101	
			218.025	.332	-.106		-.892	.352	
	4.0	1.91	226.947	.451	-.244		.791	-.274	
			219.427	.789	-.332		-.517	.212	
		1.95	227.499	.547	-.278		.720	-.252	
			221.555	.728	-.297		-.610	.243	
		2.00	228.153	.670	-.319		.600	-.212	
			223.285	-.623	.241		.725	-.284	
		2.05	229.103	.767	-.348		.472	-.169	
			224.042	.506	-.185		-.811	.316	

Table 6.2: (cont.)

A: Reactant coordinates K + NaCl

γ	R	$\mathcal{C}$	Energy	c_1	c_2	c_3	c_4	c_5	c_6
0°	4.0	2.10	230.213	.828	-.361		.365	-.134	
			223.972	.405	-.139		-.862	.338	
		2.15	231.230	.865	-.365		.284	-.108	
			223.290	.329	-.105		-.890	.351	
		2.20	232.044	.888	-.364		.226	-.090	
			222.187	-.273	.082		.904	-.360	
	4.5	2.05	229.192	.272	-.156		.886	-.320	
			220.861	.874	-.370		-.321	.126	
		2.10	228.262	.380	-.196		.838	-.308	
			222.300	.837	-.343		-.428	.163	
		2.30	227.212	.881	-.358		.264	-.110	
			222.809	.300	-.094		-.895	.348	
	5.0	2.50	218.234	.917	-.349		.166	-.076	
			214.836	.196	-.052		-.920	.350	
15°	3.5	1.80	208.408	.581	-.316	-.083	.663	-.168	-.094
			199.188	.679	-.258	-.077	-.695	.263	.078
		1.85	210.708	.660	-.334	-.090	.578	-.149	-.086
			202.242	-.611	.221	.066	.761	-.281	-.091
		1.90	212.502	.726	-.347	-.095	.494	-.129	-.078
			203.756	+.540	-.186	-.055	-.814	.296	.103
		1.95	213.827	.777	-.354	-.098	.418	-.111	-.069
			204.006	+.474	-.154	-.046	-.852	.307	.113
	3.8	1.90	225.107	.566	-.291	-.077	.692	-.209	-.092
			217.965	-.708	.269	.078	.653	-.244	-.069
		1.95	226.341	.665	-.319	-.086	.590	-.182	-.083
			220.037	-.623	.225	.066	.741	-.272	-.084
		2.00	227.588	.745	-.338	-.092	.487	-.152	-.072
			221.029	-.531	.182	+.053	.809	-.296	-.097
		2.05	228.791	.802	-.348	-.096	.396	-.126	-.062
			221.139	.448	-.145	-.042	-.854	.313	.107
		2.10	229.805	.841	-.351	-.098	.322	-.106	-.053
			220.571	.380	-.116	-.034	-.881	.324	.114
	4.0	1.90	228.266	.392	-.226	-.058	.824	-.258	-.098
			219.218	-.818	.328	.094	.478	-.182	-.041
		1.95	228.871	.501	-.260	-.068	.751	-.241	-.094
			220.037	-.761	.294	-.084	.580	-.215	-.057
		2.00	229.278	.261	-.297	-.079	.647	-.212	-.085
			223.889	-.672	.247	.071	.690	-.252	-.073
		2.05	229.919	.725	-.325	-.088	.526	-.176	-.073
			224.833	-.565	.196	.057	.782	-.285	-.089
		2.10	230.818	.798	-.341	-.094	.415	-.142	-.061
			224.977	-.462	.151	.044	.843	-.309	-.100

Table 6.2: (Cont.)

<u>A</u>: Reactant coordinates K + NaCl

χ	R	ℓ	Energy	c_1	c_2	c_3	c_4	c_5	c_6
15°	4.0	2.15	231.746	.844	-.348	-.096	.328	-.115	-.051
			224.498	.380	-.116	-.034	-.878	.324	.108
		2.20	232.549	.873	-.348	-.097	.262	-.096	-.043
			223.579	-.317	.091	.026	.897	-.334	-.114
	4.5	2.05	229.660	.243	-.151	-.037	.898	-.300	-.093
			220.404	-.885	.356	.099	.307	-.107	-.020
		2.10	228.706	.337	-.182	-.046	.858	-.294	-.092
			221.806	-.857	.335	.093	.397	-.137	-.032
		2.20	226.328	.657	-.288	-.077	.625	-.225	-.074
			223.303	.652	-.231	-.065	-.703	.248	.070
		2.30	226.499	.860	-.340	-.092	.316	-.123	-.043
			222.690	.358	-.107	-.031	-.881	.321	.097
	5.0	2.30	221.193	.261	-.138	-.034	.894	-.309	-.086
			215.630	-.890	.338	.091	.306	-.094	-.022
		2.50	217.214	-.907	.335	.089	-.204	.089	.026
			214.505	-.240	.061	.018	.915	-.327	-.093
30°	3.5	1.90	223.170	.634	-.289	-.168	.581	-.107	-.164
			213.583	.633	-.204	-.131	-.757	.248	.171
		1.95	224.722	.689	-.297	-.176	.516	-.095	-.152
			214.923	.582	-.180	-.115	-.798	.254	.189
	3.8	1.90	229.701	.488	-.242	-.135	.740	-.172	-.182
			220.243	.754	-.262	-.166	-.604	.213	.114
		1.95	230.750	.567	-.260	-.149	.672	-.158	-.172
			222.598	.703	-.235	-.150	-.673	.227	.136
		2.00	231.571	.643	-.277	-.162	.595	-.141	-.158
			224.045	.642	-.206	-.131	-.737	.241	.158
		2.05	232.332	.709	-.289	-.172	.516	-.123	-.143
			224.318	.575	-.177	-.112	-.790	.253	.178
		2.10	233.063	.762	-.297	-.179	.442	-.106	-.128
			224.357	.511	-.150	-.094	-.831	.263	+.195
		2.15	233.720	.803	-.300	-.183	.377	-.092	-.114
			224.299	.452	-.128	-.079	-.859	.270	.208
	4.0	1.95	231.555	.434	-.217	-.119	.787	-.200	-.182
			222.272	-.793	.279	.175	.537	-.190	-.094
		2.00	231.802	.521	-.240	-.136	.722	-.186	-.173
			224.188	-.704	.252	.159	.616	-.208	-.117
		2.05	231.908	.611	-.261	-.152	.641	-.167	-.160
			225.372	-.678	.220	.139	.696	-.228	-.141
		2.10	232.108	.693	-.280	-.165	.551	-.145	-.144
			225.898	.601	-.186	-.118	-.765	.246	.164

Table 6.2: (cont.)

<u>A</u>: Reactant coordinates K + NaCl

χ	R	$\mathscr{C}$	Energy	c_1	c_2	c_3	c_4	c_5	c_6
30°	4.0	2.15	232.466	.758	-.292	-.174	.463	-.123	-.126
			225.859	.523	-.155	-.097	-.818	.260	.183
	4.5	2.10	229.179	.302	-.157	-.082	.871	-.248	-.175
			220.040	-.865	.306	.186	.378	-.128	-.055
		2.30	224.860	.748	-.278	-.162	.506	-.153	-.119
			221.209	-.550	.162	.101	.793	-.249	-.158
		2.50	225.055	.906	-.292	-.175	.195	-.068	-.057
			217.062	-.251	.058	.034	.912	-.293	-.205
	5.0	2.30	220.130	.229	-.117	-.059	.906	-.265	-.163
			213.337	-.897	.308	.182	.284	-.084	-.037
		2.50	214.591	.814	-.280	-.161	.426	-.137	-.091
			212.693	-.463	.127	.079	.841	-.256	-.156
		2.70	214.337	.931	-.283	-.165	.127	-.051	-.035
			207.741	-.169	.031	.020	.928	-.295	-.190
45°	4.0	2.10	233.348	.547	-.205	-.207	.671	-.101	-.227
			224.215	-.729	.178	.205	.682	-.174	-.177
		2.20	232.511	.668	-.217	-.230	.547	-.084	-.199
			224.152	.630	-.147	-.165	-.773	.189	.224
		2.30	232.010	.759	-.223	-.243	.432	-.066	-.168
			222.845	-.531	.118	.126	.835	-.198	-.260
	4.5	2.30	223.853	.553	-.190	-.190	.697	-.139	-.213
			217.650	.742	-.178	-.199	-.648	.155	.157
		2.50	220.702	.820	-.223	-.238	.375	-.077	-.133
			214.465	-.453	.093	.100	.863	-.203	-.249
	5.0	2.50	213.026	.539	-.174	-.170	.734	-.162	-.199
			208.832	-.764	.181	.196	.607	-.136	-.135
60°	4.5	2.50	217.729	.651	-.132	-.254	.574	-.038	-.218
			209.410	.660	-.102	-.202	-.760	.131	.236
		2.70	214.274	.793	-.132	-.237	.392	-.021	-.164
			204.873	-.507	.074	.130	.857	-.124	-.295
	5.0	2.50	212.257	.418	-.103	-.174	.804	-.087	-.245
			204.067	-.824	.142	.277	.525	-.110	-.126

Table 6.2: (cont.)

B: Product coordinates Na+KCl

γ	R	ℓ	Energy	c_1	c_2	c_3	c_4	c_5	c_6
0°	4.0	2.8	223.720	.770	-.358		.454	-.151	
			216.799	-.492	.178		.825	-.323	
		2.9	224.502	.666	-.327		.598	-.201	
			218.620	-.620	.242		.731	-.288	
		3.0	225.093	.513	-.272		.745	-.253	
			218.056	-.747	.311		.583	-.237	
		3.1	225.322	.362	-.213		.844	-.286	
			215.527	-.827	.360		.433	-.186	
	4.5	3.1	231.751	.891	-.362		.226	-.093	
			223.732	-.269	.081		.904	-.359	
		3.3	228.454	.776	-.339		.470	-.179	
			225.139	.501	-.181		-.180	-.312	
		3.5	228.614	.355	-.187		.851	-.311	
			222.117	.847	-.350		-.403	.155	
	5.0	3.5	225.000	.924	-.348		.128	-.064	
			217.717	-.162	.040		.922	-.365	
		3.7	221.004	.878	-.351		.283	-.118	
			218.715	.314	-.099		-.892	.338	
15°	4.0	2.8	227.166	.800	-.346	-.108	.394	-.118	-.070
			218.646	.450	-.143	-.047	-.856	.308	.122
		2.9	227.968	.732	-.331	-.105	.502	-.152	-.085
			221.332	.544	-.185	-.064	-.801	.287	.110
		3.0	228.293	.622	-.300	-.097	.638	-.194	-.102
			222.039	.667	-.240	-.085	-.702	.251	-.091
		3.1	228.771	.475	-.254	-.082	.767	-.230	-.117
			220.967	-.776	.293	.107	.566	-.203	-.607
	4.5	3.1	232.720	.900	-.340	-.104	.198	-.079	-.037
			222.770	.252	-.066	-.020	-.911	.339	.127
		3.3	229.453	.841	-.336	-.108	.348	-.128	-.057
			224.671	.395	-.119	-.041	-.870	.312	.116
		3.5	227.498	.557	-.255	-.084	.716	-.245	-.102
			223.386	.738	-.262	-.094	-.614	.207	.073
		3.7	229.033	.200	-.141	-.043	.914	-.286	-.119
			219.371	.900	-.344	-.129	-.273	.078	.021
	5.0	3.5	224.993	.930	-.324	-.099	.110	-.056	-.210
			215.742	.152	-.031	-.010	-.924	.346	.122
		3.7	220.989	.909	-.332	-.107	.191	-.083	-.031
			216.675	.231	-.056	-.020	-.916	.328	.116
30°	4.0	3.0	234.308	.771	-.281	-.201	.419	-.087	-.138
			224.908	-.499	.138	.099	.842	-.249	-.223
		3.1	233.849	.721	-.270	-.198	.495	-.104	-.157
			225.821	-.565	.160	+.122	.802	-.239	-.206

Table 6.2: (cont.)

B: Product coordinates Na+KCl

χ	R	e	Energy	c_1	c_2	c_3	c_4	c_5	c_6
$30°$	4.0	3.3	232.832	.566	-.230	-.176	.672	-.144	-.197
			225.072	.712	-.213	-.177	-.670	.206	.156
	4.5	3.5	227.027	.839	-.274	-.201	.343	-.092	-.106
			220.694	-.408	.103	.076	.872	-.256	-.218
		3.7	224.105	.705	-.244	-.187	.555	-.143	-.155
			219.725	.603	-.165	-.134	-.762	.217	.178
		3.8	223.569	.582	-.212	-.165	.687	-.174	-.182
			218.653	.719	-.205	-.171	-.650	.185	.143
		4.0	224.023	.331	-.143	-.111	+.858	-.207	-.211
			215.806	-.859	.258	.227	.411	-.122	-.074
$45°$	4.0	3.7	228.410	.614	-.155	-.251	.587	-.041	-.232
			218.450	-.679	.124	.211	.748	-.153	-.235
	4.5	4.0	216.538	.793	-.169	-.262	.407	-.047	-.159
			208.947	.501	-.085	-.127	-.851	.155	.274

Finally it is of some concern to investigate how

sensitive these results are to details of the model,

in particular to the precise choice of pseudopotentials.

Test calculations indicate that changes of up to $2o\%$ in

the alkali ion core radii cause changes in the calculated

energy levels at thermally accessible configurations of

less than 2 Kcal/mole, except that, for close Na-K

separations, and correspondingly small values of θ

discrepancies of up to 5 Kcal/mole may occur.   These

latter configurations are relatively unimportant,

from the point of view of the reaction $K + NaCl$.   Similarly,

inside the Cl^- core, a reduction of the order of 20% in the

repulsive pseudopotential causes energy changes up to

2 Kcal/mole.   The conclusions about the stability of the

NaKCl complex and the possibility of non-adiabatic

transitions are not seriously affected by these changes.

On the other hand more drastic modifications, such as

the use of point charge potentials throughout space, or

the   complete removal of   the intra-core repulsion in the
Cl^- pseudopotential, may lead to energy changes of many tens

of Kcal/mole.   These investigations throw no further light

on the most suitable choice for these parameters, which

are selected and supported on grounds of the arguments of

chapter 3.1 and in the light of the calculations of chapter

5 on the diatomic ions. Nonetheless the latter test
calculations underline the importance of the pseudopotential
arguments, while the former indicate that the final results
are acceptably insensitive to discrepancies of the order
of 20% in the precise parametric values employed.

In summary, therefore, the results of the calculations
on K + NaCl lead to an estimated reaction exothermicity
of 6 Kcal/mole, compared with an experimental value of
4 Kcal/mole. There is no calculated activation barrier, the
potential surfaces conforming to the "attractive" classification.
The existence of a triangular complex NaKCl of dissociation
energy $D_o^o = 13.5$ Kcal/mole is predicted. Further, it is
suggested that for collisions at thermal energies, the
reaction is essentially adiabatic , but that at high
translational energies there is a plausible non-adiabatic
mechanism by which a proportion of the product atoms may
be produced in an electronically excited state. These
conclusions are not critically affected by deviations up
to 20% in the choice of ion core pseudopotential parameters.

Appendix IA   The electrostatic potentials of Na⁺, K⁺ and Cl⁻

Analytical expressions for the electrostatic
potentials of the isolated ions Na⁺, K⁺ and Cl⁻ are derived
by a method analogous to that applied to the first 36
neutral atoms by T.G. Strand and R.A. Bonham.[37]   The
electronic charge distributions are derived from
Hartree Fock numerical wavefunctions.[34-36]   Integration
of Poisson's equation then leads to numerical potential
expressions which are fitted by a modified Newton Gauss least
squares process to yield the expressions listed in chapter
3.1, equation (3.9).

The numerical self consistent field results, referred
to, list radial distribution functions, P.   On summing over
all electrons the total spherically symmetric charge
distribution, ρ , is given by

$$\rho(r) = \frac{\sum P^2(r)}{4\pi r^2} ,$$ (I.A.1)

where $\sum P^2(r)$ may be tabulated directly from the listed
wavefunctions, and interpolated by the Lagrangian technique,[61]
at any required intervals.   The potential, V, satisfies
Poisson's condition, so that

$$\nabla^2 V = -4\pi\rho = -\frac{\sum P^2(r)}{r^2} ,$$ (I.A.2)

and, since V is spherically symmetric,

$$\nabla^2 V = \frac{1}{r} \frac{d^2}{dr^2}(rV),$$ (I.A.3)

and therefore,

$$\frac{d^2 Y(r)}{dr^2} = -\frac{\sum P^2(r)}{r},$$ (I.A.4)

where $Y(r)$ $(= rV(r))$ is the total electronic charge
confined within a sphere of radius r around the nucleus.
This equation may be numerically integrated inwards point
by point, using, for the second difference of the tabulated
Y function, the equation

$$\delta^2 Y_j = (\delta r)^2 \left[-\left(\frac{\sum P^2}{r}\right)_j + \frac{1}{2}\delta^2\left(\frac{\sum P^2}{r}\right)_j \right],$$ (I.A.5)

which applies when fourth and higher order differences are
neglected.[62]   The boundary conditions are that, at
sufficiently large r, Y is equal to the total number of
electrons present and its first difference, δY, is zero.
Y may therefore be built up by applying (I.A.5) at successive
equal steps towards the origin.   It is convenient to use
a reduced step interval at smaller and more significant
r-values and interval halving is particularly easy to
introduce at any chosen stage, requiring a minimum number
of interpolations between previously calculated values.

A good check on the accuracy of the calculation, and on
the wavefunctions employed, is provided by the requirement
that Y should vanish at the origin.

The function Y obtained in this way provides the
potential due to the electronic charge distribution.
The complete electrostatic potential, V_T, contains also
the contribution due to the point nuclear charge, Z, and
corresponds to

$$\frac{V_T}{r} = Y_T = Y + Z .$$ (I.A.6)

Least squares is then used to fit Y_T by an expression of
the form:

$$Y_T = -Q + \sum_{i=1}^{2} A_i \, exp(-B_i r) + \sum_{j=1}^{m} C_j \, r \, exp(-D_j r),$$ (I.A.7)

where Q is the net charge of the ion and the A_i, B_i, C_j and
D_j are adjustable parameters.   m is taken as unity for
Na^+ and as 2 for K^+ and Cl^-.   The sum $A_1 + A_2$ is constrained
so that at the nucleus $Y_T \to Z$.   In contrast to V_T, Y_T does not
diverge at the origin, nor does it diminish so rapidly at
large r, so that least squares fitting of $Y_T(r)$ rather than
of $V_T(r)$ should lead to expressions whose accuracy is
more evenly weighted at large r, which may be important in
the calculation of molecular properties.

The fitting process is carried out by guessing initial
values for the parameters A_i, B_i, C_j and D_j and then
solving the usual Newton Gauss normal equations[61] for
a shift vector (δA_i, δB_i, δC_j, δD_j) which, if the
initial estimates are sufficiently good, will lead to a
modified expression (I.A.7) of smaller standard deviation
from the tabulated function.   Strand, Kohl and Bonham[38]
introduced a shift factor, k, to modify the length but
not the orientation of the Newton Gauss shift vector.
This device is employed here, choosing k in the range
-1.5 to 1.75, so as to minimise the sum of the squares
of the deviations, Σd^2, between the tabulated and analytical
functions.   This is achieved simply by computing Σd^2
for values of k at intervals of 0.25.   If the smallest value
occurs at either of the extremes $k = -1.5$ or $k = 1.75$,
this factor is taken.   Otherwise a parabola is fitted
through the minimum point and its two nearest neighbours,
leading to a closer estimate of the optimum factor k.
The improved estimates for the parameters form a basis for
iteration.   The straightforward Newton Gauss method, which
automatically takes $k = 1$, may lead to divergence or may
converge only very slowly when used to fit a function of the
complexity of (I.A.7), unless the initial estimates of the

parameters are inspiredly accurate.   By the introduction of
the variable shift factor convergence is considerably
speeded and made more certain.

Initial estimates of the parameters were suggested by
the tabulated values for the first 36 neutral atoms,[37] and
convergence of Σd^2 and of the parameters to five
significant figures is usually achieved in about six cycles.
The resulting expressions for the Y_r give immediately,
on division by r, the ion electrostatic potentials quoted in
equation (3.9).

Appendix IB   The Cizek approximation for the evaluation
              of multicentre integrals

   J. Cizek has proposed an elaborate method for the

approximate reduction of multicentre integrals in terms

of two centre forms.[16]   The most important step in

this method is the replacement of the overlap density of

two Slater-type orbital functions by a sum of Slater-type

charge densities on two new centres.   In the case where

the original overlap function is positive throughout space

this replacement may be written:

$$|A,m,\alpha\rangle|B,n,\beta\rangle = k_c|C,r,\gamma\rangle^2 + k_{\mathfrak{D}}|D,r,\delta\rangle^2. \qquad \text{(IB.1)}$$

A and B are the old and C and D the new centres; m, n, and

r are quantum numbers, where $r = \min(m,n)$; k_c and $k_{\mathfrak{D}}$ are

constants and α, β, γ and δ represent orbital exponents.

C and D are chosen to lie on the x-axis, AB, and their

coordinates x_c and $x_{\mathfrak{D}}$, together with the parameters $k_c, k_{\mathfrak{D}}, \gamma$

and δ are chosen so that the right hand side of (IB.1)

reproduces the monopole, dipole, quadruple and octupole

moments of the original product on the left.   That is,

integrals of the form

$$[x^i y^j z^k] \equiv \langle A,m,\alpha|x^i y^j z^k|B,n,\beta\rangle \qquad \text{(IB.2)}$$

are reproduced up to $(i + j + k) = 3$.   The six parameters

of (IB.1) are thus determined by the equations:

$$k_c + k_g = [1] = \langle 1 \rangle,$$

$$k_c x_c + k_g x_g = [x] = \langle 2 \rangle,$$

$$k_c x_c^2 + k_g x_g^2 = [x^2] - [y^2] = \langle 3 \rangle,$$

$$k_c x_c^3 + k_g x_g^3 = [x^3] - 3[xy^2] = \langle 4 \rangle,$$

$$\tau_r (k_c \gamma^{-2} + k_g \delta^{-2}) = [y^2] = \langle 5 \rangle,$$

and $\tau_r (k_c x_c \gamma^{-2} + k_g x_g \delta^{-2}) = [xy^2] = \langle 6 \rangle,$

(IB.3)

where τ_r is a simple function of the quantum number r.

In more complicated cases where the overlap function

$|A,m,\alpha\rangle | B,n,\beta\rangle$ may vary in sign in different regions of

space, a simple factorisation leads to a new product

$|A,p,\alpha\rangle | B,q,\beta\rangle$ (involving lower quantum numbers p and q)

to which the above treatment is applicable, so that

the solution of equations of the form (IB.3) is always

a crucial stage in the application of the Cizek

approximation.

It is found, however, that the solutions of (IB.3)

are frequently complex, in which case the representation

(IB.1) provides no help in the evaluation of multicentre

integrals.   Conditions under which at least one of the

parameters is complex are derived below.

The problem can be simplified by choosing the origin to lie at the centre of gravity of the overlap density, so that the dipole moment $\langle 2 \rangle$ vanishes. The first four equations of (IB.3) can be solved simultaneously to give

$$x_c = \frac{1}{2}\left\{ \frac{\langle 4 \rangle}{\langle 3 \rangle} - \sqrt{\left(\frac{\langle 4 \rangle}{\langle 3 \rangle}\right)^2 + 4\frac{\langle 3 \rangle}{\langle 1 \rangle}} \right\},$$

$$x_{\mathfrak{D}} = \frac{1}{2}\left\{ \frac{\langle 4 \rangle}{\langle 3 \rangle} + \sqrt{\left(\frac{\langle 4 \rangle}{\langle 3 \rangle}\right)^2 + 4\frac{\langle 3 \rangle}{\langle 1 \rangle}} \right\}, \qquad \text{(IB.4)}$$

$$k_c = \frac{\langle 1 \rangle \, x_{\mathfrak{D}}}{x_{\mathfrak{D}} - x_c},$$

and $\quad k_{\mathfrak{D}} = \dfrac{\langle 1 \rangle \, x_c}{x_c - x_{\mathfrak{D}}},$

where conventionally $x_{\mathfrak{D}} > x_c$. $\quad x_c$ and $x_{\mathfrak{D}}$ (and also k_c and $k_{\mathfrak{D}}$) will therefore be complex whenever

$$\frac{\langle 3 \rangle^3}{\langle 1 \rangle \langle 4 \rangle^2} < -\frac{1}{4} \qquad \text{(IB.5)}$$

$\langle 1 \rangle$ is always positive but the inequality (IB.5) will hold if $\langle 3 \rangle$ is sufficiently large and negative, i.e. if the overlap density $|A,m,\alpha\rangle|B,n,\beta\rangle$ is less spread out along the bond AB than perpendicular to it. This type of breakdown is relatively infrequent; more common is the case in which, although x_c, $x_{\mathfrak{D}}$, k_c and $k_{\mathfrak{D}}$ are real, at least one of the exponents γ and δ is imaginary.

Consider first the case in which $\langle 3 \rangle$ is positive.
It follows immediately from (IB.4) that x_c and $x_{\mathcal{D}}$ lie on
opposite sides of the origin and that k_c and $k_{\mathcal{D}}$ are both
positive.   Solving the last two of equations (IB.3) for γ^2
gives:

$$\gamma^2 = \frac{\tau_r \, k_c (x_{\mathcal{D}} - x_c)}{\langle 5 \rangle x_{\mathcal{D}} - \langle 6 \rangle} \quad . \tag{IB.6}$$

τ_r is always positive so that, if γ^2 is positive it is
necessary that

$$x_{\mathcal{D}} > \frac{\langle 6 \rangle}{\langle 5 \rangle} \quad . \tag{IB.7}$$

For both γ^2 and δ^2 to be positive the condition (IB.7) is
enlarged to:

$$x_{\mathcal{D}} > \frac{\langle 6 \rangle}{\langle 5 \rangle} > x_c \quad \tag{IB.8}$$

Consider now the case when $\langle 3 \rangle$ is negative.   If
the direction of the x-axis is chosen so that $\langle 4 \rangle$ is
negative also, then (IB.4) implies that x_c, $x_{\mathcal{D}}$ and k_c
are positive and that $k_{\mathcal{D}}$ is negative.   The condition for
both γ^2 and δ^2 to be positive becomes

$$\left(x_{\mathcal{D}} > \right) x_c > \frac{\langle 6 \rangle}{\langle 5 \rangle} \quad . \tag{IB.9}$$

Should the appropriate condition (IB.8) or
(IB.9) not hold, then at least one of the exponents γ
and δ is pure imaginary,   so that the Cizek approximation
breaks down completely, because at least one of the new
orbitals becomes a travelling wave.

It is worth noting that, to a first approximation,
it is expected that

$$\frac{\langle 6 \rangle}{\langle 5 \rangle} \equiv \frac{[xy^2]}{[y^2]} \sim \frac{[x]}{[\,]} = 0 \,. \qquad\qquad (\text{IB.10})$$

Were this rigorously true, as it is for an overlap function
with a centre of symmetry, imaginary solutions for the
exponents would never occur.   More generally (IB.10)
suggests that this breakdown should not occur when the
modulus of $\langle 3 \rangle$ is large, but that the most vulnerable
situations will be those near the transition from
condition (IB.8) to (IB.9) where $x_e \sim 0$ and where $[x^2]$
and $[y^2]$ are most nearly equal.

A more detailed analysis of the circumstances in
which the Cizek approximation fails is complicated by
the need to involve analytical forms for the two centre
integrals $[x^i y^j z^k]$.   It does appear, however, that, when
$|A,m,\alpha\rangle$ and $|B,n,\beta\rangle$ are both 1s Slater functions,
breakdown will never occur; it was largely in cases of this

type that Cizek demonstrated the value of his method.
On the other hand, frequent failures, such as those
discovered "experimentally" in the present calculations,
appear likely for higher Slater orbitals.

Part II

THE JAHN-TELLER EFFECT IN ReF$_6$

II.   The Jahn-Teller effect in ReF$_6$

II.1   Introduction

The theorem of Jahn and Teller[12,13] states that
a non-linear symmetrical molecule in an electronically
degenerate state will tend to distort in at least one
non-totally symmetrical normal coordinate and that, as
a consequence of this distortion, the electronic
degeneracy will be resolved. As a result two or more
electronic potential surfaces cross at the symmetrical
configuration.

Recalling the development outlined in the main
introduction to this thesis, the general equation
governing the nuclear wavefunctions is, in terms of the
notation there outlined,

$$\left[\sum_N \frac{\hat{p}_N^2}{2M_N} + \int \psi_m^* \left(\sum_N \frac{\hat{p}_N^2}{2M_N}\right) \psi_m \, d\tau + U_m(R) - E\right] \chi_m$$

$$+ \sum_{n \neq m} \left\{ \sum_N \frac{1}{2M_N} \left[\int \psi_m^* \hat{p}_N^2 \psi_n \, d\tau + 2\left(\int \psi_m^* \hat{p}_N \psi_n \, d\tau\right) \hat{p}_N \right] \right\} \chi_n = 0.$$

$$(II.1)$$

The coupling integrals between a given pair of electronic
states become most important in configurations of near
or actual degeneracy.   Hence it is no longer a good
approximation to treat the total wavefunction of the

system as a simple product of an electronic function and
a nuclear function.   Instead the total wavefunction must,
in such a region, be written as a sum of such products
taken over the degenerate electronic states.   Thus

$$\Psi(r, R) = \sum_n \chi_n'(R)\, \psi_n(r; R),$$ (II.2)

and the coupling between these states must be invoked
when considering the nuclear motions around these
configurations.   If the stable equilibrium geometry of
the molecule is not far removed from the crossing point,
then such coupling is important in the ordinary vibrational
motions of the molecule, and may have a striking effect
on the observed vibrational spectrum.

The first stage in any problem is to investigate the
nature of the potential energy surfaces and of the
electronic wavefunctions.   If it is anticipated that only
small deviations from the symmetrical arrangement will
be involved, then it is convenient to express the
electronic functions $\psi_n(r; R)$ at nuclear configuration
R in terms of the set of eigenfunctions $\psi_n(r; 0)$ of the
electronic hamiltonian $\hat{\mathcal{H}}_0$ relevant to the symmetrical
configuration, so that

$$\psi_m(r; R) = \sum_n c_{mn}(R)\, \psi_n(r, 0).$$ (II.3)

It is assumed that the summation need only include those electronic states $\psi_n(r;0)$ which are degenerate at $R = 0$, an approximation which is valid for sufficiently small displacements.

If the electronic hamiltonian is written in the form:

$$\hat{\mathcal{H}}_e = \hat{\mathcal{H}}_0 + V'(R) ,$$

(II.4)

where $V'(R)$ is the change in the total potential energy as the nuclear configuration is moved from $R = 0$ to $R = R$, then the coefficients $c_{mn}(R)$ in equation (II.3) and the corresponding eigenvalues, $U(R)$, may be determined as functions of nuclear geometry by solution of the secular equations:

$$\sum_n \left[V_{mn}(R) + (W_0 - U(R)) \delta_{mn} \right] c_{mn} = 0 ,$$

(II.5)

where W_0 is the electronic energy in the degenerate configuration and

$$V_{mn}(R) = \int \psi_m^*(r;0) V'(r,R) \psi_n(r;0) dr .$$

(II.6)

It is convenient to write

$$V_{mn} = V_{mn}^0 + V_{mn}^{JT}$$

(II.7)

where V_{mn}^0 is the value of the integral V_{mn} when the interactions giving rise to the Jahn-Teller effect are

switched off, V_{mn}^{JT} constituting the remaining contribution.

Expanding the diagonal element V_{mm}^{o} in a Maclaurin
series and neglecting terms of higher than quadratic order,

$$V_{mm}^{o} = \frac{1}{2} \sum_{\nu} \left(\frac{\partial^2 V_{mm}^{o}}{\partial Q_{\nu}^2} \right)_o Q_{\nu}^2 .$$

(II.8)

In (II.8) the nuclear coordinates, which have hitherto been
collected in the symbol R, are broken down into the
individual normal coordinates Q_{ν}. The origin of the Q_{ν}
can always be chosen so that there are no linear terms
in the Maclaurin series, and their forms can be chosen to
avoid the appearance of cross quadratic terms $Q_{\nu} Q_{\mu}$.
Furthermore, since the terms which relieve the degeneracy of
the ψ_n are retained in the matrix V^{JT},

$$V_{mn}^{o} = \frac{\delta_{mn}}{2} \sum_{\nu} \lambda_{\nu} Q_{\nu}^2$$

(II.9)

where $\lambda_{\nu} = \left(\frac{\partial^2 V_{11}^{o}}{\partial Q_{\nu}^2} \right)_o$

If the interactions giving rise to the Jahn-Teller effect
are relatively weak, as they must be if the expansion
(II.3) for the electronic functions is to be used, then
the Maclaurin series for the elements V_{mn}^{JT} may be truncated
after terms which are linear in the Q_{ν}. It is in any case
conventional that the phrase "Jahn-Teller effect"
encompasses only such terms. Thus

$$V_{mn}^{JT} = \sum_{\nu} \left(\frac{\partial V_{mn}}{\partial Q_{\nu}} \right)_o Q_{\nu} .$$

(II.10)

Since the electronic functions $\psi_m(r;0)$ are independent of the Q_∂, it follows that

$$\left(\frac{\partial V_{mn}}{\partial Q_\partial}\right)_0 = \int \psi_m^*(r;0) \left(\frac{\partial V(r,R)}{\partial Q_\partial}\right)_0 \psi_n(r;0)\,dr. \quad \text{(II.11)}$$

For any given molecular symmetry and class of electronic degeneracy, the Q_∂ which give rise to non zero coupling integrals (II.10) have been documented.[12,13]

The solution of the secular equation (II.5) rests on the evaluation of the λ_∂ and of the elements of the matrix V^{JT}.   If the expansion (II.8) is valid throughout the range of configurations which concern the vibrational motions of the molecule, the λ_∂ are given simply by the experimental force constants derived from the vibrational spectrum.   Thus

$$\lambda_\partial = 4\pi^2 \mu_\partial \omega_\partial^2 c^2, \quad \text{(II.12)}$$

where μ_∂ is the reduced mass of the vibration whose observed spectral frequency is $\omega_\partial c$ sec^{-1}.   The evaluation of V^{JT} thus represents the largest obstacle to the calculation.

If indeed the Jahn-Teller distortion is small, the most striking consequences appear in the vibrational motions of the molecule, which couple together the different electronic states, leading in particular to an anomalous

vibrational spectrum.   The total wavefunction may be
written as

$$\Psi(r, R) = \sum_n \chi_n(R) \Psi_n(r; 0),$$ (II.13)

where the sum, as in (II.3) is over the degenerate
electronic functions of the symmetrical geometry.   The
coupled equations for the nuclear functions then take the
form:

$$\left[\sum_N \frac{\hat{P}_N^2}{2M_N} + V_{mm}^{JT} + W_c + \frac{1}{2} \sum_v \lambda_v Q_v^2 - E \right] \chi_m$$

$$+ \sum_{n \neq m} V_{mn}^{JT} \chi_n = 0,$$ (II.14)

and may be set up immediately.   It can be shown that the
use of this formalism, in terms of the fixed $\Psi_n(r;0)$,
rather than that of (II.1), in terms of the instantaneous
$\Psi_n(r;R)$, transfers the burden of the calculation from
kinetic to potential energy.[63]

Rhenium hexafluoride in an octahedral configuration
is in a four-fold degenerate (Γ_8) electronic state,[64]
and will therefore exhibit the Jahn-Teller effect.   The
calculations here described are aimed at achieving a
measure of the direction and extent of the effect in this
case.   One reason for this calculation is that features of
the ReF_6 vibrational spectrum have been ascribed to the

influence of the Jahn-Teller effect.[65]

In the homologous hexafluoride of tungsten there are
six valence electrons on the central atom which may be
assigned to the W-F bonding orbitals. The molecule
is of regular octahedral geometry and has the characteristic
vibrational spectrum.[66] ReF_6 has an extra valence electron
on the central atom and this is assigned to the non-bonding
rhenium 5d- (t_{2g}) orbital, leading in the octahedral
arrangement to a four-fold degeneracy when spin orbit coupling
is taken into account. The coupling terms, V_{mn}^{JT} , giving
rise to the Jahn-Teller effect in this case arise
principally from the sensitivity to the nuclear geometry
of the disposition of this single electron.   In this
calculation it is assumed that these terms arise simply
from the electrostatic interactions between this non-
bonding electron and the bonded fluorine atoms. The
integrals V_{mn}^{JT} thus depend only on the coordinates of a
single electron, which is a further encouragement for
considering this particular case.

The course of the work may be briefly summarised.
The electronically degenerate states of octahedral ReF_6
are discussed and the normal coordinates Q_j which contribute
to V^{JT} are enumerated.   An analytical form is postulated

for the electrostatic interaction potential between the
non-bonding electron and the fluorine atoms and the
necessary integrals (II.11) are evaluated using postulated
parameters governing the size of the Re 5d-orbital, the
ionic character of the Re-F bond and the extent of sp-
hybridisation of the bonding F orbitals. The results
are relatively insensitive to reasonable choices of
these parameters and are in good agreement with the
large splitting observed in the ω_2 band of the vibrational
spectrum. A very small (~ 0.005Å) tetragonal distortion
from octahedral geometry is predicted.

II.2 The degenerate wavefunctions in an octahedral field

The electronic structure of octahedral transition
metal hexafluorides may be envisaged in the following way.
Each fluorine atom contributes a 2s2p σ-hybrid atomic
orbital and a single electron to the bonding. Linear
combinations of these six fluorine orbitals may be
constructed to give one group orbital of symmetry a_{ig} ,
two of symmetry e_g and three of symmetry t_{iu}. These interact,
respectively, with the central atom 6s, $5d_{z^2}$, $5d_{x^2-y^2}$, $6p_x$,
$6p_y$ and $6p_z$ orbitals, yielding a set of six bonding
orbitals and six antibonding orbitals.   The metal $5d_{xy}$,

$5d_{yz}$ and $5d_{zx}$ orbitals, of symmetry t_{2g}, are not involved in the binding. The six bonding orbitals are expected to lie lowest in energy, followed by the t_{2g} non-bonding levels and then, at a somewhat higher energy, the e_g antibonding levels. In the ground state of ReF_6 according to this picture, the six bonding orbitals are fully occupied, leaving a single electron occupying the degenerate t_{2g} levels.

In ReF_6 there will also be coupling between the spin and orbital angular momenta of the non bonding electron. Spin orbit coupling effects increase in magnitude through the periodic table as the **square** of the atomic number and are far from negligible in the third row transition metals. The six spin orbit states arising from the $^2T_{2g}$ state are split into an upper doublet and a lower quartet. In the ground state, octahedral ReF_6 is therefore, fourfold degenerate, belonging to the representation Γ_8 of the extended octahedral point group O_h^r .[67] This quartet of states correlates with the $^2D_{\frac{3}{2}}$ levels of the isolated atom and may conveniently be written in terms of the d_{xy}, d_{yz} and d_{zx} orbitals as

$$|\tfrac{3}{2}\rangle = \tfrac{1}{\sqrt{2}} \left(|zx,\alpha\rangle - i|yz,\alpha\rangle \right),$$
$$|\tfrac{1}{2}\rangle = \tfrac{1}{\sqrt{6}} \left(2i|xy,\alpha\rangle + |zx,\beta\rangle - i|yz,\beta\rangle \right),$$
$$|-\tfrac{1}{2}\rangle = \tfrac{1}{\sqrt{6}} \left(2i|xy,\beta\rangle + |zx,\alpha\rangle + i|yz,\alpha\rangle \right),$$

$$(II.15)$$

and $|-\tfrac{3}{2}\rangle = -\tfrac{1}{\sqrt{2}} \left(|zx,\beta\rangle + i|yz,\beta\rangle \right),$

where α and β represent the spin functions $m_s = \frac{1}{2}$ and $m_s = -\frac{1}{2}$ respectively.   This assignment, and in particular the validity of treating the spin orbit interaction as a perturbation of the crystal field states, is based on an analysis of the electronic spectrum of ReF_6.[64]

II.3 The Jahn-Teller active modes of vibration

The integrals V_{mn}^{JT} ranging over the functions (II.15) can easily be expressed in terms of similar integrals over the simple d_{xy}, d_{yz} and d_{zx} orbitals.   The normal coordinates which contribute to the Jahn-Teller effect are therefore, by (II.11) restricted to Q_ν for which

$$\langle m | \left(\frac{\partial V(r, R)}{\partial Q_\nu} \right)_0 | n \rangle \neq 0 , \qquad (II.16)$$

where m and n range over the t_{2g} functions.   Following the original arguments of Jahn and Teller[12] non zero contributions arise only for those Q_ν which belong to irreducible representations, of the octahedral point group, O_h, contained in the symmetrised product of T_{2g} with itself. Now

$$[T_{2g}^2] = A_{1g} + E_g + T_{2g} , \qquad (II.17)$$

so that the "vibronically active" Q_ν are the totally symmetric vibration Q_1, and the modes Q_2 and Q_5 which are doubly and triply degenerate respectively.   These

Q_1 Q_{2a} Q_{2b}

Q_{5x} Q_{5y} Q_{5z}
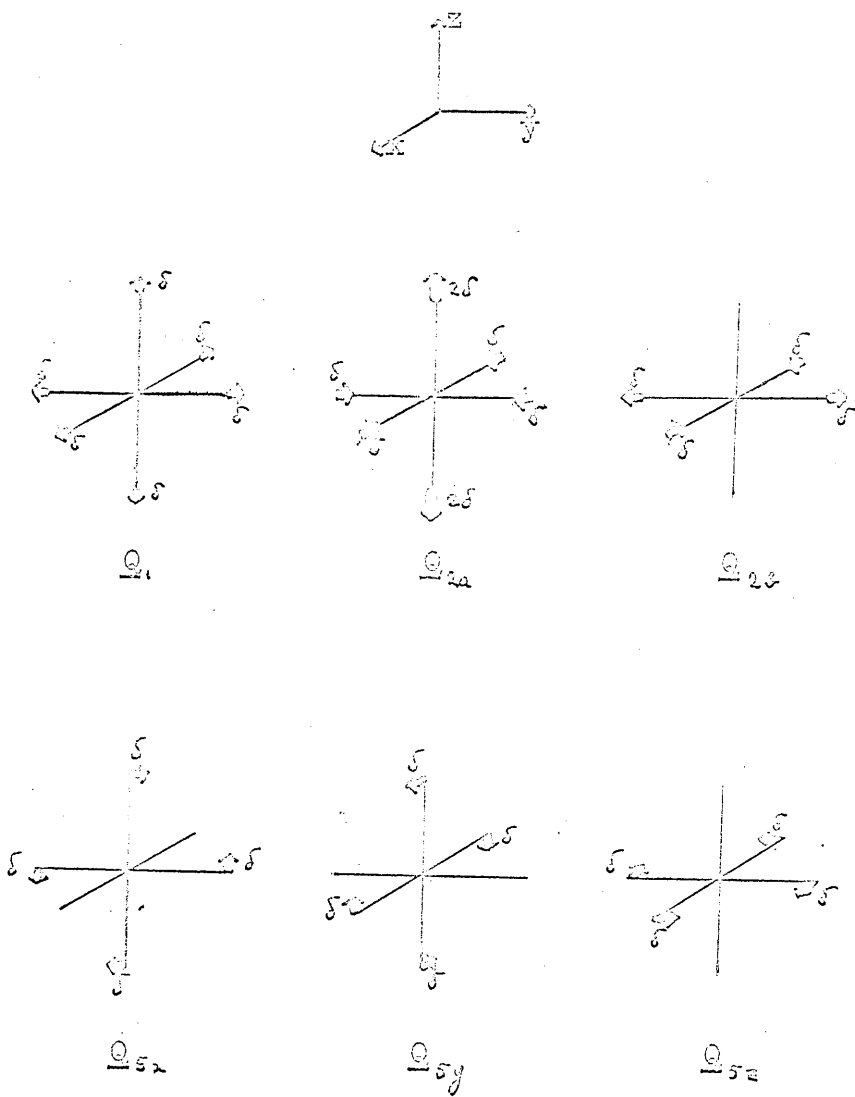
vibrations are illustrated in figure II.1.   It is

apparent that Q_1 and Q_2 involve changes in bond lengths,

while Q_5 involves changes in bond angles.

The non zero integrals (II.16), which are interrelated

by symmetry, may be expressed in terms of three constants

k_1, k_2 and k_5, defined by

$$k_1 = \langle xy | \left(\tfrac{\partial V}{\partial Q_1}\right)_0 | xy \rangle,$$

$$k_2 = -\tfrac{1}{2} \langle xy | \left(\tfrac{\partial V}{\partial Q_{2a}}\right)_0 | xy \rangle,$$

$$\text{and} \quad k_5 = -\tfrac{1}{\sqrt{3}} \langle xy | \left(\tfrac{\partial V}{\partial Q_{5x}}\right)_0 | zx \rangle, \tag{II.18}$$

and when taken over the Γ_8 states (II.15), the matrix of

V^{JT} becomes

$$V_{JT} = \begin{bmatrix} k_1 Q_1 + k_2 Q_{2a} & k_5(Q_{5y} - i Q_{5x}) & k_2 Q_{2b} - i k_5 Q_{5z} & 0 \\ k_5(Q_{5y} + i Q_{5x}) & k_1 Q_1 - k_2 Q_{2a} & 0 & -k_2 Q_{2b} + i k_5 Q_{5z} \\ k_2 Q_{2b} + i k_5 Q_{5z} & 0 & k_1 Q_1 - k_2 Q_{2a} & k_5(Q_{5y} - i Q_{5x}) \\ 0 & -k_2 Q_{2b} - i k_5 Q_{5z} & k_5(Q_{5y} + i Q_{5x}) & k_1 Q_1 + k_2 Q_{2a} \end{bmatrix} \tag{II.19}$$

The constants k_1, k_2 and k_5 are most conviently expressed

in terms of basic integrals involving the interaction with a

single fluorine atom. If $v(x,y,z)$ is the potential between

the non bonding electron and a single fluorine atom at the

point (x,y,z), then simple symmetry considerations show
that

$$\langle xy|\left(\frac{\partial V}{\partial Q_v}\right)_0|xy\rangle = \frac{1}{\sqrt{6}}\left\{2\langle xy|v_z(0,0,R_0)|xy\rangle + 4\langle zx|v_z(0,0,R_0)|zx\rangle\right\},$$

$$\langle xy|\left(\frac{\partial V}{\partial Q_{2q}}\right)_0|xy\rangle = \frac{1}{2\sqrt{3}}\left\{4\langle xy|v_z(0,0,R_0)|xy\rangle - 4\langle zx|v_z(0,0,R_0)|zx\rangle\right\}, \qquad (II.20)$$

and $\langle xy|\left(\frac{\partial V}{\partial Q_{5x}}\right)_0|zx\rangle = \frac{1}{2}\left\{4\langle xy|v_y(0,0,R_0)|zx\rangle\right\}$,

where v_y and v_z are the appropriate derivatives of the
function v and R_0 is the equilibrium bondlength in the
absence of the Jahn-Teller interactions.   Furthermore

$$\langle xy|v_y(0,0,R_0)|zx\rangle = \lim_{\omega \to 0}\left\{\frac{\langle xy|v(0,R_0\sin\omega,R_0)|zx\rangle - \langle xy|v(0,0,R_0)|zx\rangle}{R_0\sin\omega}\right\}$$

$$= \frac{\langle zx|v(0,0,R_0)|zx\rangle - \langle xy|v(0,0,R_0)|xy\rangle}{R_0}, \qquad (II.21)$$

so that only four basic two centre integrals are required.
These are

$$v'_{xy} = \langle xy|v_z(0,0,R_0)|xy\rangle,$$

$$v'_{zx} = \langle zx|v_z(0,0,R_0)|zx\rangle,$$

$$v_{xy} = \langle xy|v(0,0,R_0)|xy\rangle, \qquad (II.22)$$

and $v_{zx} = \langle zx|v(0,0,R_0)|zx\rangle.$

In terms of these quantities the coupling constants
k_1, k_2 and k_5 become

$$k_1 = \sqrt{\frac{2}{3}}\left(v'_{xy} + v'_{zx}\right),$$

$$k_2 = \frac{1}{\sqrt{3}}\left(v'_{zx} - v'_{xy}\right),$$

and $k_5 = \frac{2}{\sqrt{3}}\left(\frac{v_{xy} - v_{zx}}{R_0}\right).$ (11.23)

II.4 Calculation of the integrals

The evaluation of the integrals (II.22) requires expressions for the electrostatic potential due to the fluorine atom on the positive z-axis and for the rhenium 5d-orbitals.

If the bonding were completely ionic the electrostatic fluorine potential would closely approximate that of a fluoride ion, for which an analytical expression, derived from self consistent field calculations[68] is available.[69] In order to correct for covalency, the bonding fluorine orbital is assumed to be a hybrid 2s2p Slater-type function with exponent c. Thus

$$|F\rangle \propto r_F \exp(-c\,r_F)\{\sqrt{3}\,h\cos\alpha + (1-h)\}, \qquad (II.24)$$

where h is a hybridisation parameter (h=0 corresponds to a pure s-orbital and h=1 to a pure p-function). The angle α is measured from the F-Re bond. The electrostatic potential v (r_F,α) may be expressed as

$$v(r_F,\alpha) = v_{F^-}(r_F) - (1-g)\langle F|\frac{1}{r_F}|F\rangle, \qquad (II.25)$$

where completely covalent and totally ionic situations correspond to g=0 and g=1 respectively. On substituting for the fluoride ion potential v_{F^-}, and performing the

integration in (II.25) the following expression is
obtained:

$$
v(r_F, \alpha) = \left\{ \frac{1}{r_F} - \frac{10}{r_F} \exp(-2.674 r_F) - 147 r_F^2 \exp(-5.365 r_F) \right\}
$$

$$
- (1-g) \left\{ \frac{1}{r_F} - \exp(-2c r_F) \left[\frac{1}{r_F} + \frac{3c}{2} + c^2 r_F + \frac{c^3 r_F^2}{3} \right] \right.
$$

$$
- h \left(1 - 3\cos^2\alpha \right) \left[\frac{3}{2c^2 r_F^3} - \exp(-2c r_F) \left(\frac{3}{2c^2 r_F^3} + \frac{3}{c \cdot r_F^2} \right. \right.
$$

$$
\left. \left. \left. + \frac{3}{r_F} + 2c + c^2 r_F + \frac{c^3 r_F^2}{3} \right) \right] \right\} .
$$

(II.26)

The radial part for the rhenium 5d-orbitals is taken
in Slater-type form:

$$
| Re \rangle \propto f(\theta, \phi) \, r^3 \exp(-p r).
$$

(II.27)

Since the true radial variation of these functions is
uncertain the exponent p is varied widely about the value
p=1.4 estimated by Slater's rules.[31]

Because of the terms in r^{-2} and r^{-3} in the expression
(II.26) for v, the two centre integrals (II.22) are best
computed numerically. Gaussian quadrature [42] using
confocal ellipsoidal coordinates was adopted, with an
integration grid whose mesh was reduced until the desired
accuracy was obtained. The integrals v'_{xy} and v'_{zx}
which involve the derivative of v, with respect to the
z-coordinate of the fluorine atom on which it is centred,
are best performed by carrying out the differentiation

after transforming to ellipsoidal coordinates.   The bond
length R_e in equations (II.22) was taken as 1.830Å,
the observed internuclear distance in WF_6.[70]

II.5 Results and discussion

The measurable consequences of the Jahn-Teller effect
fall into two categories.   In the static aspect the form of
the lowest potential surface determines the (distorted)
equilibrium geometry of the molecule.   In the dynamical
problem the coupling between the surfaces induced by the
nuclear motions determines the vibrational spectrum of
the molecule.

Once the integrals (II.22) have been evaluated it is
possible to set up the secular equations, (II.5), whose
eigenvalues determine the electronic potential surfaces.
Thus, in matrix notation,

$$\left\{ V^{JT} + \left(W_0 + \tfrac{1}{2} \sum_{\nu} \lambda_{\nu} Q_{\nu}^2 \right) \mathbf{1} \right\} C = \mathcal{U} C ,$$ (II.28)

where C is the matrix of eigenvectors and U is that of
eigenvalues; V^{JT} is constructed from (II.19) and   is the
unit matrix.   The potential surfaces in this situation
have been derived by Moffitt and Thorson.[71]   They
correspond to two Kramer doublet levels whose energies may

be written

$$U = W_o + \frac{1}{2}(\lambda_1 Q_1^2 + \lambda_2 r^2 + \lambda_5 R^2) + k_1 Q_1 \pm \sqrt{k_2^2 r^2 + k_5^2 R^2},\qquad \text{(II.29)}$$

where $r^2 = Q_{2a}^2 + Q_{2e}^2$ and $R^2 = Q_{5x}^2 + Q_{5y}^2 + Q_{5z}^2$.

If $k_5^2/\lambda_5 > k_2^2/\lambda_2$ the minima lie at

$$Q_1 = -k_1/\lambda_1, \quad r = 0, \quad R = |k_5|/\lambda_5, \qquad \text{(II.30)}$$

where $U_{min} = W_o - \frac{1}{2}\frac{k_1^2}{\lambda_1} - \frac{1}{2}\frac{k_5^2}{\lambda_5}$

On the other hand, when $k_5^2/\lambda_5 < k_2^2/\lambda_2$, the minima lie at

$$Q_1 = -k_1/\lambda_1, \quad Q_{2a} = \pm|k_2|/\lambda_2, \quad R = 0, \qquad \text{(II.31)}$$

where $U_{min} = W_o - \frac{1}{2}\frac{k_1^2}{\lambda_1} - \frac{1}{2}\frac{k_2^2}{\lambda_2}$,

In the latter case, where the asymmetric distortion is in the Q_2 mode, it has been shown [72] that any quadratic coupling terms (neglected in this work) will cause the absolute minimum to lie in Q_{2a} rather than in the Q_{2e} component.

It can be shown [73] that the vibrational consequences of the Jahn-Teller effect depend on the dimensionless ratio D_i to the ith vibrational quantum, of the depression of the energy minimum caused in that mode. Thus

$$D_i = \frac{1}{2}\frac{k_i^2}{\lambda_i \omega_i}. \qquad \text{(II.32)}$$

The force constants λ_ν, required in equations (II.29-II.32), are evaluated from the vibrational frequencies

Table II

p	g	h	$r_{max}(\text{Å})$	D_1	D_2	D_5	$\beta_2^2/\lambda_2\,(\text{cm}^{-1})$	$\beta_5^2/\lambda_5(\text{cm}^{-1})$	$\Delta Q_1\,(\text{Å})$	$\Delta Q_2(\text{Å})$	$\Delta Q_5(\text{Å})$	$\Delta\omega(\text{cm}^{-1})$
1.0	0	1	2.12	0.038	0.0069	0.068	9.27	40.2	−0.0055		±0.014	13
1.4	0	1	1.51	0.413	0.062	0.188	82.3	111	−0.018		±0.025	130
1.7	0	1	1.35	0.760	0.101	0.188	136	111	−0.024	±0.0067		190
2.0	0	1	1.06	0.866	0.101	0.140	135	82.4	−0.026	±0.0067		190
2.5	0	1	0.85	0.714	0.061	0.068	81.0	39.9	−0.024	±0.0052		130
1.0	0	0	2.12	0.065	0.0093	0.092	12.4	54.1	−0.0072		±0.017	20
1.4	0	0	1.51	0.543	0.079	0.200	106	118	−0.021		±0.025	160
1.7	0	0	1.35	0.815	0.117	0.164	157	96.7	−0.025	±0.0072		210
2.0	0	0	1.06	0.738	0.104	0.096	139	56.7	−0.024	±0.0068		200
2.5	0	0	0.85	0.371	0.048	0.029	64.4	16.9	−0.017	±0.0046		110
1.4	0.01	1	1.51	0.413	0.062	0.188	82.3	111	−0.018		±0.025	130
1.435	0.1	1	1.47	0.222	0.063	0.110	83.9	65.0	−0.013	±0.0053		140
1.505	0.3	1	1.41	0.0034	0.059	0.015	78.6	8.62	−0.0016	±0.0051		130
1.61	0.6	1	1.31	0.482	0.043	0.041	57.9	24.2	0.019	±0.0044		100
1.75	1.0	1	1.21	3.693	0.016	0.394	21.4	232	0.054		∓0.034	40

r_{max} = radial distribution maximum of t_{2g} orbital.
ΔQ_1 = increase in average bond length.
ΔQ_2 = increase in equatorial bond length = $\frac{1}{2}$(decrease in axial bond length).
ΔQ_5 = atomic displacement in a Q_5 mode.

$\omega_1 = 755$ cm^{-1} , $\omega_2 = 670$ cm^{-1} and $\omega_5 = 295$ cm^{-1} . Of these ω_1 is taken direct from the Raman spectrum[65] but ω_2 and ω_5 are interpolated from the sequence WF_6 , IrF_6 and PtF_6[66,74,75] because the observed ReF_6 frequencies are dependent on the Jahn-Teller effect. These spectra have been reviewed at length.[65]

In the results, collected in table II, a value of 2.425 has been used throughout for the fluorine bonding orbital exponent c. This value is in accordance with Slater's rules and in one case the choice c=2.6 was found to alter the calculated coupling constants by only about 2%, so that the accuracy of this choice does not appear to be crucial. On the other hand the t_{2g} orbital exponent, p, is varied widely, though the extreme values of 1.0 and 2.5 appear unrealistic when the corresponding orbital maxima, at 2.12Å and 0.85Å respectively, are compared with the molecular dimensions (Re-F $\sim$1.8Å).

Horizontally, the table is divided into three sections. The first two correspond to purely covalent binding (g=0), using 2p- and 2s- fluorine orbitals respectively, and in each case varying the rhenium exponent p over a wide range. It appears that the hybridisation of the fluorine orbital has little influence on the results, though significant

variations do occur on changing the rhenium exponent.
Order of magnitude consistency is however maintained,
especially over the physically reasonable range $1.4 \leq p \leq 2.0$.
The effect on the results of a gradual introduction of bond
polarity is shown in the last section of the table, where
g is the charge transferred to each fluorine atom and the
rhenium exponent is at each step derived by applying
Slater's rules to the configuration Re $5d_{t_{2g}}' \left[5d_{e_g}^4 \ 6s^2 \right]^{(1-g)}$,
thereby taking account of the increasing effective nuclear
charge of the central atom. The increasing ionic character
appears to have little influence on the magnitude of D_2,
but to cause a rapid diminution of D_1 and D_5, both of
which pass through zero before $g = 0.4$. Since the
positive charge on the central atom is 6g it is unlikely
that g will exceed 0.3.

The calculated equilibrium geometry of the molecule
may be derived by superimposing the atomic displacements
ΔQ_1, ΔQ_2 and ΔQ_5 on to the unperturbed (WF_6) geometry. The
predicted values of these displacements and an explanation
of the symbols are given in the table. It is apparent that
neither Q_2 nor Q_5 distortions predominate over the entire
range of values of p. A small degree of ionicity tends to

favour Q_2, however, and a distortion in this mode seems
the more likely. In order of magnitude, therefore, it
seems probable that there will be a net decrease in
bondlength ($\sim$0.01Å) compared with WF_6 and that superimposed
on this will be a small tetragonal distortion corresponding
to a change in the equatorial bondlength of $\sim$0.005Å.
Since the mean amplitude of vibrational motion in the ReF
bonds is of the order of 0.02Å, it appears improbable
that the net asymmetry would be detectable.

The influence of the Jahn-Teller effect on the
vibrational spectrum, however, is more striking. The Q_1
displacement does not reduce the molecular symmetry, nor
relieve the electronic degeneracy.   It marks only the
influence of the non bonding electron on the net stability
of the molecule. The values of D_2 and D_5, however,
determine the expected splitting in the ω_2 and ω_5 bands in
the Raman spectrum. If $k_5 \ll k_2$ or if it is assumed that
the vibrational interactions in Q_2 and Q_5 may be treated
separately, then the vibronic problem in Q_2 reduces to
that treated by Longuet-Higgins and others[76] and the
predicted splittings $\Delta\omega_2$ quoted in the last column are
derived from their tables of energy levels. An experimental
value of 168 cm^{-1} has been reported[65] for this splitting,
and this figure is in reasonable agreement with values

calculated for $1.4 \leq p \leq 2.0$.   The necessary data is not
available for a similar estimate of the structure of the ω_5
band.

This calculation is of necessity rather crude. It
does, however, show that a simple electrostatic interaction
accounts for the observed anomalous Jahn-Teller splitting in
the ω_2 band of the spectrum of ReF_6. It also predicts
that the net geometric distortion will be very small, a
conclusion which is susceptible to test. In this
straightforward electrostatic approach no allowance has
been made for the Pauli exclusion effects which were
shown to be of such significance in the calculation in part I.
This omission should be relatively unimportant here as the
t_{2g} rhenium orbital expressions have nodes in the
octahedral directions, and are thus of small amplitude
within the fluorine cores, and overlap in any case only
with the occupied fluorine $2p_\pi$ orbitals. Neglect of such
other factors as exchange should be entirely justifiable
within the framework of this calculation, since the
fundamental uncertainties in the detailed electronic
distributions restrict the reasonable objectives of the
work to a demonstration of the applicability of Jahn-Teller
theory to ReF_6 and an order of magnitude estimate of the

detailed effects. A more precise calculation would

require a very much more elaborate treatment of the

problem. The results of this work have been published.[77]

References

1. Born,M., and Oppenheimer, R.J.,1927, Ann. Physik, 84, 457.

2. Born,M., 1951, Festschrift Gött. Nachr. Math , Phys.Kl.l.

3. Hobey,W.D., and McLachlan,A.D., 1960, J.Chem. Phys. 33, 1695.

4. Thorson,W.R., 1963, J. Chem. Phys. 39, 1431.

5. Landau, L.D., 1932, Z. Phys. Sowj. 2, 46.

6. Zener,C., 1932, Proc. Roy. Soc. A.137, 696.

7. Steueckelberg, E.G.C., 1932, Helv. Phys. Acta, 5, 369.

8. Laidler, K.J., and Polanyi,J.C., 1965, Prog. React. Kinet. 3,1.

9. Herschbach, D.R., 1966, Adv. Chem. Phys. 10, 319.

10. Herschbach, D.R., 1965, Appl. Opt. 4, Supplement, p 128.

11. Taylor, E.H., and Datz,S., 1955, J. Chem. Phys.23, 1711.

12. Jahn,H.A., and Teller,E., 1937, Proc.Roy.Soc. A.161, 220

13. Jahn,H.A., 1938, Proc.Roy.Soc. A164, 117.

14. Longuet-Higgins,H.C., 1960, Adv. Spect. 2,249.

15. Austin,B.J., Heine,V., and Sham,L.J., 1962, Phys. Rev. 127, 276.

16. Cizek, J., 1963, Mol. Phys. 6, 19.

17. Rittner,E.S., 1951, J. Chem. Phys., 19, 1030.

18. London, F., 1937, Z. Physik, 74, 143.

19. Renninger, M., 1952, Acta Cryst. 5, 711.

20. Gordy, W., 1951, J. Chem. Phys. 19, 792.

21. Pauling, L., 1927, Proc. Roy. Soc. A. 114, 181.

22. London, F., 1930, Z. Physik, 63, 245.

23. Born, M., and Mayer, J.E., 1932, Z. Physik, 75, 1.

24. Amdur, I., and Ross, J., 1958, Combust. Flame, 2, 412.

25. Pauling, L.C., 1940, "The Nature of the Chemical Bond"
            (Cornell Univ. Press, Ithaca, New York) 2nd edition

26. Clementi, E., 1964, J. Chem. Phys. 41, 295.

27. Clementi, E., 1963, J. Chem. Phys. 38, 996 and 1001

28. Clementi, E., 1963, Document Nos. 7440, 7441, ADI
            Auxiliary Publications Project, Photoduplication
            Service, Library of Congress, Washington 25, D.C.

29. Atomic Energy Levels, 1949, Circular 467, United States
            Dept. of Commerce, National Bureau of Standards.

30. Sternheimer, R.M., 1962, Phys. Rev. 127, 1220.

31. Slater, J.C., 1930, Phys. Rev. 36, 57.

32. Clementi, E., 1963, J. Chem. Phys. 39, 175.

33. Clementi, E., 1965, J. Chem. Phys. 42, 2783.

34. Hartree, D.R., and Hartree, W., 1948, Proc. Roy. Soc.
            A. 193, 299.

35. Hartree, D.R., and Hartree, W., 1938, Proc. Roy. Soc.
            A. 166, 450.

36. Hartree, D.R., and Hartree, W., 1936, Proc. Roy. Soc.
            A. 156, 45.

37. Strand, T.G., and Bonham, R.A., 1964, J. Chem. Phys.
            40, 1686.

38. Strand, T.G., Kohl, D.A., and Bonham, R.A., 1963,
            J. Chem. Phys. 39, 1307.

39. Mulliken,R.S., Rieke,C.A., Orloff,D., and Orloff,H.,
        1949, J. Chem. Phys. 17, 1248.

40. Magnusson,E.A., 1964, Rev. Pure Appl. Chem. 14, 57.

41. Mulliken,R.S., 1949, J. Chim. phys. 46, 497, 500 and 521.

42. Lowan,A.N.,Davids,N., and Levenson,A., 1942, Bull. Amer.
        Math. Soc. 48,739.

43. Pope,D.A., and Tomkins, C.,1957, J. Assoc. Comp. Mach.
        4, 459.

44. Leifer,L. Cotton,F.A., and Leto,J.R., 1958, J. Chem.Phys.
        28, 364.

45. Hafemeister,D.W.,and Flygare,W.H.,1965, J. Chem.Phys.
        43, 795.

46. Mayer,J.E., and Helmholz,L., 1932,Z.Phys. 75, 19.

47. Herzberg,G., 1950, "Spectra of Diatomic Molecules"
        (D. Van Nostrand Company, Inc., New York)2nd
        edition.

48. Rosen,N., and Ikehara,S., 1932, Phys. Rev. 43, 5.

49. Barrow,R.F., Travis,N., and Wright,C.V.,1960, Nature,
        187, 141.

50. Robertson,E.W., and Barrow,R.F.,1961, Proc.Chem. Soc.
        329.

51. James,H.M., 1935, J. Chem.Phys. 3,9.

52. Lee,Y., and Mahan,B.H., 1965, J. Chem Phys. 42, 2893.

53. Sinanoglu,O., and Mortensen,E.M., 1961, J. Chem Phys.
        34, 1078.

54. Faulkner,J.E., 1957, J. Chem. Phys. 27, 369.

55. Morse,P.M., 1929, Phys. Rev. 34, 57.

56. Kachhava,C.M., and Saxena,S.C., 1963, Mol. Phys. 7, 465.

57. Bunker,D.L., and Blais,N.C., 1964, J. Chem. Phys.,
        41, 2377.

58. Chupka,W.A., 1959, J. Chem. Phys. 30, 458.

59.   Dixon,R.N., 1964, Trans. Farad. Soc. 60, 1363.

60.   Moulton,M.C., and Herschbach, D.R., 1966,J. Chem.Phys.
              44, 3010.

61.   Margenau,H., and Murphy,G.M., 1956, "The Mathematics of
              Physics and Chemistry" (D. Van Nostrand
              Company Inc.,New York) 2nd edition.

62.   Hartree,D.R., 1955, "Numerical Analysis" (Oxford Univ.
              Press.)

63.   McLachlan,A.D., 1961, Mol. Phys. 4, 417.

64.   Moffitt,W., Goodman,G.L., Fred,M., and Weinstock,B.,
              1959, Mol. Phys. 2, 109.

65.   Weinstock,B., and Goodman,G.L.,1965, Adv. Chem. Phys.9,
              169.

66.   Burke,T.G.,Smith,D.F., and Nielsen,A.H., 1952, J. Chem.
              Phys. 20, 447.

67.   Bethe, H., 1929, Ann. Phys. 3, 133.

68.   Froese,C., 1957, Proc. Camb. Phil. Soc. 53, 206.

69.   Craig,D.P., and Zauli,C., 1962,J. Chem Phys. 37, 601.

70.   Weinstock,B., and Malm,J.G., 1958, Proc. U.N. Intern.
              Conf. Peaceful Uses At. Energy, 2nd,
              Geneva, 28, 125.

71.   Moffitt,W. and Thorson,W.R., 1957, Phys.Rev. 108,1251.

72.   Balhausen,C.J., and Liehr,A.D., 1958, Annals of Physics,
              3, 304.

73.   Moffitt,W., and Thorson,W.R., 1958, Rec. Mém. Centre
              Nat. Rech. Sci., November.

74.   Weinstock,B., Claassen,H.H., and Malm,J.G., 1960,
              J. Chem. Phys. 32, 181.

75,   Claassen,H.H., Malm,J.G., and Selig,H., 1962, J. Chem.
              Phys. 36, 2890.

76.   Longuet-Higgins, H.C., Öpik,U., Price,M.H.L., and Sack,
                R.A., 1958., Proc. Roy. Soc. A.244, 1.

77.   Child, M.S., and Roach, A.C., 1965, Mol. Phys., 9, 281.